Diffusions and Laplacians on Laakso, Barlow-Evans, and other Fractals

Benjamin Steinhurst, Ph.D.
University of Connecticut, 2010

The study of self-adjoint operators on fractal spaces has been well developed on specific classes of fractals, such as post-critically finite and finitely ramified. In Part I, we begin by discussing the spectrum of a self-similar Laplacian on a family of post-critically finite fractals, calculating the spectrum for a general member of this family. To complement this we then discuss a source of post-critically finite fractals from self-similar groups that are associated with the Hanoi Towers game and certain modifications of these groups. Part II develops the spectral analysis of a self-adjoint Laplacian on Laakso spaces. The spectrum of this operator is calculated in general with multiplicities and supported by numerical calculations for many specific Laakso spaces.

Diffusions and Laplacians on Laakso, Barlow-Evans, and other Fractals

Benjamin Steinhurst

M.Sc. Mathematics, University of Connecticut, 2007
B.A. Mathematics, Williams College, 2005

A Dissertation
Submitted in Partial Fullfilment of the
Requirements for the Degree of
Doctor of Philosophy
at the
University of Connecticut

2010

APPROVAL PAGE

Doctor of Philosophy Dissertation

Diffusions and Laplacians on Laakso, Barlow-Evans, and other Fractals

Presented by
Benjamin Steinhurst, M.Sc. Math.

Major Advisor _____
Alexander Teplayaev

Associate Advisor _____
Richard Bass

Associate Advisor _____
Luke Rogers

University of Connecticut
2010

Dedicated to my lovely wife who kept me going while compiling this document.

ACKNOWLEDGEMENTS

I thank my advisor Alexander Teplyaev and the other members of my committee, Richard Bass and Luke Rogers for all of their help throughout the entire process. The research presented in this document has been supported by the National Science Foundation grant DMS-0505622. Chapters two through six were originally produced as independent papers and so I make my acknowledgements for those chapters separately.

Chapter 2: Daniel Ford and I thank Alexander Teplyaev for his guidance and support. We also thank Kevin Romeo, Robert Strichartz, and Denglin Zhou for their comments throughout the process.

Chapter 3: Shotaro Makisumi, Grace Stadnyk and I thank Alexander Teplyaev, Volodymyr Nekrashevych, Luke Rogers, Matt Begué, Levi DeValve, and David Miller.

Chapter 4: I thank Alexander Teplyaev for his guidance in the original framing of this chapter. I also thank Piotr Hajłasz, Luke Rogers, and Robert Strichartz for their useful questions and comments. Comments from anonymous referees have proved invaluable in improving this paper.

Chapter 5: Kevin Romeo and I thank Alexander Teplyaev, Daniel Ford, and Robert Strichartz for their support and feedback throughout the production of this paper.

Chapter 6: Matthew Begue, Levi DeValve, David Miller and I thank Alexander Teplyaev, Luke Rogers, Robert Strichartz, Shotaro Makisumi, Grace Stadnyk, Jun Kigami, and Naotaka Kajino.

TABLE OF CONTENTS

LIST OF FIGURES

LIST OF TABLES

Chapter 1

Introduction

Fractals have been studied for most of the $20th$ century by mathematicians including Cantor, Julia, Fatou, Hausdorff, Sierpinski, and others. For example the Cantor set became a common textbook example of a perfect set with zero Lebesgue measure. They were also a rich source of examples in developing various notions of dimensions that take non-integer values. A renewed interest in fractals came about when it became clear that they could also be useful in modeling physical processes. This was also at the time when computer aided renderings became available. With these renderings of fractals applications suggested themselves such as questions of the length of coastlines, diffusion in porous media such as air flowing through lungs, and the more involved service as models for quantum field theory, and industrial applications such as pre-fractal antennae and road-side sound barriers.

The analysis on fractals field has made it possible to consider functions with high orders of smoothness on fractals, despite the fact that fractals are non-smooth spaces. In this context a function is smooth if it is in the domain of any positive integer power of a Laplacian operator. The definition of this Laplacian is usually a non-trivial task. The price one pays for this rich class of smooth functions is that one much demand high levels of regularity in the fractals. Examples include the class of post-critically finite fractals explored by Kigami [43] and many others, and finitely ramified fractals as in Bajorin et al. [6]. Both of these classes share a cell structure whose cells have very small boundary. In contrast to this program of introducing highly regular spaces, analysis on metric measure spaces allows for much rougher spaces while considering only the equivalent of a single derivative. The spaces are even rougher reducing the amount of smoothness available. Depending on how rough the metric measure space is this first derivative may not even be canonical [36]. For instance, Cheeger, Hajłasz and Koskela have constructed various types of Sobolev spaces on metric measure spaces which do not always coincide even in Euclidean domains [36] when the boundary is not Lipschitz. Related notions have further been developed by Heinonen, Shanmugalingam, and Tyson.

In this document we compile five papers [29,59,71,66,16]. The first two papers explore the construction and spectral analysis of Laplacians on post-critically

finite fractals and Laplacians on them in Part I. Then the third, fourth, and fifth papers in Part II we bring together methods from analysis on fractals, the analysis of metric measure spaces, and potential theory to explore diffusions and the spectrum of a Laplacian on Laakso spaces. As will be seen in Chapter 4 there are many choices of Laplacian. We conclude Chapter 6 an analysis of the short-time asymptotics of the heat kernel associated to a particular Laplacian on a Laakso space constructed in Chapter 4.

1.1 Laakso Space

What we call Laakso spaces were introduced by Tomi Laakso in [52] as examples of metric measure spaces supporting Poincaré inequalities with Hausdorff dimension greater than one. His original construction began with the product $[0,1]\times K$, where K is a Cantor set, and formed the quotient space by an equivalence relation. The quotient space is a path-connected metric measure space with a Hausdorff dimension determined by certain choices made in the definition of the equivalence relation can be encoded by a sequence of integers. In [12], Martin Barlow and Steven Evans commented, without giving a proof, that their projective limit construction of Markov process-state space pairs could also be used to construct Laakso spaces with diffusions living on them.

We will use Laakso spaces as a setting to explore what aspects of the theory of differential equations on fractals can be extended to more general metric measure spaces. It will be proved in Chapter 4 that the constructions of Laakso and of Barlow-Evans do give homeomorphic spaces. Using Laakso's construction we will define a Dirichlet form from minimal generalized upper gradients. We show that it is equivalent to the Dirichlet form associated to the Markov process from Barlow and Evan's construction applied to reflected Brownian motion on the unit interval as the base process. The proofs of these results also develop the methods used to analyze the spectrum of the Laplacian in Chapters 5 and 6. With an undergraduate advisee, Kevin Romeo, we performed the numerical calculation in Chapter 5 and then provided a theoretical proof that the spectrum of the Laplacian associated to these Dirichlet forms has the form

$$\sigma(A)=\bigcup_{n=0}^{\infty}\bigcup_{k=0}^{\infty}\left\{\frac{k^2\pi^2}{d_n^2}\right\}\cup\bigcup_{n=2}^{\infty}\bigcup_{k=1}^{\infty}\left\{\frac{k^2\pi^2}{4d_n^2}\right\}\cup\bigcup_{n=1}^{\infty}\bigcup_{k=0}^{\infty}\left\{\frac{(2k+1)^2\pi^2}{4d_n^2}\right\},$$

where the sequence d_n is part of the data used to construct the Laakso space. Which can be chosen to produce a desired Hausdorff dimension. Our argument includes an account of how the graph Laplacian approximates the continuously defined Laplacian. The analysis in this chapter completely characterizes the spectrum, but leaves an account of the multiplicity of the eigenvalues for the next chapters. We turn to this matter in Chapter 6 then continues this analysis with

an expansion of the numerical experiments conducted in Chapter 5 extending the characterization of the spectrum to include an exact statement of the multiplicities. Many of these calculations were done with another group of undergraduate advisees, Matthew Begue, Levi DeValve, and David Miller. As a corollary to the spectral results the spectral dimension is calculated directly from the short-time asymptotics of the heat kernel associated to this Laplacian. The calculation of the spectral dimension was inspired by the interests of some authors in the physics literature [2].

Chapters 4, 5, and 6 together develop an analysis of metric-measure spaces using only their weak self-similarity and cell structure that they have without relying on strict self-similarity or upon the types of probabilistically controlled departures from strict self-similarity (e.g choosing between two sets of contraction maps according to a given distribution) that have previously been studied [11] and elsewhere. However this still demands more regularity in the structure of Laakso spaces than is usually assumed by the metric measure space community which may be no more than assuming that the measure is volume doubling. Considering the kind of results that are accessible using the methods demonstrated it is reasonable to suspect that further results may be obtained by similar methods in the future. For example, it has been shown for generalized Sierpinski carpets that under certain symmetry conditions that Brownian motion on these fractals is unique up to a time change [11]. It is reasonable to suspect this might also be true on Laakso spaces, but this is still being worked on [72]. A related question is: what are the best bounds possible on the heat kernel on a Laakso space? Again, this is still being worked on. Alternatively, one could consider more general self-adjoint operators than this single Laplacian, and ask how wave packets would evolve under Schrödinger operators. Perhaps most interestingly, one may ask how far these constructions can be extended, and can they be used to construct metric measure spaces with more direct applications to physical problems?

1.2 Self-Similar Groups

Recently there has been a coming together of group theory and analysis on fractals. Using the notion of finite state automata, Nekrashevych [61], Grigorchuk, Šuník and others have, with reasonable specified conditions, defined groups of automorphisms of rooted infinite trees that can to be associated to fractals. One of the more tangible examples [24,25] is the group representing the legal moves in the Towers of Hanoi game, which is related the Sierpinski gasket. There has been a technical obstacle to generalizing this result to versions of the Towers of Hanoi game that have more than three pegs. Such a generalization would yield an algebraic generalization of the Sierpinski gasket which may be different than the wide supply of geometric generalizations. An algebraically natural generalization is provided in Chapter 3, where we produce sufficient extra conditions on the

group of legal moves when there are more than three pegs are sufficient to show that these groups retain the critical "contracting" property that is required for the correspondence between the groups and the fractals. This work was originally developed in cooperation with two REU students Shotaro Makisumi and Grace Stadnyk.

1.3 Post Critically Finite Fractals

In the study of fractals and operators on functions defined on fractals it is necessary to make assumptions on the geometry of the fractal to be able to give reasonable definitions to the operators one wants to study. For a fractal to be post critically finite we require that the set of boundary points between cells and finite and that they can only be approached by finitely many asymptotically equivalent paths. Analysis on post critically finite fractals has a well established tradition with much work having been done [40,43,6,74] since the 1980's.

Part I of this document explores spectral decimation, the method of spectral analysis that is often used when working with post critically finite fractals. Spectral decimation was first introduced in [32] and has been used widely since. The benefit of spectral decimation is that it reduces the problem of determining the spectrum of a Laplacian to an iterative process using small order matrices. In the spectral decimation calculations on the Sierpinski gasket [6] the matrices were three by three. In Chapter 2 a class of post critically finite fractals is constructed, analyzed, and the spectrum of the Laplacian on them determined. Chapter 3, as mentioned above, describes a class of post critically finite fractals derived from generalizing the Towers of Hanoi game. These two chapters will serve as a demonstration of traditional methods in analysis on fractals before moving into Part II where the focus moves towards the methods of the analysis of metric measure spaces.

Part I

Chapter 2

Vibration Spectra of the m-Tree

This chapter first appeared as [29] with co-author Daniel Ford who worked as a REU student under the author's supervision.

Abstract: We introduce a family of post-critically finite fractal trees indexed by the number of branches they possess. Then we produce a Laplacian operator on graph approximations to these fractals and use spectral decimation to describe the spectrum of the Laplacian on these trees. Lastly we consider the behavior of the spectrum as the number of branches increases.

MCS: 28A80, 34B45, 15A18, 60J45, 94C99, 31C25

2.1 Introduction

There have been many studies using spectral decimation to calculate the spectrum of a Laplacian operator on finitely ramified fractals [6,7,70,77,78]. These authors have studied many fractals in both specific cases, in families, or in general. We shall consider a Laplacian for a family of fractals, the m-Branch Trees and in one general calculation find the spectrum of Laplacians on the entire family. This work is done via the spectral decimation process by which the spectra of Laplacians on graph approximations are used to calculate the spectrum of a limiting Laplacian on the fractal or on an infinite graph. Our notation is complicated by the fact that we do the spectral decimation calculations for an arbitrary m, effectively doing every fractal in this family at one time. Trees have been a well studied topic in fractal literature, for example Vicsek sets in [77,78] and dendrites in [41].

In [43], Kigami set out a framework by which post-critically finite fractals can be thought of as abstract spaces independent of an embedding in an ambient space. This is accomplished by labeling a point by an "address" determined by the cell structure of the fractal. The space of addresses is isomorphic to the fractal. Because of this point of view it is natural to consider graph approximations to the fractal as truncations of these addresses. Kigami also proved that the graph Laplacian operators on the approximating graphs converge to a Laplacian on the fractal when the fractal has certain characteristics, i.e. is post critically finite.

Strichartz, [74], builds upon Kigami's point of view and considers differential equations on post-critically finite fractals using the types of operators that Kigami constructed. Strichartz included a discussion of the spectral decimation method for calculating the spectrum of these Laplacians from the spectra of the graph Laplacians, though the method goes back to [32].

The m-Branch Trees, $m \geqslant 3$, are post-critically finite fractals whose approximating graphs are defined for $m \geqslant 3$ and are constructed with m-simplices. For the sake of working with concrete matrices we run through the calculations of the spectrum for the 3-branch tree in Section 2.4 first. Then in Section 2.5 the general case is presented, and finally in Section 2.6 we observe the behavior of the spectra of the Laplacians on the m-branch trees as the number of branches increases. But first we describe the trees in Section 2.2 and the spectral decimation method in Section 2.3.

2.2 m-Branch Tree Fractals

The m-branch tree fractal, F_m, is a post-critically finite fractal with m defining contraction mappings. The zero-level graph approximation, $V_{m,0}$, consists of a complete graph of m vertices, when $m = 3$, $V_{3,0}$ is a triangle, when $m = 4$, $V_{4,0}$ is a tetrahedron. The iterated function system that generates the fractal scales, duplicates, and translates the simplex to m simplices sharing a common point at the epicenter of the previous simplex and with each vertex from $V_{m,0}$ as a vertex of one of the new simplices, this is the graph $V_{m,1}$. This process is iterated and the countable set of vertices is completed in the effective resistance metric to form a tree with m branches. With the graphs $V_{m,0}$ and $V_{m,1}$ defined we refer to the appendix of [40] for the detailed construction of the post-critically finite fractal and proofs of its properties.

Below we construct a Laplacian operator, Δ_m, on F_m as a limit of Laplacians, $\Delta_{m,n}$, on $V_{m,n}$ from which we will calculate the spectrum of Δ_m by spectral decimation. All of the calculations that are done in the spectral decimation process do not depend on any particular embedding into an Euclidean space and in fact when we calculate the Hausdorff dimension of these spaces in Section 2.5 we will use the intrinsic effective resistance metric. This metric capitalizes on the analogy between graphs and electrical networks to calculate the effective resistance between two points as if the edges of the graph were resistors and the vertices nodes in an electrical network. This analogy has been used by many authors but a useful reference for the mechanics of these calculations and a more extensive bibliography is [74]. It is a straight forward calculation to show that in the effective resistance metric the contraction mappings forming the trees have contraction factor one half for all m.

There has recently been developed a connection between fractals and certain groups, most specifically cellular autonoma and iterated monodromy groups. Nekra-

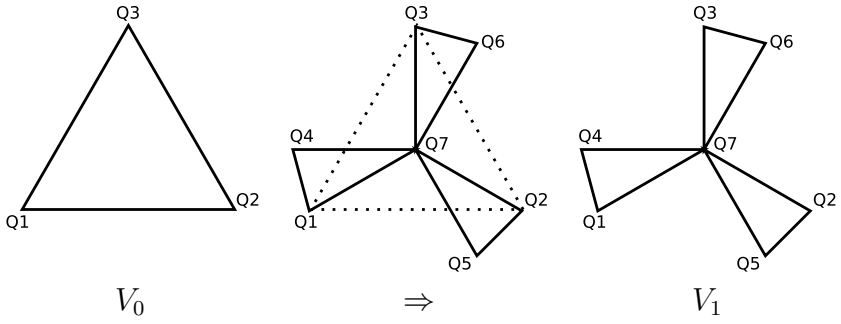

Fig. 2.1: The progression of the three-branch tree from its $V_{3,0}$ to $V_{3,1}$ network

shevych has written a survey [61] exploring self-similar groups such as iterated monodromy groups involving Schreier graphs as pictoral representations of the groups. In [14] and [15] there is consideration of a particular self-similar group, which is a subgroup of the automorphism group of a rooted $p-$tree. This particular self-similar group is sometimes called the Gupta-Fabrykowski group. Bartholdi, Grigorchuk, and Nekrashevych explore limits of the Schreier graphs as fractals combining algebraic and analytic perspectives. The Schreier graphs for the Gupta-Fabrykowski groups are the same as the $V_{m,n}$ graphs for the m-Branch Tree when m is a prime. This is the topic of the next chapter.

Figures 2.1 and 2.2 give a visual guide to what the iterated function system does in the $m = 3$ case. Note that all triangles are equilateral in the intrinsic effective resistance geometry but when embedded in $\mathbb{R}^2$ they would overlap if they were drawn as equilateral in the geometry of $\mathbb{R}^2$. Since the theoretical machinery that we use in this chapter is independent of an embedding into an Euclidean space we won't be using the geometry of any $\mathbb{R}^n$ so the issue of overlap is moot.

The Laplacian operator we use is analogous to the second difference operator on a continuous space because it takes the average value of the function at neighboring points and subtracts that from the value of the function, $\Delta_{m,n} f(x) = f(x) - \sum_{x \sim y} \frac{f(y)}{\deg(x)}$. Where the sum is over neighboring points in the graph and $\deg(x)$ is the number of neighbors that x has. Because the matrix representation of this operator on a graph has ones on the diagonal this is known as a probabilistic Laplacian. We construct a matrix representation for the Laplacian $\Delta_{m,n}$ associated to the graph $V_{m,n}$ as in [6,7,74,77,78]. Let $M_{m,n}$ denote this matrix which is the level-n graph approximation to the Laplacian on F_m. The on-diagonal entries of $M_{m,n}$ are 1 as already noted. The off-diagonal entries are:

- 0 if x_i and x_j are not connected;
- $\frac{-1}{deg(x_i)}$ if x_i and x_j *are* connected.

Kigami proved that the sequence of operators $\rho^n M_n$ converge in an appropriate sense to an operator $\widehat{\Delta}_m$ on F_m in [43,44] where ρ is the "energy renormalization

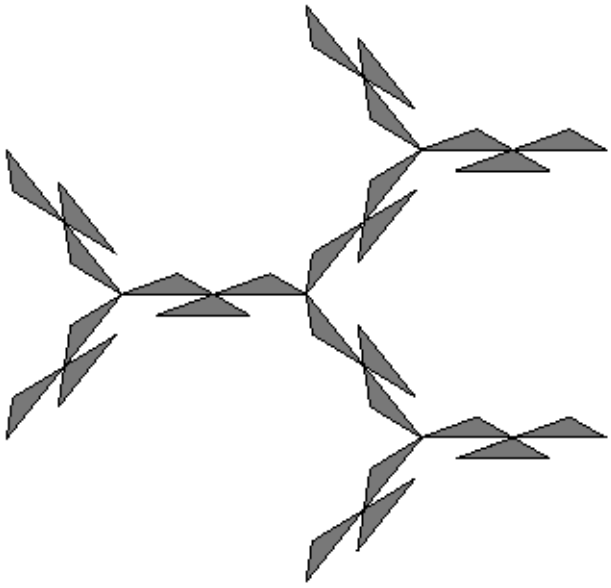

Fig. 2.2: The graph $V_{3,3}$, note that the branches only connect to each other at the center point.

constant." If we view the distance between adjacent vertices always being constant as the level of approximation increases, then we get an infinite graph where $\rho = 1$ instead of a compact fractal where the graphs are scaled at each step so that the limiting fractal is bounded in which case $\rho > 1$. We will calculate the spectrum of the bounded operator $\lim_{n\to\infty} M_{m,n} = \Delta_m$ and will not be concerned with ρ. Since there are $deg(x_i)$ points connected to x_i and the diagonal entry is 1, then we have the property that the row sums of $M_{m,n}$ are always equal to zero which is a very useful aid in the calculations to follow.

2.3 Spectral Decimation

Spectral decimation is a means of extending the eigenvalues for the n-level Laplacian to those of the $n+1$-level Laplacian. Used inductively, this means only the zero- and first-level Laplacians must be explicitly calculated. These will include the so-called forbidden eigenvalues. The process, which dates back to [32,46,70], is presented in terms of the calculations shown in [7] and discussed in more abstract detail in [6,70,74]. We first write the level-one Laplacian as a block matrix. For the time being we drop the m from the notation.

$$M = M_1 = \begin{pmatrix} A & B \\ C & D \end{pmatrix}, \tag{2.3.1}$$

where $A = I_m$ since the boundary points are not neighbors in V_1. The Schur complement of the matrix $M - Iz$ is the matrix-valued function:

$$S(z) = (A - z) - B(D - z)^{-1}C. \tag{2.3.2}$$

Schur complements are discussed in more detail in [6,7], also note that $S(z)$ has a pole when z is an eigenvalue of the matrix D. If $v = (v_0, v_1')^T$ is an eigenvector of M with corresponding eigenvalue z, the eigenvalue equation can be written as

$$\begin{pmatrix} A & B \\ C & D \end{pmatrix} \begin{pmatrix} v_0 \\ v_1' \end{pmatrix} = z \begin{pmatrix} v_0 \\ v_1' \end{pmatrix}. \tag{2.3.3}$$

A function on V_1 is split into two portions, the values on V_0 are collected in v_0, and the values on $V_1 \setminus V_0$ into v_1'. This system of linear equations yields two equations: $v_1' = -(D - z)^{-1}Cv_0$, provided that $z \notin \sigma(D)$, and $(A - z)v_0 + Bv_1' = 0$. The set $\sigma(D)$ are the eigenvalues of the matrix D. It is worth noting that the map $-(D - z)^{-1}C$ takes the eigenvector v_0 on the boundary points and determines the values required at the interior vertices so that $\begin{pmatrix} v_0 \\ v_1' \end{pmatrix}$ is an eigenvector on V_1. This is actually the eigenvector extension mentioned below. When the two equations are combined with the Schur complement they imply that

$$S(z)v_0 = 0. \tag{2.3.4}$$

If v_0 is *also* an eigenvector of M_0 with corresponding eigenvalue z_0, then

$$(M_0 - z_0)v_0 = 0. \tag{2.3.5}$$

By combining (2.3.4) and (2.3.5), and setting $z_0 = R(z)$ for a rational function $R(z)$, we have,

$$S(z) = \phi(z)\,(M_0 - R(z)) \tag{2.3.6}$$

where $\phi(z)$ and $R(z)$ are scalar-valued rational functions whose existence is shown in [6,46,70,74]. It can be observed from the proof of their existence that $\phi(z)$ is dependent on $S_{1,2}$ and $R(z)$ is dependent on both $S_{1,1}$ and $\phi(z)$. The role of $R(z)$ is as an "eigenvalue projector" taking eigenvalues of one level and projecting them down to a lower level's eigenvalues. To calculate these functions we then only need two entries from the matrix $S(z)$, $S_{1,2}$ and $S_{1,1}$. The formulae are:

$$\phi(z) = -(m-1)S_{1,2} \qquad \textit{and} \qquad R(z) = 1 - \frac{S_{1,1}}{\phi(z)}. \tag{2.3.7}$$

These equations are *a priori* rational functions on $\mathbb{C}$ so the locations of possible zeroes and poles require special attention. If they are off the real axis they won't be an issue since Δ_m are bounded symmetric operators so have real spectrum,

only zeros and poles on the real axis are of concern. The location of these possible zeroes and poles are what we call exceptional values. The exceptional values are $E(M_0, M) = \sigma(D) \cup \{z : \phi(z) = 0\}$. These values are exceptional because $(D - z)$ is not invertible when $z \in \sigma(D)$, which causes (2.3.4) to not be defined, and if $\phi(z) = 0$ then either (2.3.4) or (2.3.5) fail to be defined, i.e. the poles of R and ϕ and zeroes of ϕ.

It is the rational functions $R(z)$ and $\phi(z)$ that are the main tools used throughout this paper. Proposition 2.5.4 will produce a general form for the values of $S_{1,1}$ and $S_{1,2}$ to obtain the functions $\phi(z)$ (Corollary 2.5.5) and $R(z)$ (Corollary 2.5.6) in the general m-branch case. The function $R(z)$ projects level-$n+1$ eigenvalues to level-n eigenvalues, so the primary use of $R(z)$ is to take inverse images. We will call the depth-n eigenvalue z the offspring of the depth-$n+1$ eigenvalue $R^{-1}(z)$.

The process of extending eigenvalues from one approximation to the next is summarized in the following proposition from [6]. The extension map, $-(D - z)^{-1}C$, which was mentioned above, will extend an eigenfunction on V_0 by filling in the values needed on $V_1 \setminus V_0$ provided that z is not an exceptional value and is an eigenvalue at the first level. To find those eigenvalues at the next level we will use this proposition. Denote by $\text{mult}_D(z)$ the multiplicity of z as an eigenvalue of D. Similarly, $\text{mult}_n(z)$ is the multiplicity of z as an eigenvalue of M_n. Again the subscript m has been removed to simplify notation, so everything here is for a given value of m.

Remark 2.3.1. Here and throughout, $\dim_n$ is the dimension of the function space on V_n for a given m. Since V_n is a finite collection of points, the dimension of the space of functions on V_n is just the number of points in V_n.

Proposition 2.3.2. [6]

1. If $z \notin E(M_0, M)$, then

$$\text{mult}_n(z) = \text{mult}_{n-1}(R(z)), \tag{2.3.8}$$

   and every corresponding eigenfunction at depth n is an extension of an eigenfunction at depth $n - 1$.

2. If $z \notin \sigma(D)$, $\phi(z) = 0$ and $R(z)$ has a removable singularity at z, then

$$\text{mult}_n(z) = \dim_{n-1}, \tag{2.3.9}$$

   and every corresponding eigenfunction at depth n is localized.

3. If $z \in \sigma(D)$, both $\phi(z)$ and $\phi(z)R(z)$ have poles at z, $R(z)$ has a removable singularity at z, and $\frac{d}{dz}R(z) \neq 0$, then

$$\text{mult}_n(z) = m^{n-1}\text{mult}_D(z) - \dim_{n-1} + \text{mult}_{n-1}(R(z)), \tag{2.3.10}$$

   and every corresponding eigenfunction at depth n vanishes on V_{n-1}.

4. If $z \in \sigma(D)$, but $\phi(z)$ and $\phi(z)R(z)$ do not have poles at z, and $\phi(z) \neq 0$, then
$$\text{mult}_n(z) = m^{n-1}\text{mult}_D(z) + \text{mult}_{n-1}(R(z)). \tag{2.3.11}$$
In this case $m^{n-1}\text{mult}_D(z)$ linearly independent eigenfunctions are localized, and $\text{mult}_{n-1}(R(z))$ more linearly independent eigenfunctions are extensions of corresponding eigenfunction at depth $n-1$.

5. If $z \in \sigma(D)$, but $\phi(z)$ and $\phi(z)R(z)$ do not have poles at z, and $\phi(z) = 0$, then
$$\text{mult}_n(z) = m^{n-1}\text{mult}_D(z) + \text{mult}_{n-1}(R(z)) + \dim_{n-1} \tag{2.3.12}$$
provided $R(z)$ has a removable singularity at z. In this case there are $m^{n-1}\text{mult}_D(z) + \dim_{n-1}$ localized and $\text{mult}_{n-1}(R(z))$ non-localized corresponding eigenfunctions at depth n.

6. If $z \in \sigma(D)$, both $\phi(z)$ and $\phi(z)R(z)$ have poles at z, $R(z)$ has a removable singularity at z, and $\frac{d}{dz}R(z) = 0$, then
$$\text{mult}_n(z) = \text{mult}_{n-1}(R(z)), \tag{2.3.13}$$
provided there are no corresponding eigenfunctions at depth n that vanish on V_{n-1}. In general we have
$$\text{mult}_n(z) = m^{n-1}\text{mult}_D(z) - \dim_{n-1} + 2\text{mult}_{n-1}(R(z)). \tag{2.3.14}$$

7. If $z \notin \sigma(D)$, $\phi(z) = 0$ and $R(z)$ has a pole z, then $\text{mult}_n(z) = 0$ and z is not an eigenvalue.

8. If $z \in \sigma(D)$, but $\phi(z)$ and $\phi(z)R(z)$ do not have poles at z, $\phi(z) = 0$, and $R(z)$ has a pole z, then
$$\text{mult}_n(z) = m^{n-1}\text{mult}_D(z) \tag{2.3.15}$$
and every corresponding eigenfunction at depth n vanishes on V_{n-1}.

The proof of this proposition can be found in [6] and in a large part depends on the Schur Complement formula and the eigenvector equations from earlier in the section. It is also shown how the eigenspace projection matrices are constructed, these matrices are related to the map $-(D-z)^{-1}C$ and project eigenvectors on V_n onto V_{n-1}. This proposition is used constantly as we recursively extend eigenvalues from the V_1 approximation, which are calculated explicitly, to the full fractal F_m. A necessary condition for $\sigma(M_{m,n})$ capturing all of $\sigma(\Delta_m)$ is that the spectral dimension is less than two [70] however it is known that for p.c.f. fractals this is always the case.

2.4 The Three-Branch Tree

We analyze the spectrum of the Laplacian, Δ_3, on the three-branch tree as a special case to demonstrate the calculations involved with spectral decimation as found in [6,7] while the approximating graphs and matrices are still relatively small. For this section assume that $m = 3$ throughout with will drop the m from the notation. Spectral decimation uses the spectra of M_0, M_1, D, and the Schur Complement of $M_1 - Iz$ yielding the spectrum of M_n as the output. We will then take the limit as n grows to infinity to find $\sigma(\Delta_3)$. The process will also be used in the next section as we consider the general case of the m-branch tree.

First we consider V_0, which is a triangle (Figure 2.1). The Laplacian matrix for V_0 is

$$M_0 = \begin{pmatrix} 1 & -\frac{1}{2} & -\frac{1}{2} \\ -\frac{1}{2} & 1 & -\frac{1}{2} \\ -\frac{1}{2} & -\frac{1}{2} & 1 \end{pmatrix}.$$

Since V_0 is a complete graph there are no zeros in this matrix. The eigenvalues of M_0 written with multiplicities are:

$$\sigma(M_0) = \left\{0, \frac{3}{2}, \frac{3}{2}\right\}.$$

Next we consider the Laplacian on V_1, which is a set of three triangles with a common vertex (Figure 2.1). There are seven vertices in V_1, and the depth-one Laplacian matrix is:

$$M_1 = \begin{pmatrix} 1 & 0 & 0 & -\frac{1}{2} & 0 & 0 & -\frac{1}{2} \\ 0 & 1 & 0 & 0 & -\frac{1}{2} & 0 & -\frac{1}{2} \\ 0 & 0 & 1 & 0 & 0 & -\frac{1}{2} & -\frac{1}{2} \\ -\frac{1}{2} & 0 & 0 & 1 & 0 & 0 & -\frac{1}{2} \\ 0 & -\frac{1}{2} & 0 & 0 & 1 & 0 & -\frac{1}{2} \\ 0 & 0 & -\frac{1}{2} & 0 & 0 & 1 & -\frac{1}{2} \\ -\frac{1}{6} & -\frac{1}{6} & -\frac{1}{6} & -\frac{1}{6} & -\frac{1}{6} & -\frac{1}{6} & 1 \end{pmatrix}.$$

Recall from (2.3.1) that A will be the identity matrix I_3.

The Schur Complement is $S(z) = (A - z) - B(D - z)^{-1}C$, as stated earlier. With these small matrices $S(z)$ can easily be computed:

$$S(z) = \begin{pmatrix} -\frac{(2z-3)(6z^2-6z+1)}{6(z-1)(2z-1)} & \frac{2z-3}{12(z-1)(2z-1)} & \frac{2z-3}{12(z-1)(2z-1)} \\ \frac{2z-3}{12(z-1)(2z-1)} & -\frac{(2z-3)(6z^2-6z+1)}{6(z-1)(2z-1)} & \frac{2z-3}{12(z-1)(2z-1)} \\ \frac{2z-3}{12(z-1)(2z-1)} & \frac{2z-3}{12(z-1)(2z-1)} & -\frac{(2z-3)(6z^2-6z+1)}{6(z-1)(2z-1)} \end{pmatrix}.$$

From this, we have

$$\phi(z) = -(m-1)S_{1,2} = \frac{3-2z}{6(-1+z)(-1+2z)}$$

and

$$R(z) = 1 - \frac{S_{1,1}}{\phi(z)} = 6z - 6z^2,$$

as defined in [6,7]. These two functions allow us to use Proposition 2.3.2 to determine the multiplicities of eigenvalues for M_n, without writing the matrix M_n down. These recursive formulae utilize the spectrum of M_1 to recursively list all eigenvalues of M_n.

The eigenfunction extension map that fills in the interior values when eigenvectors are extended is:

$$(D-z)^{-1}C = \begin{pmatrix} \frac{-2+3z}{3(-1+z)(-1+2z)} & \frac{-1}{6(-1+z)(-1+2z)} & \frac{-1}{6(-1+z)(-1+2z)} \\ \frac{-1}{6(-1+z)(-1+2z)} & \frac{-2+3z}{3(-1+z)(-1+2z)} & \frac{-1}{6(-1+z)(-1+2z)} \\ \frac{-1}{6(-1+z)(-1+2z)} & \frac{-1}{6(-1+z)(-1+2z)} & \frac{-2+3z}{3(-1+z)(-1+2z)} \\ \frac{1}{3(-1+2z)} & \frac{1}{3(-1+2z)} & \frac{1}{3(-1+2z)} \end{pmatrix}.$$

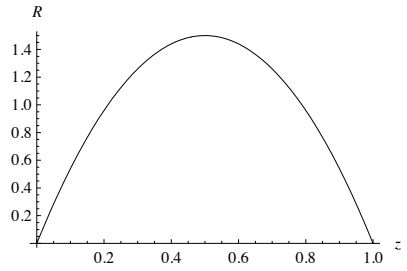

Fig. 2.3: The graph of $R(z)$ for the three-branch tree

Now we list the eigenvalues of M_1, written with multiplicities, to provide a check for the calculations.

$$\sigma(M_1) = \left\{\frac{3}{2}, \frac{3}{2}, \frac{3}{2}, \frac{3}{2}, \frac{1}{2}, \frac{1}{2}, 0\right\}.$$

The corresponding eigenvectors are {-1, -1, -1, 0, 0, 0, 1}, {0, 0, -1, 0, 0, 1, 0}, {0, -1, 0, 0, 1, 0, 0}, {-1, 0, 0, 1, 0, 0, 0}, {-1, 0, 1, -1, 0, 1, 0}, {-1, 1, 0, -1, 1, 0, 0}, and {1, 1, 1, 1, 1, 1, 1} respectively.

To find the exceptional set we need the eigenvalues of D, which are written with multiplicities:

$$\sigma(D) = \left\{\frac{3}{2}, 1, 1, \frac{1}{2}\right\},$$

with corresponding eigenvectors of {-1, 1, -1, 1}, {-1, 0, 1, 0}, {-1, 1, 0, 0}, and {1, 1, 1, 1} respectively.

The equation $\phi(z) = 0$ has only one solution, $\left\{\frac{3}{2}\right\}$, so the exceptional set is:

$$E(M_0, M_1) = \sigma(D) \cup \{z : \phi(z) = 0\} = \left\{\frac{3}{2}, 1, \frac{1}{2}\right\}.$$

The multiplicities of these exceptional values are found by using Proposition 2.3.2. For the value of $z = \frac{3}{2}$, which is in $\sigma(D)$, is not a pole of $\phi(z)$, and $\phi(z) = 0$, use Proposition 2.3.2(5) to find the multiplicities:

$$\begin{aligned} &\mathrm{mult}_0(\tfrac{3}{2}) = 2, \\ &\mathrm{mult}_1(\tfrac{3}{2}) = 4, \\ &\mathrm{mult}_2(\tfrac{3}{2}) = 10. \end{aligned}$$

For the values of $z = \frac{1}{2}$ and $z = 1$, which are poles of $\phi(z)$ and in $\sigma(D)$, we use Proposition 2.3.2(3):

$$\begin{aligned} &\mathrm{mult}_0(\tfrac{1}{2}) = 0, \quad \mathrm{mult}_0(1) = 0, \\ &\mathrm{mult}_1(\tfrac{1}{2}) = 2, \quad \mathrm{mult}_1(1) = 0, \\ &\mathrm{mult}_2(\tfrac{1}{2}) = 4, \quad \mathrm{mult}_2(1) = 0. \end{aligned}$$

For the value of $z = 0$, since $0 \notin E(M_0, M)$, we use Proposition 2.3.2(1) to determine that $\mathrm{mult}_n(0) = 1$.

Using the inverse function $R^{-1}(z)$, we can calculate the ancestors of $z = \frac{1}{2}$ to be $R^{-1}(1/2) = \frac{3\pm\sqrt{6}}{6}$. From Proposition 2.3.2(1), since $\frac{3\pm\sqrt{6}}{6} \notin E(M_0, M_1)$, their multiplicity at depth n will be the multiplicity of $R(\frac{3\pm\sqrt{6}}{6}) = \frac{1}{2}$ at depth $n-1$.

Table 2.1 shows the ancestor-offspring structure of the eigenvalues of the three-branch tree. The symbol * indicates an ancestor of $\frac{3\pm\sqrt{6}}{6}$, calculated by the branches of the inverse function $R^{-1}(z)$ computed at the ancestor value z. By Proposition 2.3.2(1) the ancestor and the offspring have the same multiplicity. The empty columns represent exceptional values. If they are eigenvalues of the appropriate M_n, then their multiplicity is shown in the right hand part of the same row.

Proposition 2.4.1. The dimension of the function space on V_n, $\dim_n$, as was commented in Remark 2.3.1, is the same as the number of points in V_n. For the three-branch tree, this is:

$$\dim_n = 1 + 2 \cdot 3^n.$$

Likewise, $\mathrm{mult}_n(z)$ is given as follows for $n \geqslant 0$ and $1 \leqslant k \leqslant n$:

$$\begin{aligned} &\mathrm{mult}_n(0) = 1, \\ &\mathrm{mult}_n(1) = 0, \\ &\mathrm{mult}_n(\tfrac{3}{2}) = 1 + 3^n, \\ &\mathrm{mult}_n(\tfrac{1}{2}) = 1 + 3^{n-1}, \\ &\mathrm{mult}_n(\tfrac{3\pm\sqrt{6}}{6}) = 1 + 3^{n-2}, \\ &\quad \vdots \\ &\mathrm{mult}_n(R^{-k}(\tfrac{3}{2})) = 1 + 3^{n-k}. \end{aligned}$$

$z\in\sigma(M_0)$	0				$\frac{3}{2}$							
$\text{mult}_0(z)$	***1***				***2***							
$z\in\sigma(M_1)$	0			1	$\frac{1}{2}$				$\frac{3}{2}$			
$\text{mult}_1(z)$	***1***				***2***				***4***			
$z\in\sigma(M_2)$	0		1		$\frac{3\pm\sqrt{6}}{6}$				$\frac{1}{2}$		$\frac{3}{2}$	
$\text{mult}_2(z)$	***1***				***2***		***2***		***4***		***10***	
$z\in\sigma(M_3)$	0	1			$*$	$*$	$*$	$*$	$\frac{3\pm\sqrt{6}}{6}$		$\frac{1}{2}$	$\frac{3}{2}$
$\text{mult}_3(z)$	***1***				***2***	***2***	***2***	***2***	***4***	***4***	***10***	***28***

Table 2.1: Ancestor-offspring structure of the eigenvalues on the three-branch tree.

Proof. For F_3, the number of vertices begins with 3 in V_0 then increases by $3^{n-1}+3^n$ for each subsequent level. Therefore, the partial sum of this sequence yields $\dim_n = 1 + 2\cdot 3^n$. In Proposition 2.5.1, we will prove $\dim_n$ for the general case.

By applying Proposition 2.3.2 to the eigenvalues of M_1, and by using $\dim_n = 1+2\cdot 3^n$, $\phi(z)$, and $R(z)$, the multiplicities of $\sigma(M_n)$ are calculated inductively. ***Qed***

Lemma 2.4.2. The spectrum of Δ_3 is $\bigcup_{i\geq 0}\left\{R^{-i}\left(\frac{3}{2}\right)\right\}\cup\{0\}$. This spectrum is bounded, $\sigma(\Delta_3)\subseteq[0,1)\cup\{\frac{3}{2}\}$, and accumulates to the Julia set of $R(z)$.

Proof. From Figure 2.3 we can see that $R(z)$ is a parabola with zeros $\{0,1\}$ and apex $(\frac{1}{2},\frac{3}{2})$. By applying inverses of $R(z)$, we have $R^{-1}(z)\in[0,1]$ so long as $z\in[0,\frac{3}{2}]$. Since $R^{-1}(0)=\{0,1\}$ and $\text{mult}_n(1)=0$, the only ancestor of 0 will be itself. Since $\bigcup_{i\geq 0}\left\{R^{-i}\left(\frac{3}{2}\right)\right\}\subseteq(0,1)\cup\{\frac{3}{2}\}$, we have

$$\sigma(\Delta_3)=\bigcup_{i\geq 0}\left\{R^{-i}(\tfrac{3}{2})\right\}\cup\{0\}\subseteq[0,1)\cup\{\tfrac{3}{2}\}.$$

The statement about the Julia set is a special case of the discussion in [28] Chapter 14. ***Qed***

2.5 The m-Branch Tree

This section focuses on the use of spectral decimation on the m-branch tree and its Laplacian, Δ_m. We follow the same process as in Section 2.4, however the

inverse of $(D - z)$ is more difficult to compute since it must be done for arbitrary m so we must use a different method for this computation.

Proposition 2.5.1. For F_m, the number of vertices in $V_{m,n}$, which is equal to the dimension of the function space on $V_{m,n}$ (Remark 2.3.1), is

$$\dim_{m,n} = 1 + (m-1)m^n,$$

where m and n are integers with $m \geqslant 3$ and $n \geqslant 0$.

Proof. Beginning with $V_{m,0}$ in F_m, $dim_{m,0} = m$. At each subsequent level, the number of vertices introduced by the defining iterated function system is $(m-2)m^n + m^{n-1}$. Thus,

$$\dim_{m,n} = m + \sum_{i=1}^{n} (m-2)m^i + m^{i-1}.$$

For any level $n \geqslant 0$, the partial sum of the sequence is $\dim_n = 1 + (m-1)m^n$. ***Qed***

Proposition 2.5.2. For the depth-zero Laplacian matrix, $\text{mult}_0(0) = 1$ and $\text{mult}_0(\frac{m}{m-1}) = m - 1$.

Proof. For F_m, we will have an $m \times m$ depth-zero Laplacian matrix of the form

$$M_{m,0} = \begin{pmatrix} 1 & \frac{-1}{m-1} & \frac{-1}{m-1} & \cdots & \frac{-1}{m-1} \\ \frac{-1}{m-1} & 1 & \frac{-1}{m-1} & \cdots & \frac{-1}{m-1} \\ \frac{-1}{m-1} & \frac{-1}{m-1} & 1 & \cdots & \frac{-1}{m-1} \\ \vdots & & & \ddots & \vdots \\ \frac{-1}{m-1} & \frac{-1}{m-1} & \frac{-1}{m-1} & \cdots & 1 \end{pmatrix}.$$

We are looking for the values of z and vectors, v, such that $M_{m,0}v = zv$. Since $M_{m,0}$ has a row-sum of zero, $v = \{1, \ldots, 1\} \in \mathbb{R}^m$ will be an eigenvector of $M_{m,0}$ with corresponding eigenvalue $z = 0$. So this is our first pair.

Consider $v = \{0, \ldots, 0, 1, -1, 0, \ldots, 0\} \in \mathbb{R}^m$, where 1 and -1 occur consecutively and all other elements of v are 0, we get a corresponding eigenvalue $z = \frac{m}{m-1}$. There are $m - 1$ of these vectors, so $\text{mult}_0(\frac{m}{m-1}) = m - 1$.

These vectors are linearly independent by standard methods, so they form a full set of eigenvectors for $M_{m,0}$. ***Qed***

For the m-branch tree, $M_{m,1}$ is a square matrix with $m^2 - m + 1$ rows and columns. Take A to be the $m \times m$ identity matrix, then D is a square matrix with

$(m-1)^2$ rows and columns. Likewise, B will have dimension $m \times (m-1)^2$ and C will have dimension $(m-1)^2 \times m$. Let

$$\delta = \begin{pmatrix} \frac{-1}{m-1} & 0 & \cdots & 0 \\ 0 & \frac{-1}{m-1} & \cdots & 0 \\ \vdots & & \ddots & \vdots \\ 0 & 0 & \cdots & \frac{-1}{m-1} \end{pmatrix}_{m \times m} = \frac{-1}{m-1} I_m.$$

We will then have:

$$M_{m,1} = \left(\begin{array}{c|c} A & B \\ \hline C & D \end{array}\right) = \left(\begin{array}{c|ccc|c} I & \delta & \cdots & \delta & \frac{-1}{m-1} \\ \hline \delta & I & \cdots & \delta & \frac{-1}{m-1} \\ \vdots & & \ddots & & \vdots \\ \delta & \delta & \cdots & I & \frac{-1}{m-1} \\ \hline \frac{-1}{m(m-1)} & \frac{-1}{m(m-1)} & \cdots & \frac{-1}{m(m-1)} & 1 \end{array}\right).$$

In the last row and column the entries are row and column vectors with the indicated values in every entry. The lower right hand entry is a single entry however.

Proposition 2.5.3. For the m-branch tree, $\sigma(D) = \left\{\frac{m}{m-1}, \frac{2}{m-1}, \frac{1}{m-1}\right\}$ with multiplicities $\text{mult}_D(\frac{m}{m-1}) = m^2 - 3m + 1, \text{mult}_D(\frac{2}{m-1}) = m-1$, and $\text{mult}_D(\frac{1}{m-1}) = 1$.

Proof. We can observe that D has a row-sum of $\frac{1}{m-1}$. Therefore,

$$v_1 = \{1, \ldots, 1\}$$

will be an eigenvector of D with corresponding eigenvalue $\lambda_1 = \frac{1}{m-1}$.

We propose the remaining eigenvectors and their eigenvalues. If

$$v_{2a} = \{-1, \ldots, -1, 0, \ldots, 0, 1\},$$

where -1 occurs in the first m entries of the vector, v_{2a} will be an eigenvector of D with eigenvalue $\lambda_2 = \frac{m}{m-1}$. Consider

$$v_{2b} = \{x_1^1, x_2^1, \ldots, x_m^1, x_1^2, \ldots, x_m^{m-2}, 0\},$$

where $\sum_{i=1}^{m-2} x_j^i = 0 \ j = 1, \ldots, m$, note that the sum is across the upper index. If we choose $x_1^1 = -1$, for some $i > 1$, $x_i^1 = 1$, and all other $x_j = 0$, v_{2b} will be an eigenvector of D with eigenvalue $\lambda_2 = \frac{m}{m-1}$. Since the 1 can occur in one of m entries, and the corresponding -1 can occur in one of $m-3$ entries, v_{2b} occurs in $m(m-3) = m^2 - 3m$ linearly independent variations, and consequently λ has a multiplicity of $m^2 - 3m + 1$ (including the vector v_{2a}).

Consider also

$$v_3 = \{c_1, c_2, \ldots, c_m, c_1, \ldots, c_m, \ldots, 0\},$$

where $\sum_{i=1}^{m} c_i = 0$. If we choose $c_1 = -1$, some $c_i = 1$, and all other $c_j = 0$, v_3 will be an eigenvector of D with eigenvalue $\lambda_3 = \frac{2}{m-1}$. Since there are $m-1$ of these vectors, λ has a multiplicity of $m-1$.

It can be checked that v_1, v_{2a}, v_{2b}, and v_3 are linearly independent, so these vectors form a spanning set of eigenvectors. ***Qed***

Proposition 2.5.4. The two entries of the Schur complement used in calculating $R(z)$ and $\phi(z)$ are:

$$S_{1,1} = (1-z) - \frac{m - z(m-1)^2}{m(1-z(m-1))(2-z(m-1))}$$

and

$$S_{1,2} = -\frac{m - z(m-1)}{m(m-1)(1-z(m-1))(2-z(m-1))}$$

for any $m \geqslant 3$.

Proof. To find the Schur Complement, one must invert the increasingly large matrix $D - z$, where D is an $(m-1)^2 \times (m-1)^2$ matrix. This is most conveniently done by forming a spectral resolution of D. Since D has 3 distinct eigenvalues, we can express D as:

$$D = \lambda_1 \cdot P_1 + \lambda_2 \cdot P_2 + \lambda_3 \cdot P_3,$$

where λ_i is an eigenvalue of D and P_i is the projection matrix onto the eigenspace, E_i, corresponding to the eigenvector λ_i. This can be done since the listed eigenvectors are all linearly independent [65]. Once the projectors are written, then,

$$(D-z)^{-1} = \frac{1}{\lambda_1 - z} \cdot P_1 + \frac{1}{\lambda_2 - z} \cdot P_2 + \frac{1}{\lambda_3 - z} \cdot P_3.$$

To find the projection matrices, we must find matrices that have the following properties:

1. map each eigenspace to itself, $P_i(E_i) = E_i$;
2. $P_i^2 = P_i$;
3. $P_i \cdot v = 0$ when $v \in \bigoplus_{j \neq i} Range(P_j)$; and
4. $P_1 + P_2 + P_3 = I$.

First we set P_1 and P_3, both of which are $(m-1)^2 \times (m-1)^2$ matrices:

$$P_1 = \frac{1}{m(m-1)} \begin{pmatrix} 1 & \cdots & 1 & m \\ \vdots & & \vdots & \vdots \\ 1 & \cdots & 1 & m \end{pmatrix}_{(m-1)^2 \times (m-1)^2},$$

$$P_3 = \frac{1}{m(m-2)} \begin{pmatrix} J & \cdots & J & 0 \\ \vdots & & \vdots & \vdots \\ J & \cdots & J & 0 \\ 0 & \cdots & 0 & 0 \end{pmatrix}_{(m-1)^2 \times (m-1)^2}$$

where J is the $m \times m$ matrix

$$J = \begin{pmatrix} m-1 & -1 & \cdots & -1 \\ -1 & m-1 & \cdots & -1 \\ \vdots & & \ddots & \vdots \\ -1 & -1 & \cdots & m-1 \end{pmatrix}_{m \times m}.$$

Then we set $P_2 = I - (P_1 + P_3)$ to ensure the fourth requirement for the projection matrices listed above. While adding P_1 and P_3, we obtain a new $m \times m$ matrix, K. Subtracting $P_1 + P_3$ from I, we have:

$$P_2 = \begin{pmatrix} I-K & -K & \cdots & -K & \frac{-1}{m-1} \\ -K & I-K & \cdots & -K & \frac{-1}{m-1} \\ \vdots & & \ddots & & \vdots \\ -K & -K & \cdots & I-K & \frac{-1}{m-1} \\ \frac{-1}{m(m-1)} & \frac{-1}{m(m-1)} & \cdots & \frac{-1}{m(m-1)} & \frac{m-2}{m-1} \end{pmatrix}_{(m-1)^2 \times (m-1)^2}$$

where

$$K = \frac{1}{m(m-1)(m-2)} \begin{pmatrix} m^2-m-1 & -1 & \cdots & -1 \\ -1 & m^2-m-1 & \cdots & -1 \\ \vdots & & \ddots & \vdots \\ -1 & -1 & \cdots & m^2-m-1 \end{pmatrix}_{m \times m}.$$

It is not difficult to show that these are projecting onto the correct subspaces by checking their action on the eigenvectors.

Now that we have our projection matrices and their corresponding eigenvalues, and since matrix multiplication is distributive, we can write the Schur Complement as: $S(z) = (A - z) - \sum_{i=1}^{3} \frac{1}{\lambda_i - z} B P_i C$. The $1,1$ and $1,2$ entries are the only

ones we need to calculate $\phi(z)$ and $R(z)$. The relevant entries from the summands are:

	P_1	P_2	$P3$
$\frac{1}{\lambda_i - z} BP_iC_{1,1}$	$\frac{1}{m(1-z(m-1))}$	0	$\frac{m-2}{m(2-z(m-1))}$
$\frac{1}{\lambda_i - z} BP_iC_{1,2}$	$\frac{1}{m(1-z(m-1))}$	0	$\frac{-(m-2)}{m(m-1)(2-z(m-1))}$

Since $(B(D-z)^{-1}C)_{1,1} = \sum_{i=1}^{3} \frac{1}{\lambda_i - z}(BP_iC)_{1,1}$ and $(B(D-z)^{-1}C)_{1,2} = \sum_{i=1}^{3} \frac{1}{\lambda_i - z}(BP_iC)_{1,2}$, we have

$$S_{1,1} = (1-z) - \frac{m - z(m-1)^2}{m(1-z(m-1))(2-z(m-1))}$$

and

$$S_{1,2} = -\frac{m - z(m-1)}{m(m-1)(1-z(m-1))(2-z(m-1))}.$$

Qed

Corollary 2.5.5. For any $m \geqslant 3$, the function $\phi(z) = -(m-1)S_{1,2}$ is:

$$\phi(z) = \frac{m - (m-1)z}{m(2-(m-1)z)(1-(m-1)z)}.$$

Corollary 2.5.6. For any $m \geqslant 3$, the function $R(z) = 1 - \frac{S_{1,1}}{\phi(z)}$ is:

$$R(z) = 2mz - m(m-1)z^2.$$

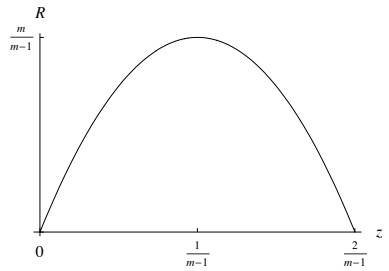

Fig. 2.4: The graph of $R(z)$ for the m-branch tree

Theorem 2.5.7. For any $m \geqslant 3$, $n \geqslant 0$, and $1 \leqslant k \leqslant n$, the depth-$n$ Laplacian matrix will have eigenvalues such that:

$$\begin{aligned}
&\text{mult}_n(0) = 1,\\
&\text{mult}_n(\tfrac{m}{m-1}) = 1 + (m-2)\cdot m^n,\\
&\text{mult}_n(R^{-k}(\tfrac{m}{m-1})) = 1 + (m-2)\cdot m^{n-k}.
\end{aligned}$$

In the limit as $n \to \infty$, $\sigma(\Delta_m) = \bigcup_{i \geq 0} \left\{R^{-i}(\frac{m}{m-1})\right\} \cup \{0\} \subseteq [0, \frac{2}{m-1}) \cup \{\frac{m}{m-1}\}$, where the inverse images of $\frac{m}{m-1}$ accumulate to the Julia set of $R(z)$.

Proof. We first define the exceptional set, $E(M_{m,0}, M_m) = \sigma(D) \cup \{z : \phi(z) = 0\}$, as in Section 2.3. Since $\phi(z) = 0$ only when $z = \frac{m}{m-1}$, we have

$$E(M_{m,0}, M_m) = \left\{ \frac{m}{m-1}, \frac{2}{m-1}, \frac{1}{m-1} \right\}.$$

We can find the multiplicities of these exceptional values using Proposition 2.3.2. For $z = \frac{m}{m-1}$, which is in $\sigma(D)$, is not a pole of $\phi(z)$, and $\phi(z) = 0$, we use Proposition 2.3.2(5) to find its multiplicities:

$$\begin{aligned}
&\text{mult}_0(\tfrac{m}{m-1}) = m - 1,\\
&\text{mult}_1(\tfrac{m}{m-1}) = m^2 - 2m + 1,\\
&\text{mult}_2(\tfrac{m}{m-1}) = m^3 - 2m^2 + 1,\\
&\quad\vdots\\
&\text{mult}_n(\tfrac{m}{m-1}) = 1 + (m-2) \cdot m^n.
\end{aligned}$$

For $z = \frac{2}{m-1}$, which is in $\sigma(D)$, is a pole of $\phi(z)$, and $R'(z) \neq 0$, we use Proposition 2.3.2(3) to find its multiplicities:

$$\begin{aligned}
&\text{mult}_0(\tfrac{2}{m-1}) = 0,\\
&\text{mult}_1(\tfrac{2}{m-1}) = 0,\\
&\text{mult}_2(\tfrac{2}{m-1}) = 0,\\
&\quad\vdots\\
&\text{mult}_n(\tfrac{2}{m-1}) = 0.
\end{aligned}$$

For $z = \frac{1}{m-1}$, which is in $\sigma(D)$, is a pole of $\phi(z)$, and $R'(z) = 0$, we use Proposition 2.3.2(6) to find its multiplicities. Note that $\text{mult}_0(\frac{1}{m-1}) = 0$ so:

$$\begin{aligned}
&\text{mult}_0(\tfrac{1}{m-1}) = 0,\\
&\text{mult}_1(\tfrac{1}{m-1}) = m - 1,\\
&\text{mult}_2(\tfrac{1}{m-1}) = m^2 - 2m + 1,\\
&\quad\vdots\\
&\text{mult}_n(\tfrac{1}{m-1}) = \text{mult}_{n-1}(\tfrac{m}{m-1}) = 1 + (m-2) \cdot m^{n-1}.
\end{aligned}$$

When $z = 0$, since $z \notin E(M_{m,0}, M_m)$, we use Proposition 2.3.2(1) to find its multiplicities. Given $\text{mult}_0(0) = 1$ and $R(0) = 0$,

$$\text{mult}_n(0) = 1.$$

Since $R^{-1}(0) = \{0, \frac{2}{m-1}\}$ and $\text{mult}_n(\frac{2}{m-1}) = 0$, there are no additional ancestors from 0. However, as n increases, one must consider $R^{-k}(\frac{m}{m-1})$ for $1 \leqslant k \leqslant n$. Since $R^{-k}(\frac{m}{m-1}) \notin E(M_0, M)$ when $k > 1$, we use Proposition 2.3.2(1) to determine that

$$\text{mult}_n\left(R^{-k}\left(\tfrac{m}{m-1}\right)\right) = \text{mult}_{n-k}\left(\tfrac{m}{m-1}\right) = 1 + (m-2) \cdot m^{n-k}.$$

As $n \to \infty$, the only ancestor from $z = 0$ is itself. However, since $R(z)$ has zeros at $z = \{0, \frac{2}{m-1}\}$ and maximum at $R(\frac{1}{m-1}) = \frac{m}{m-1}$, $R^{-1}(z) \in [0, \frac{2}{m-1}]$ so long as $z \in [0, \frac{m}{m-1}]$, as seen in Figure 2.4. Since $\bigcup_{i\geq 0} \left\{R^{-i}\left(\frac{m}{m-1}\right)\right\} \subseteq (0, \frac{2}{m-1}) \cup \{\frac{m}{m-1}\}$, we have

$$\sigma(\Delta_m) = \bigcup_{i\geq 0} \left\{R^{-i}(\tfrac{m}{m-1})\right\} \cup \{0\} \subseteq [0, \tfrac{2}{m-1}) \cup \{\tfrac{m}{m-1}\}.$$

As before, the inverse images accumulate to the Julia set of $R(z)$ as discussed in [28]. ***Qed***

Table 2.2 shows the ancestor-offspring structure of the eigenvalues of the m-branch tree for the first few Laplacian matrices. In the table, we denote $R^{-1}(\frac{1}{m-1}) = \psi_i$ and $R^{-1}(\psi_i) = *$ denote either of the inverse images. Blank entries denote exceptional values and if they have non-zero multiplicity they are added at the right hand end of the table.

$z \in \sigma(M_0)$	0				$\frac{m}{m-1}$							
$\text{mult}_0(z)$	***1***				$m-1$							
$z \in \sigma(M_1)$	0		$\frac{2}{m-1}$		$\frac{1}{m-1}$		$\frac{m}{m-1}$					
$\text{mult}_1(z)$	***1***				$m-1$		$(m-1)^2$					
$z \in \sigma(M_2)$	0		$\frac{2}{m-1}$		ψ_1	ψ_2	$\frac{1}{m-1}$		$\frac{m}{m-1}$			
$\text{mult}_2(z)$	***1***				$m-1$	$m-1$	$(m-1)^2$		m^3-2m^2+1			
$z \in \sigma(M_3)$	0	$\frac{2}{m-1}$			$*$	$*$	$*$	$*$	ψ_1	ψ_2	$\frac{1}{m-1}$	$\frac{m}{m-1}$
$\text{mult}_3(z)$	***1***				$m-1$	$m-1$	$m-1$	$m-1$	$(m-1)^2$	$(m-1)^2$	m^3-2m^2+1	m^4-2m^3+1

Table 2.2: Ancestor-offspring structure of the eigenvalues on the m-branch tree

Proposition 2.5.8. The eigenvalues and multiplicities established in Theorem 2.5.7 represent all the eigenvalues of $M_{m,n}$. That is, at any level n, the number of eigenvalues is equal to $\dim_n$.

Proof. We can conclude from Theorem 2.5.7 and Table 2.2 that all eigenvalues for any level n in F_m lie in either $[0, \frac{2}{m-1})$ or $\{\frac{m}{m-1}\}$. The number of eigenvalues in

the depth-n Laplacian of the m-branch tree will be

$$\begin{aligned} & \text{mult}_n(0) + \text{mult}_n(\tfrac{m}{m-1}) + \sum_{i=1}^{n} \text{mult}_n\left(R^{-i}(\tfrac{m}{m-1})\right) \\ = \;& 1 + (1 + (m-2)m^n) + \sum_{i=1}^{n} (2^{i-1}(1 + (m-2)m^{n-i})) \\ = \;& 1 + (1 + (m-2)m^n) + (2^n - 1) + (m^n - 2^n) \\ = \;& 1 + (m-1)m^n = \dim_n. \end{aligned}$$

The equation holds because $R^{-1}(z)$ will yield exactly two values for all $z \in (0, \frac{2}{m-1})$. Since $\dim_n = 1 + (m-1)m^n$, we have found every eigenvalue for the depth-n Laplacian matrix. ***Qed***

It is of some interest as well to have some idea of the geometric properties of the fractal as well as its vibrational behavior. To this end we need more detailed information about the generating iterated function system than the qualitative description given in the original description of the fractals.

Proposition 2.5.9. For any $n \geqslant 0$ and $m \geqslant 3$, the common contraction factor c_m for all functions in the IFS as measured in the effective resistance metric is:

$$c_m = \frac{1}{2}.$$

Proof. The idea behind this is that if two elements of V_0 are separated by resistance one, then those same points viewed in V_1 still should have resistance one between them. Then paring off the uninvolved branches, we see that they are now at opposite ends of a chain of two copies of V_0 each of which would have equal resistance by symmetry so they must have resistance one half. So the distance between neighboring points goes down by a factor of one half each time the level of approximation is increased. For a more formal treatment of these types of calculations see [41,74]. ***Qed***

Once the contraction factor is known it is a direct corollary to calculate the dimension of a given $m-$branch tree. These fractals satisfy the open set condition which is a prerequisite of the formula in this proposition.

Proposition 2.5.10. Since the m-Branch Trees satisfy the open set condition and are generated by m contraction mappings the Housdorff dimension s_m is given by:

$$s_m = \frac{-\log(m)}{\log\left(\frac{1}{2}\right)}.$$

Proof. A formula for the Hausdorff dimension of a fractal generated by an IFS with a finite number of functions is given in [28]. The formula is:

$$\sum_{i=1}^{m} c_i^{s_m} = 1.$$

In our case $c_i = \frac{1}{2}$ so the calculations are simple and yield

$$s_m = \frac{-\log(m)}{\log(\frac{1}{2})}.$$

Qed

This confirms the reasonable intuition that as the number of branches grows so does the dimension of the space.

2.6 Towards the Infinite-Branch Tree

With the full spectrum of the m-branch tree established in Theorem 2.5.7, we can observe what happens as the number of branches goes towards infinity. From Propositions 2.3.2 and 2.5.1 and Theorem 2.5.7, it is clear that the multiplicities of eigenvalues and $\dim_{m,n}$ both go to infinity. However, we can observe what occurs to the density of the spectra as $m \to \infty$.

As a tool to describe what happens to the spectra of the Δ_m as m grows we introduce a measure on the complex plane supported on $\sigma(\Delta_m)$. For a $z \in R^{-k}\left(\frac{m}{m-1}\right)$ then for some n large enough $\text{mult}_n(z)$ is positive. Also 0 is an eigenvalue with $\text{mult}_n(0) = 1$ for all n. Points, z, of these two forms are dense in $\sigma(\Delta_m)$ so we define the measure as follows

$$\kappa_m = \lim_{n\to\infty} \frac{1}{\dim_n} \sum_{z\in\sigma(\Delta_m)} \text{mult}_n(z)\delta_z.$$

Now we consider the weak limit of these measures and the support of the limit measure.

Theorem 2.6.1. As $\lim_{m\to\infty} \sigma(\Delta_m) = \{0, 1\}$ in the Hausdorff metric. Also $\lim_{m\to\infty} \kappa_m = \delta_1$ where the limit is in the weak topology.

Proof. From Theorem 2.5.7, we have that

$$\bigcup_{i\geq 0} \left\{ R^{-i}\left(\frac{m}{m-1}\right)\right\} \subseteq \left[0, \frac{2}{m-1}\right] \cup \left\{\frac{m}{m-1}\right\}$$

and

$$\sigma(\Delta_m) = \bigcup_{i\geq 0} \left\{ R^{-i}\left(\tfrac{m}{m-1}\right)\right\} \cup \{0\} \subseteq \left[0, \tfrac{2}{m-1}\right] \cup \left\{\tfrac{m}{m-1}\right\}.$$

It is easy to see that the only points in the complex plane about any open ball will intersect infinitely many of the $\sigma(\Delta_m)$ are the points $\{0\}$ and $\{1\}$.

Since $\text{mult}_n(\frac{m}{m-1}) = 1 + (m-2)m^n$ and $\dim_n = 1 + (m-1)m^n$, the density $\mathcal{F}$ of $\frac{m}{m-1}$ in the spectrum of M_n as $m \to \infty$ is

$$\mathcal{F}\left(\frac{m}{m-1}\right) = \frac{1+(m-2)m^n}{1+(m-1)m^n} = \frac{m^{n+1}-2m^n+1}{m^{n+1}-m^n+1} \to_{m\to\infty} 1.$$

And similarly the density of all other eigenvalues which are the ones tending towards zero is $O(\frac{1}{m})$ as $m \to \infty$.

Qed

In this paper we have applied the method of spectral decimation to a family of post critically finite fractals of interest to the program begun by Kigami [40,41,43]. The novelty of our work rests in the class of examples addressed and the technical aspects of the calculation especially the use of symmetry arguments to spectrally decompose the matrices D and M_0 in the $m-$branch case.

Chapter 3

Modified Hanoi Towers Groups and Limit Spaces

This chapter first appeared as [59] with co-authors Shotaro Makisumi and Grace Stadnyk who worked as REU students under the author's supervision.

Abstract: We introduce the k-peg Hanoi automorphisms and Hanoi self-similar groups, a generalization of the Hanoi Towers groups, and give conditions for them to be contracting. We analyze the limit spaces of a particular family of contracting Hanoi groups, $H_c^{(k)}$, and show that these are the unique maximal contracting Hanoi groups under a suitable symmetry condition. Finally, we provide partial results on the contractiveness of Hanoi groups with weaker symmetry.

3.1 Introduction

The Hanoi Towers game consists of n graduated disks on k pegs. The object of the game is to move all n disks from one peg to another by moving one disk at a time so that no disk is on top of a smaller disk at any step. For the 3-peg case, the well known optimal solution is given recursively; for this and other known results about the game, see [17].

This chapter examines the Hanoi Towers game from two perspectives. The first is the theory of self-similar groups—groups with a self-similar action by automorphism on regular rooted trees—a branch of geometric group theory developed in the last few decades. Any contracting self-similar group has an associated limit space with fractal-like properties that capture the group's self-similarity. The standard reference on self-similar groups is [61]. The other is analysis on fractals, which has developed analytic structures such as measures, metrics, and Laplacians on post-critically finite (p.c.f. for short) fractals (see [43,74]) as well as the wider classes of finitely ramified and even infinitely ramified fractals, for example in [6,39,2]. A p.c.f. fractal obtained as a limit space can thus be equipped with both algebraic and analytic structures, an interplay that has driven considerable recent developments (see [62] and references therein).

The recursive nature of the Hanoi Towers game allows us to model it using self-similar groups. In [24] and [25], Grigorchuk and Šuník introduced the Hanoi Towers groups—self-similar groups whose generators correspond to the game's

legal moves—and derived some analytic results on their limit spaces. This paper aims to extend this development to modifications of the Hanoi Towers game.

After a brief introduction to self-similar groups in Section 3.2, we define the k-peg Hanoi Towers groups, $H^{(k)}$, in Section 3.3 as the self-similar group generated by automorphisms $\{a_{ij},\, 0 \leq i < j \leq k-1\}$, each of which corresponds to a legal move between pegs i and j under the identification of the rooted tree with the legal states of the k-peg game. Though $H^{(3)}$, corresponding to the standard 3-peg game, is contracting, we find that $H^{(k)}$ for $k > 3$, and in fact any non-trivial group generated by these automorphisms, is not contracting. As these non-contracting groups have no known association to fractal or self-similar limit spaces (although there are some prospects in non-commutative geometry for handling these), we are led to introduce a larger class of automorphisms. In Section 3.4 we define Hanoi automorphisms, and Hanoi groups as self-similar groups with subsets of these automorphisms as generators. The rest of the section develops sufficient conditions for these groups to be contracting. In particular, Theorem 3.4.8 reduces determining whether or not a Hanoi group is contracting to a finite calculation.

Section 3.5 studies a particular family $H_c^{(k)}$ of contracting Hanoi groups and their limit spaces, denoted by $\mathcal{J}^{(k)}$. We show that there exist compact sets $K^{(k)}$ in $\mathbb{R}^{k+1}$ defined by an iterated function system that are homeomorphic to $\mathcal{J}^{(k)}$, and that this self-similar structure is p.c.f. Following the standard theory for p.c.f. self-similar sets [43], we solve the renormalization problem for $\mathcal{J}^{(k)}$ and equip $K^{(k)}$ with a self-similar energy and effective resistance metric. From this, we calculate the Hausdorff and spectral dimensions of $K^{(k)}$.

To reflect the symmetry of pegs in the original Hanoi Towers game, we introduce a symmetry condition on the generating set of the Hanoi groups in Section 3.6. Under strong enough conditions, we show that $H_c^{(k)}$ is the unique maximal contracting k-peg Hanoi group, in the sense that all other contracting Hanoi groups are subgroups of $H_c^{(k)}$. Finally, we present partial results on contracting Hanoi groups that arise when these symmetry conditions are relaxed.

The Appendix deals with Hanoi Networks, HN3 and HN4, introduced in [19,18], which are partially inspired by the Hanoi Towers game and also possess self-similar qualities. Though they are primarily of interest in the physics literature for their small-world properties which give rise to anomalous diffusion, there are some connections to the automata which arise from a different construction.

3.2 Self-Similar Groups

In this section we review the necessary background on self-similar groups. For more details, see [61] and [62].

Let X be a finite set, called the alphabet. Write X^n for the set of words of length n over X, $w = x_n \dots x_1$, where $x_i \in \mathsf{X}$. The length of w is denoted $|w|$. The union of all finite words, including the empty word $\varnothing$, is denoted $\mathsf{X}^* = \bigcup_{n=0}^{\infty} X^n$.

The free monoid, X^*, has a rooted tree structure with root $\varnothing$ and an edge between w and xw for every word w and every $x \in \mathsf{X}$. An automorphism of X^* is a permutation that fixes $\varnothing$ and preserves adjacency; we write $\operatorname{Aut}\mathsf{X}^*$ for the group of these automorphisms under composition. Any automorphism acts as a permutation of the vertices of X^n for each $n \geq 0$.

Let $g \in \operatorname{Aut}\mathsf{X}^*$. Identifying X^1 with X, the restriction of g to X^1 becomes a permutation of X. This is called the root permutation of g and denoted σ_g. For each $x \in \mathsf{X}$, g is an adjacency-preserving bijection from $x\mathsf{X}^*$ to $\sigma_g(x)\mathsf{X}^*$. Identifying both subtrees with X^*, g restricted to $x\mathsf{X}^*$ becomes another automorphism of X^*, called the section of g at x and denoted $g|_x$. That is,

$$g(xw) = \sigma_g(x)g|_x(w) \tag{3.2.1}$$

for all $x \in \mathsf{X}$ and $w \in \mathsf{X}^*$. For $w = x_n \dots x_1 \in \mathsf{X}^n$, $n \geq 2$, we define the section at a word inductively by $g|_w = (g|_{x_n})|_{x_{n-1}\dots x_1}$.

The action of g on X^1 is determined by σ_g. Thereafter, the action on X^{n+1} is given by the action on X^n by (3.2.1). The root permutation and the set of length-one sections uniquely determine an automorphism. Fixing $\mathsf{X} = \{0, \dots, k-1\}$, we use "wreath recursion" notation to express this dependence:

$$g = \sigma_g(g|_0, g|_1, \dots, g|_{k-1}).$$

This allows us to compute compositions. Given g, $h \in \operatorname{Aut}\mathsf{X}^*$,

$$gh(xw) = g(\sigma_h(x)h|_x(w)) = \sigma_g\sigma_h(x)g|_{\sigma_h(x)}h|_x(w)$$

for all $x \in \mathsf{X}$ and $w \in \mathsf{X}^*$. Therefore,

$$gh = \sigma_g\sigma_h(g|_{\sigma_h(1)}h|_1, \dots, g|_{\sigma_h(k-1)}h|_{k-1}).$$

We obtain the following lemma by applying $(gh)|_j = g|_{\sigma_h(j)}h|_j$ repeatedly to $(\cdots((a_m a_{m-1})a_{m-2})\cdots a_2)a_1$.

Lemma 3.2.1. Let $a_i \in \operatorname{Aut}(\mathsf{X}^{-\omega})$ with root permutation σ_i. Then for any $j \in \mathsf{X}$,

$$(a_m \cdots a_2 a_1)|_j = a_m|_{j_m} \cdots a_2|_{j_2} a_1|_{j_1},$$

where $j_1 = j$ and $j_l = \sigma_{l-1}\cdots\sigma_2\sigma_1(j)$ for $l \geq 2$.

Definition 3.2.2. A self-similar group (G, X) is a group G together with a faithful action of G by automorphisms on X^* such that, for every $g \in G$ and every $x \in \mathsf{X}$, there exists some $h \in G$ such that

$$g(xw) = g(x)h(w)$$

for every $w \in \mathsf{X}^*$. We identify G with its image in $\operatorname{Aut}\mathsf{X}^*$. As with tree automorphisms, we define the root permutation of g and its section at x by $\sigma_g = g|_{\mathsf{X}}$ and $g|_x = h$. Where there is no risk of confusion, we write G for the self-similar group.

The following property plays a central role in the theory of self-similar groups.

Definition 3.2.3. A self-similar group (G, X) is contracting if there exists a finite set $\mathcal{N} \subset G$ such that for every $g \in G$ there exists $k \in \mathbb{N}$ such that $g|_v \in \mathcal{N}$ for all $v \in \mathsf{X}^*$ with $|v| \geq k$. The minimal such $\mathcal{N}$ is called the nucleus of G.

Note that if (G, X) is contracting with nucleus $\mathcal{N}$, then in particular $\mathcal{N}$ contains all $g \in G$ such that $g|_i = g$ for some $i \in \mathsf{X}$.

Definition 3.2.4. An automaton A over X is given by

1. the set of states, denoted A and
2. a map $\tau : \mathsf{A} \times \mathsf{X} \to \mathsf{X} \times \mathsf{A}$.

An automaton is finite if its set of states is finite.

An automaton A can be represented by its Moore diagram, a digraph with vertex set A. For each $(g, x) \in \mathsf{A} \times \mathsf{X}$, there is an edge from g to h labeled (x, y), where h and y are defined by $\tau(g, x) = (y, h)$.

The nucleus $\mathcal{N}$ of a contracting group can be viewed as a finite automaton with states $\mathcal{N}$ and $\tau(g, x) = (\sigma_g(x), g|_x)$. In the Moore diagram, the edge from g to $g|_x$ is labeled $(x, g(x))$.

A set $S \subset \operatorname{Aut} \mathsf{X}^*$ of automorphisms is said to be state-closed if every section of $g \in S$ is also in S. Consider a group G generated by a state-closed set S of automorphisms with finite order. Then every element of G can be written as a product of generators, without using inverses. Then by Lemma 3.2.1, G is also state-closed and hence is a self-similar group.

> The 3-peg Hanoi Towers group $(H^{(3)}, \{0, 1, 2\})$ is the self-similar group generated by
>
> $$S = \{1\} \cup \left\{ \begin{array}{l} a_{01} = (0\ 1)(1, 1, a_{01}) \\ a_{02} = (0\ 2)(1, a_{02}, 1) \\ a_{12} = (1\ 2)(a_{12}, 1, 1) \end{array} \right\}.$$
>
> Here and elsewhere, we write 1 for the identity automorphism. Note that $a_{01}^2 = a_{02}^2 = a_{12}^2$ and that, since 1 is included, S is state-closed. We will later show that $H^{(3)}$ is contracting with nucleus S. Figure 1 shows the Moore diagram of S. The three self-loops of the identity automorphism, at the center, are not shown.

Contracting self-similar groups have an associated topological space, called their limit space, that is often also self-similar. It is this space that connects the theory of self-similar groups to analysis on fractals.

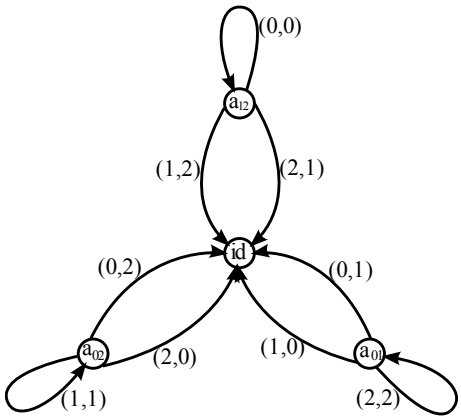

Fig. 3.1: Moore diagram for the nucleus of $H^{(3)}$

Definition 3.2.5. Let (G, X) be a contracting self-similar group. We write $\mathsf{X}^{-\omega}$ for the set of left-infinite sequences $\dots x_2 x_1$, $x_i \in \mathsf{X}$, and give it the product topology, where each copy of X has the discrete topology. Two left-infinite sequences $\dots x_2 x_1$, $\dots y_2 y_1 \in \mathsf{X}^{-\omega}$ are said to be asymptotically equivalent if there exists a sequence $g_k \in G$, taking only finitely many different values, such that $g_k(x_k \dots x_2 x_1) = y_k \dots y_2 y_1$ for all $k \geq 1$. The quotient of $\mathsf{X}^{-\omega}$ by the asymptotic equivalence relation is called the limit space of G and is denoted $\mathcal{J}_G$.

The next proposition allows us to read off asymptotically equivalent sequences from the Moore diagram of the nucleus.

Proposition 3.2.6. (part of Theorem 3.6.3 in [61]) Two sequences $\dots x_2 x_1$, and $\dots y_2 y_1$ are asymptotically equivalent if and only if there exists a left-infinite path $\dots e_2 e_1$ in the Moore diagram of the nucleus such that the edge e_i is labeled by (x_i, y_i).

For example, from Figure 3.1, we see that pairs of asymptotically equivalent sequences for $H^{(3)}$ have the form $(\dots llli, \dots llli)$, where $i, j, l \in \{0, 1, 2\}$ are all distinct. We can also associate a sequence of finite graphs to any self-similar group with a fixed generated set.

Definition 3.2.7. Let (G, X) be a self-similar group generated by S. The *nth* level Schreier graph of G with respect to S, denoted Γ_n, is the graph with vertices identified with X^n and whose vertices w, v are connected if $s(w) = v$ for some automorphism $s \in S \cup S^{-1}$.

When G is contracting, it is known that $\{\Gamma_n\}$ limits to $\mathcal{J}_G$ in an appropriate sense (see Section 3.6.3 in [61]).

3.3 Hanoi Towers Groups

The Hanoi Towers groups, $\{H^{(k)} \mid k \geq 3\}$, are self-similar groups introduced in [24] to model the k-peg Hanoi Towers game. Fix the alphabet $\mathsf{X}_k = \{0, 1, \ldots, k-1\}$, and identify it with the k pegs. Consider a game with n-disks labeled 1 through n from largest to smallest. The word $x_n x_{n-1} \ldots x_1$ uniquely determines a legal n-disk configuration where disk i is on peg x_i. For each $n \geq 1$, X_k^n is identified with the legal states of the n-disk game.

Recall $a_{01} = (0\ 1)(1, 1, a_{01})$ from $(H^{(3)}, \mathsf{X}_3)$ in Example 3.2. Then

$$a_{01}(x_n x_{n-1} \ldots x_1) = a_{01}(x_n) a_{01}|_{x_n}(x_{n-1} \ldots x_1).$$

If $x_n = 0$ or 1, a_{01} replaces it with the other letter, and the remaining word is unchanged; if $x_n = 2$, then x_n remains unchanged, and a_{01} acts on $x_{n-1} \ldots x_1$. Thus a_{01} looks for the leftmost occurrence of either 0 or 1 and replaces it according to its root permutation. In the context of the game, a_{01} ignores all disks on peg 2 and moves the smallest disk on either peg 0 or peg 1 to the other. This is the legal move between pegs 0 and 1.

In general, for $k \geq 3$, we define a_{ij}, $0 \leq i < j < k$, as the automorphism of X_k^* with root permutation $(i\ j)$ and

$$a_{ij}|_l = \begin{cases} 1 & \text{if } l = i, j \\ a_{ij} & \text{otherwise.} \end{cases}$$

As with a_{01}, a_{ij} corresponds to the legal move between pegs i and j. This motivates the following definition from [24].

Definition 3.3.1. The k-peg Hanoi Towers Group $(H^{(k)}, \mathsf{X}_k)$, $k \geq 3$, is the self-similar group generated by $\{a_{ij} \mid 0 \leq i < j < k\}$.

Definition 3.3.2. Given a group G with a fixed generating set, S, a representation of $g \in G$ is any expression $g = s_n \ldots s_2 s_1$, where $s_i \in S \cup S^{-1}$. Then the length of the representation is n. minimal representation is a representation of shortest length. The length of g, denoted $l(g)$, is 0 if g is the identity element, and otherwise is the length of a minimal representation.

Theorem 3.3.3 (Theorem 2.1 in [24])**.** The 3-peg Hanoi Towers group, $(H^{(3)}, \mathsf{X}_3)$, is contracting.

Proof. Let $\mathcal{N} = \{1, a_{01}, a_{02}, a_{12}\} \subset H^{(3)}$. We induct on $l(g)$ to show that $l(g|_i) < l(g)$ for any $g \in H^{(3)}$ with $l(g) \geq 2$ and any $i \in \mathsf{X}_3$.

First consider the base case $l(g) = 2$. Since each a_{ij} has order 2, it suffices to consider $a_{01}a_{12} = (1\ 2\ 0)(a_{12}, a_{01}, 1)$, all of whose sections have length less than

2. Now consider $g \in H^{(3)}$ with $l(g) = n+1$, $n \geq 2$. Without loss of generality, $g = g'a_{01}$ for some $g' \in G$ with $l(g') = n$. Then

$$g = g'a_{01} = \sigma_{g'}(0\ 1)(g'|_1, g'|_0, g'|_2 a_{01}).$$

Assuming the claim for n, we have $l(g'|_1) < n$ and $l(g'|_0) < n$ and $l(g'|_2 a_{01}) < n+1$, which proves the $n+1$ case.

Since $\mathcal{N}$ is state-closed, this shows that for any $g \in G$ with $l(g) = n$, we have $g|_v \in \mathcal{N}$ for all $v \in \mathsf{X}^*$ with $|v| \geq n-1$. Thus $H^{(3)}$ is contracting. ***Qed***

It happens that $H^{(k)}$ is not contracting for any $k > 3$. In fact, we can make a stronger statement.

Proposition 3.3.4. Any self-similar group (G, X_k), $k > 3$, that contains the automorphisms a_{ij} and a_{jl} for i, j, and l all distinct is not contracting.

We first give a lemma that provides a sufficient condition for a group to not be contracting.

Lemma 3.3.5. Let (G, X) be a self-similar group. Suppose some $g \in G$ satisfies the following conditions:

1. σ_g is nontrivial with order $n > 1$.
2. There exists $i \in \mathsf{X}$ fixed by σ_g such that $g|_i = g$.
3. There exists $j \in \mathsf{X}$ such that $g^n|_j = g^m$ for some integer m, $0 < |m| < n$.

Then G is not contracting.

Proof. Note that if $g \in G$ satisfies these conditions, then so does g^{-1} with the same data. Suppose G is contracting with nucleus $\mathcal{N}$ and that these conditions hold for some $g \in G$. The second condition implies that $g^l|_i = g^l$, so $g^l \in \mathcal{N}$ for all positive integers l. Since $\mathcal{N}$ is finite, we can take l to be the smallest positive integer for which $g^l = 1$. Then $l = nl'$ for some integer l', since otherwise g^l has a nontrivial root permutation. But by the third condition, $g^{nl'}|_j = g^{ml'} = 1$, contrary to the minimality of l. ***Qed***

Proof of Proposition 3.3.4. Without loss of generality, we may assume that the two elements are $a = a_{01}$ and $b = a_{12}$. That is,

$$a = (0\ 1)(1, 1, a, a, \ldots, a) \qquad b = (1\ 2)(b, 1, 1, b, \ldots, b).$$

Then $ab = (0\ 1\ 2)(b, a, 1, ab, \ldots, ab)$ and $(ab)^3|_0 = ab$, $(ab)^3|_3 = (ab)^3$, so Lemma 3.3.5 applies with $g = ab$, $i = 3$, and $j = 0$. ***Qed***

This means that any contracting self-similar group (G, X_k), $k > 3$, with generators a_{ij} represents an uninteresting game, such as a 4-peg game with two legal moves: between pegs 0 and 1 and between pegs 2 and 3. In order to obtain modifications of the Hanoi Towers groups that are contracting, we are led to consider a larger class of possible generators.

3.4 Hanoi Automorphisms and Groups

In this section a class of automorphisms is defined that generalize the generators a_{ij} that were used in the previous section.

Definition 3.4.1. An automorphism $a \in \operatorname{Aut} \mathsf{X}_k^{-\omega}$ is called a k-peg Hanoi automorphism if there are disjoint subsets of X_k, P_a and Q_a, such that

1. $P_a \cup Q_a = \mathsf{X}_k$;
2. for each $i \in P_a$, $a|_i = 1$;
3. for each $j \in Q_a$, $a|_j = a$;
4. σ_a fixes each element of Q_a.

For $a \neq 1$, P_a and Q_a, if they exist, are uniquely determined; we call them the sets of active and inactive pegs of a, respectively. The set of inactive pegs of the identity automorphism is defined to be X_k.

Write $S_{k,q}$ for the set of automorphisms of X_k that have q inactive pegs, and $S_k = \bigcup_q S_{k,q}$. The root permutation of an automorphism, a, is naturally regarded as a permutation of both X_k and of P_a.

In terms of the game, $a \in S_{k,q}$ corresponds to ignoring some set Q_a of q pegs and moving the smallest disk among the remaining pegs, P_a, according to σ_a. For example, the 5-peg Hanoi automorphism $a = (0\ 1\ 2)(1, 1, 1, a, a) \in S_{5,2} \subset S_5$ ignores pegs 3 and 4 and applies (0 1 2) to the smallest disk among pegs 0, 1, and 2. A k-peg Hanoi automorphism a is thus determined by Q_a and $\sigma_a \in \operatorname{Sym}(\mathsf{X}_k \setminus Q_a)$. Note that $b = (0\ 1)(1, 1, 1, b, b) \in S_{5,2} \subset S_5$ also has two inactive pegs 3 and 4, even though peg 2 is also fixed by (0 1). If the smallest disk among pegs 0, 1, and 2 is on peg 2, then b does nothing.

Definition 3.4.2. A k-peg Hanoi group (G, X_k) is a group together with a fixed generating set $S \subset S_k$ with $1 \in S$. The corresponding Hanoi game is the k-peg game whose legal moves correspond to the non-identity generators.

Since every section of an automorphism $a \in S_k$ is either 1 or a itself, any such $S \subset S_k$ is state-closed. Moreover, the order of a Hanoi automorphism is the order of its root permutation; in particular this order is finite. Hence every Hanoi group is a self-similar group.

For example, $H^{(k)}$ is the Hanoi group generated by $S_{k,k-2}$. The remainder of this section studies when Hanoi groups are contracting or non-contracting.

Lemma 3.4.3. Let G be a Hanoi group. Consider $g \in G$ with representation $g = s_n \cdots s_2 s_1$. Since the inverse of a Hanoi automorphism is another Hanoi automorphism (with the same inactive pegs and with the inverse root permutation), we can define Q_i to be the set of inactive pegs of s_i. Define the essential set of this representation to be $Q = \bigcap_{i=1}^n Q_i$. If $g \neq 1$, then

1. $g|_j = g$ when $j \in Q$ and
2. $l(g|_j) < n$ when $j \notin Q$. In particular, $l(g|_j) < l(g)$ if $g = s_n \cdots s_2 s_1$ is a minimal representation.

Proof. Write σ_i for the root permutation of s_i.

1. By Lemma 3.2.1 for a given $j \in Q$ we have $g|_j = s_n|_j s_2|_j \cdots s_n|_j = g$.
2. Induct on n. Clearly $n = 1$ holds since $j \notin Q_1$ implies $s_1|_j = 1$. Assuming the claim for $n-1$, consider $g = s_n \cdots s_2 s_1$, $n \geq 2$, and $j \notin Q$. If $j \notin Q_1$, then
$$g|_j = (s_n \cdots s_2)|_{\sigma_1(j)} s_1|_j = (s_n \cdots s_2)|_{\sigma_1(j)}.$$
By Lemma 3.2.1, this is a product of sections of the s_i, so $l(g|_j) < n$. Now suppose $j \in Q_1$, so $g|_j = (s_n \cdots s_2)|_j s_1$. If $s_n \cdots s_2 = 1$, then $l(g|_j) = 1$. Otherwise, since $j \notin Q_2 \cap \cdots \cap Q_n$, we have $l((s_n \ldots s_2)|_j) \leq n-2$ by the $n-1$ case, and so again $l(g|_j) < n$. ***Qed***

Proposition 3.4.4. The following conditions are equivalent for an element g of a Hanoi group (G, X_k):

1. $g|_j = g$ for some $j \in \mathsf{X}_k$,
2. The essential set Q is nonempty for some representation of g,
3. The essential set Q is nonempty for all minimal representations of g.

The set of all g satisfying these conditions is called the prenucleus of G, and is state-closed.

Proof. The three conditions clearly hold for the identity automorphism, so assume $g \neq 1$. Then $3 \Rightarrow 2$ is trivial, $2 \Rightarrow 1$ is part 1 of Lemma 3.4.3, and the contrapositive of $1 \Rightarrow 3$ follows from part 2 of the same lemma.

It remains to show that the prenucleus is state-closed. Suppose $g = s_m \cdots s_2 s_1$ satisfies the three conditions, and $j \in \mathsf{X}_k$. Taking the section of g at j gives
$$g|_j = s_m|_{j_m} \cdots s_2|_{j_2} s_1|_{j_1}$$
with $j_1 = j$ (see Lemma 3.2.1 for the notation). The sections of the generators are equal to either the identity automorphism or themselves and so the essential set of the representation of $g|_j$ contains the essential set of the representation of g and is thus non-empty. Hence $g|_j$ is in the prenucleus for any $j \in \mathsf{X}_k$ and g in the prenucleus. ***Qed***

Theorem 3.4.5. A Hanoi group G is contracting if and only if its prenucleus, $\mathcal{N}$, is finite. In this case, $\mathcal{N}$ is the nucleus of G.

Proof. If G is contracting, its nucleus contains $\mathcal{N}$ by characterization 1 in Proposition 3.4.4. So if $\mathcal{N}$ is infinite, G cannot be contracting.

Suppose $\mathcal{N}$ is finite, and consider $g \in G$ of length n. We show that any length-n section $g|_{x_n x_{n-1} \ldots x_1}$ is in $\mathcal{N}$. Assume otherwise, then since $\mathcal{N}$ is state-closed, none of the sections $g|_{x_n}$, $g|_{x_n x_{n-1}}$, $\ldots$, $g|_{x_n x_{n-1} \ldots x_1}$ can be in $\mathcal{N}$. By characterization 3 in Proposition 3.4.4, each of these has a minimal representation with empty essential set. Thus by part 2 of Lemma 3.4.3, the length decreases from one section to the next, and so $l(g|_{x_n x_{n-1} \ldots x_1}) \leq 0$, a contradiction since $1 \in \mathcal{N}$.

Thus $\mathcal{N}$ meets the condition for the finite set in the definition of the contraction property. We already noted that the nucleus contains $\mathcal{N}$. Since the nucleus is the smallest such set, it must equal $\mathcal{N}$. ***Qed***

Definition 3.4.6. Let G be a Hanoi group with prenucleus $\mathcal{N}$. By the second characterization in Proposition 3.4.4, every $g \in \mathcal{N}$ has a representation with a nonempty essential set. Define $d(g)$ as the least number of distinct generators among all such representations of g.

Definition 3.4.7. Let (G, X_k) be a k-peg Hanoi group generated by S. For a subset $T \subset S$ with fixed indexing $T = \{s_i\}_{i=1}^M$, write Q_i for the set of inactive pegs of s_i, and σ_i for the root permutation of s_i. The essential set of T is defined to be $Q = \bigcap_{i=1}^M Q_i$.

The subgroup of $\mathrm{Sym}(\mathsf{X}_k)$ generated by $\{\sigma_i\}_{i=1}^M$ acts by permutation on X_k. Write $\mathrm{Fix}(T)$ for the set of elements of X_k that are fixed by every σ_i, and $\mathrm{Orb}_T(j)$ for the orbit of $j \in \mathsf{X}_k$ under this action.

Note that the essential set of a representation (see Lemma 3.4.3) coincides with the essential set of the set of generators it uses.

Theorem 3.4.8. Let (G, X_k) be a k-peg Hanoi group generated by S. Then G is contracting if and only if the following condition holds:

($*$) For any $T = \{s_i\}_{i=1}^M \subset S$ with nonempty essential set and any $j \notin \mathrm{Fix}(T)$, there exists some i such that $\mathrm{Orb}_T(j) \cap Q_i = \emptyset$.

We will use the next lemma in the proof of the theorem.

Lemma 3.4.9. Assume a Hanoi group G satisfies condition ($*$). Suppose that $g \in G$ has a representation $g = a_m \ldots a_1$, with a nonempty essential set Q, using M distinct generators, $T = \{s_i\}_{i=1}^M$. Then for any $j \in \mathsf{X}_k$, either $g|_j = g$ or $d(g|_j) < M$.

Proof. If $j \in \mathrm{Fix}(T)$, then $g|_j = a_m|_j \cdots a_2|_j a_1|_j$ by Lemma 3.2.1. If $s_i|_j = 1$ for any i then this representation does not use s_i, so $d(g|_j) < N$. Otherwise, $s_i|_j = s_i$ for every i and $g|_j = g$.

Now suppose $j \notin \mathrm{Fix}(T)$. By Lemma 3.2.1, $g|_j = a_m|_{j_m} \cdots a_2|_{j_2} a_1|_{j_1}$, where $j_l \in \mathrm{Orb}_T(j)$ for all l, $m \geq l \geq 1$. Using $(*)$ to choose i so that $\mathrm{Orb}_T(j) \cap Q_i = \emptyset$, we have $j_l \notin Q_i$ for all l, so this representation does not use s_i. Again the essential set is nonempty, so $d(g|_j) < M$. ***Qed***

Proof of Theorem 3.4.8. First suppose condition $(*)$ holds. Let $\mathcal{N}$ be the prenucleus of G, and $\mathcal{N}_M = \{g \in \mathcal{N} \mid d(g) \leq M\}$. We induct on M to show that every $\mathcal{N}_M$ is finite. Clearly, $\mathcal{N}_1$ is finite. For $g \in \mathcal{N}_M$, $M \geq 2$, by Lemma 3.4.9, every section of g either is g or is in $\mathcal{N}_{M-1}$. Because wreath recursion defines g recursively, g depends only on σ_g and its sections that are not g. If $\mathcal{N}_{M-1}$ is finite, then there are only finitely many such distinguishing choices, and so $\mathcal{N}_M$ is also finite. Hence $\mathcal{N} = \mathcal{N}_{|S|}$ is finite, and G is contracting by Theorem 3.4.5.

Now suppose $(*)$ does not hold. That is, for some subset $T = \{s_i\}_{i=1}^N$ of S with nonempty essential set Q and some $j \notin \mathrm{Fix}(T)$, we have $\mathrm{Orb}_T(j) \cap Q_i \neq \emptyset$ for every i, $1 \leq i \leq M$. It suffices to show that $H = \langle T \rangle \leq G$ is infinite; since the prenucleus of G contains H by characterization 1 in Proposition 3.4.4, this would imply by Theorem 3.4.5 that G is not contracting.

We follow the idea in the proof of infinite cardinality of the Grigorchuk group (original proof in Russian in [23]; see Theorem 1.6.1 in [61] for an exposition in English). With $j \in \mathsf{X}_k$ chosen as above, let $H_j \leq H$ be the subgroup of automorphisms whose root permutation fixes j. Then $\phi : H_j \to H$ defined by $\phi(g) = g|_j$ is a homomorphism. Since $j \notin \mathrm{Fix}(T)$, H_j is a proper subgroup of H. For each generator s_i of H, we construct below some $h_i \in H_j$ such that $\phi(h_i) = h_i|_j = s_i$, which shows that ϕ is a surjection. Then H must be infinite since a proper subgroup $H_j < H$ maps onto H.

Fix i, $1 \leq i \leq M$. By the assumption, $\mathrm{Orb}_T(j) \cap Q_i \neq \emptyset$, so there exists some $s_{n_L} \ldots s_{n_2} s_{n_1} \in H$ with root permutation satisfying $\sigma_{n_L} \ldots \sigma_{n_2} \sigma_{n_1}(j) \in Q_i$. Let $j_1 = j$ and let $j_{l+1} = \sigma_{n_l}(j_l)$ for $1 \leq l \leq L$. By removing any σ_{n_l} with $j_{l+1} = j_l$, we may assume that σ_{n_l} does not fix j_l and j_{l+1}. This implies $s_{n_l}|_{j_l} = s_{n_l|_{j_{l+1}}} = 1$ for all l, $L \geq l \geq 1$.

Take

$$\begin{aligned} h_i &= (s_{n_L} \cdots s_{n_2} s_{n_1})^{-1} s_i (s_{n_L} \cdots s_{n_2} s_{n_1}) \\ &= (s_{n_1}^{-1} s_{n_2}^{-1} \cdots s_{n_L}^{-1}) s_i (s_{n_L} \cdots s_{n_2} s_{n_1}) \end{aligned}$$

with root permutation $(\sigma_{n_1}^{-1} \sigma_{n_2}^{-1} \cdots \sigma_{n_L}^{-1}) \sigma_i (\sigma_{n_L} \cdots \sigma_{n_2} \sigma_{n_1})$. Since σ_i fixes $\sigma_{n_L} \cdots \sigma_{n_2} \sigma_{n_1}(j) = j_{L+1} \in Q_i$,

$$\begin{aligned} \sigma_{n_l} \cdots \sigma_{n_2} \sigma_{n_1}(j) &= j_{l+1} \text{ for } L \geq l \geq 1 \\ \sigma_i \sigma_{n_L} \cdots \sigma_{n_2} \sigma_{n_1}(j) &= j_{L+1} \\ \sigma_l \sigma_{n_{l+1}} \cdots \sigma_{n_L} \sigma_i \sigma_{n_L} \cdots \sigma_{n_2} \sigma_{n_1}(j) &= j_l \text{ for } 2 \leq l \leq L \\ \sigma_{n_1} \sigma_{n_2} \cdots \sigma_{n_L} \sigma_i \sigma_{n_L} \cdots \sigma_{n_2} \sigma_{n_1}(j) &= j_{l-1}. \end{aligned}$$

The last equation shows $h_i \in H_j$. Using the remaining equations in Lemma 3.2.1,

$$h_i|_j = \left(s_{n_1}^{-1}|_{j_2} s_{n_2}^{-1}|_{j_3} \cdots s_{n_l}^{-1}|_{j_{l+1}}\right) s_i|_{j_{l+1}} \left(s_{n_l}|_{j_l} \cdots s_{n_2}|_{j_2} s_{n_1}|_{j_1}\right) = s_i,$$

as we wanted. ***Qed***

Given $S \subset S_k$, checking $(*)$ is a finite computation. Moreover, since $T_1 \subset T_2 \subset S$ implies $\mathrm{Fix}(T_2) \subset \mathrm{Fix}(T_1)$ and $\mathrm{Orb}_{T_1}(j) \subset \mathrm{Orb}_{T_2}(j)$, it suffices to check the maximal sets among subsets $T \subset S$ with nonempty essential set.

3.5 Contracting Hanoi Groups and Their Limit Spaces

In view of Theorems 3.4.5 and 3.4.8, $H^{(k)}$ is noncontracting for $k \geq 4$ because two generators had distinct but overlapping sets of inactive pegs (common inactive peg 3 in the proof of Proposition 3.3.4). This is avoided if only one peg is inactive, which leads us to the following definition.

Definition 3.5.1. $H_c^{(k)}$ is the k-peg Hanoi group generated by $S_{k,1}$.

Corollary 3.5.2. $H_c^{(k)}$ is contracting for every $k \geq 3$.

Proof. Since the prenucleus of $H_c^{(k)}$ is $S_{k,1}$, the result follows from Theorem 3.4.5. ***Qed***

Alternatively, this follows since $H_c^{(k)}$ is contained in the group of bounded automorphisms of X_k^* (see [20] and Theorem 3.9.12 in [61]). In Section 3.6, we will use Theorem 3.4.8 in a case where this result is not applicable.

For $k = 3$, $S_{3,1} = \{1, a_{01}, a_{12}, a_{02}\}$, and $H^{(3)} = H_c^{(3)}$. We can thus view $H_c^{(k)}$ as higher-peg analogues that preserve contraction. In the Hanoi game corresponding to $H_c^{(k)}$, the nth smallest disk can be moved only when the $n-1$ smallest disks are on the same peg. As a result, for any number of pegs, the optimal move count h_n for moving n disks from one peg to another satisfies the same recurrence $h_n = 2h_{n-1} + 1$ as for three pegs (see [17]). Additional pegs, while providing more solution paths, do not make the game any shorter.

Because these groups are contracting we have a well-defined limit space to analyze as was done in [25] for $H^{(3)}$. By construction, $S_{k,1}$ is the nucleus of $H_c^{(k)}$, so by Proposition 3.2.6 asymptotically equivalent pairs of left-infinite sequences have the form $(\ldots llliv, \ldots llljv)$, where $i, j, l \in \mathsf{X}_k$ are all distinct and $v \in \mathsf{X}_k^*$. For simplicity's sake abbreviate $\mathcal{J}_{H_c^{(k)}}$ as $\mathcal{J}^{(k)}$ for the limit space of $H_c^{(k)}$. We will show for each $k \geq 3$ that $\mathcal{J}^{(k)}$ can be obtained as a self-similar set $K^{(k)} \subset \mathbb{R}^{k-1}$. We first, however, need some basic definitions and results about self-similar sets.

Definition 3.5.3. (Definitions 1.2.1 and 1.3.1 in [43]) For a finite set $S = \{s_i\}_{i=1}^N$, the shift space $\Sigma(S) = S^{-\omega}$ is the set of all left-infinite sequences of elements of S, with the product topology where S has the discrete topology. For each $s_i \in S$, define $s_i : \Sigma(S) \to \Sigma(S)$ by $s_i(\ldots x_3x_2x_1) = \ldots x_3x_2x_1s_i$.

Let K be a compact metric space. For each $s_i \in S$, let F_i be a continuous injection from K to itself. Then $(K, S, \{F_i\}_{s_i \in S})$ is called a self-similar structure if there exists a continuous surjection $\pi : \Sigma(S) \to K$ such that $\pi \circ s_i = F_i \circ \pi$ for any $s_i \in S$. We call K a self-similar set.

Theorem 3.5.4. (Theorems 1.1.4 and 1.2.3 in [43]) Let (X, d) be a complete metric space and $S = \{s_1, s_2, \ldots, s_N\}$. For each $s_i \in S$, let $F_i : X \to X$ be a contraction. For any $A \subset X$, define $F(A) = \bigcup_{i=1}^N F_i(A)$. Then there exists a unique nonempty compact set K satisfying $F(K) = K$.

For $w = x_m \ldots x_2x_1$, $x_i \in S$, set $F_w = F_{x_m} \circ \cdots \circ F_{x_2} \circ F_{x_1}$ and $K_w = F_w(K)$. Each K_w, $|w| = m$, is called an m-cell. Then for any $w = \ldots x_2x_1 \in \Sigma(S)$, $\bigcap_{m \geq 1} K_{x_m \ldots x_2x_1}$ contains only one point. The map $\pi : \Sigma(S) \to K$ defined by taking $\pi(w)$ as this unique point is a continuous surjection. Moreover, $\pi \circ s_i = F_i \circ \pi$ for all $s_i \in S$.

Fix $k \geq 3$. Let $\{p_i \mid i \in \mathsf{X}_k\}$ be the vertices of a regular k-simplex in $\mathbb{R}^{k-1}$. For each i, the points $\{p_j \mid j \neq i\}$ form the vertices of a regular $(k-1)$-simplex; let q_i be its centroid. Define F_i, $i \in \mathsf{X}_k$, as the unique affine map satisfying

$$F_i(p_j) = \begin{cases} p_j & \text{if } i = j \\ q_j & \text{otherwise.} \end{cases}$$

Since each F_i is a contraction with respect to the Euclidean metric, by Theorem 3.5.4 there is a unique nonempty compact set $K^{(k)}$ with $F(K^{(k)}) = K^{(k)}$, and $(K^{(k)}, \mathsf{X}_k, \{F_i\}_{i \in \mathsf{X}_k})$ is a self-similar structure.

Before proving that $K^{(k)}$ is homeomorphic to $\mathcal{J}^{(k)}$, we need an observation.

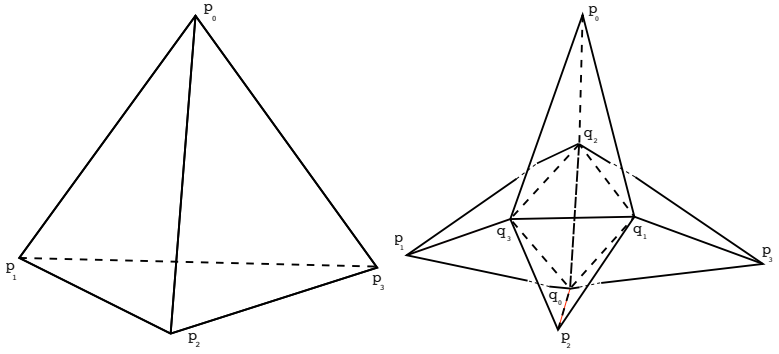

Fig. 3.2: $E^{(4)}$ and $F(E^{(4)})$ in $\mathbb{R}^3$

Lemma 3.5.5. Let $E^{(k)}$ be the k-simplex with vertices $\{p_i \mid 0 \leq i \leq k-1\}$. Then for $i \neq j$,

$$F_i(F(E^{(k)})) \cap F_j(F(E^{(k)})) = \{q_l \mid l \neq i, j\}.$$

Since $K \subset F(E^{(k)})$, it follows that $F_i(K) \cap F_j(K) = \{q_l \mid l \neq i, j\}$.

Proof. Without loss of generality, assume $i = 0$ and $j = 1$. It is clear that $F_0(F(E^{(k)})) \cap F_1(F(E^{(k)})) \supset \{q_l \mid l \geq 2\}$, so we show the reverse inclusion.

Let $Conv(X)$ be the convex hull of the points X where X is a finite collection of points in a vector space be the set of points $\sum_{i=1}^{N} \alpha_i x_i$, where α_i are nonnegative reals satisfying $\sum_{i=1}^{N} \alpha_i = 1$. Given such a representation, we call α_i the coefficient of x_i $E = \text{Conv}(\{p_i \mid 0 \leq i \leq k-1\})$. For a simplex, it is easily shown that $(\alpha_0, \ldots, \alpha_{k-1})$ gives a unique representation of every point in E. Since the F_i are affine maps,

$$f_0(E) = \text{Conv}(\{p_0, q_1\} \cup \{q_i \mid i \geq 2\})$$
$$f_1(E) = \text{Conv}(\{p_1, q_0\} \cup \{q_i \mid i \geq 2\}).$$

Since q_j is a weighted average of $\{p_i \mid i \neq j\}$, $\alpha_i > 0$ for every $i \neq j$. Thus for points of $F_0(E)$, $\alpha_0 > \alpha_1$ if the coefficient of either p_0 or q_1 is nonzero. For points of $F_1(E)$, $\alpha_1 > \alpha_0$ if the coefficient of either p_1 or q_0 is nonzero. Hence $F_0(E) \cap F_1(E) \subset \text{Conv}(\{q_i \mid i \geq 2\})$, and since $F(E^{(k)}) \subset E$,

$$F_0(F(E^{(k)})) \cap F_1(F(E^{(k)})) \subset \text{Conv}(\{q_i \mid i \geq 2\}). \tag{3.5.1}$$

For any q_j, at least one of α_0 and α_1 is positive. Then p_i is the only element of $F_i(F(E))$ that can possibly lie in $\text{Conv}(\{p_j \mid j \geq 2\})$. Since $F(E^{(k)}) = \bigcup F_i(E)$, we have $F(E^{(k)}) \cap \text{Conv}(\{p_j \mid j \geq 2\}) \subset \{p_i \mid j \geq 2\}$. Applying F_i, $i \in \{0, 1\}$, to both sides and taking their intersection,

$$[F_0(F(E^{(k)})) \cap F_1(F(E^{(k)}))] \cap \text{Conv}(\{q_j \mid j \geq 2\}) = \{q_j \mid j \geq 2\}.$$

The result follows by this and (3.5.1). ***Qed***

Proposition 3.5.6. For all $k \geq 3$, $K^{(k)}$ is homeomorphic to $\mathcal{J}^{(k)}$.

Proof. Let $\pi : \mathsf{X}_k^{-\omega} \to K^{(k)}$ be as in Proposition 3.5.4, and suppose $\pi(\ldots x_3 x_2 i) = \pi(\ldots y_3 y_2 j) = p$ with $i \neq j$. Then $p \in F_i(K) \cap F_j(K) \subset \{q_l \mid l \neq i, j\}$ by Lemma 3.5.5. It is easy to see that $p = q_l$ if and only if $x_n = y_n = l$ for all $n \geq 2$. Since the F_i are injective, by Proposition 1.2.5 in [43], $\pi(w) = \pi(\tau)$ for $w \neq \tau$ if and only if $(w, \tau) = (\ldots lliv, \ldots lljv)$ for $i, j, l \in \mathsf{X}_k$ all distinct and $v \in \mathsf{X}_k^*$.

Since this is the asymptotic equivalence relation in $\mathcal{J}^{(k)}$, π induces a continuous bijection $p : \mathcal{J}^{(k)} \to K^{(k)}$. The limit space, $\mathcal{J}^{(k)}$, is compact by Theorem 3.6.3 in [61], and $K^{(k)}$ is Hausdorff; hence p is a homeomorphism. ***Qed***

It is known that $K^{(3)}$ is the Sierpiński gasket. Unlike in the usual construction, each F_i here involves a reflection as well as a contraction. This reflects a symmetry of the Hanoi Towers game (see Section 3.7.1).

Except for when $k = 3$, F_i is not a similitude since $F_i(E^{(k)})$ is not a regular k-simplex; that is, there is no constant r for which $|F_i(x) - F_i(y)| = r|x - y|$. While the F_i become similitudes if q_i is taken outside $E^{(k)}$, the resulting invariant set is not homeomorphic to $\mathcal{J}^{(k)}$. Since the available theory is limited for sets invariant under affine contractions, the Euclidean metric on $K^{(k)}$ is of limited use. However, analytic structures such as energy, measure, and Laplacians have been constructed on the following special class of self-similar structures, independent of an Euclidean embedding [43].

Definition 3.5.7. For a self-similar structure $(K, S, \{F_s\}_{s\in S})$, define the critical set $\mathcal{C}$ and the post critical set $\mathcal{P}$ by $\mathcal{C} = \pi^{-1}(\cup_{i,j\in S, i\neq j}(F_i(K) \cap F_j(K)))$ and $\mathcal{P} = \cup_{n\geq 1}\sigma^n(\mathcal{C}_{\mathcal{L}})$. If $\mathcal{P}$ is finite, the self-similar structure is said to be post critically finite (*p.c.f.* for short).

Proposition 3.5.8. The self-similar structure $(K^{(k)}, \mathsf{X}_k, \{F_i\}_{i\in\mathsf{X}_k})$ is p.c.f.

Proof. By Lemma 3.5.5, $\mathcal{C} = \{\ldots lli \mid i \neq l\}$ and hence $\mathcal{P} = \{\ldots ll \mid l \in \mathsf{X}_k\}$. ***Qed***

Analysis can thus be developed on $K^{(k)}$ following the standard theory of p.c.f. self-similar sets (see [43]), and moreover, we expect the high symmetry of $K^{(k)}$ to simplify computations. As examples, in the rest of this section we compute the Hausdorff and spectral dimensions of $K^{(k)}$. We provide only a sketch of the theory; for details see [43] and Chapter 4 of [74].

Let $V_0 = \pi(\mathcal{P}) = \{p_i \mid i \in \mathsf{X}_k\}$, and let Γ_0 be the complete graph on V_0. Inductively define $V_{m+1} = F(V_m)$ and Γ_{m+1}, a graph on V_{m+1}, where x and y are connected in Γ_{m+1} if $x = F_i(x')$, $y = F_i(y')$ for some F_i and $x', y' \in V_m$ are connected in Γ_m. Given positive weights $\{c_{ij} \mid i, j \in \mathsf{X}_k, i < j\}$, define an energy form on V_0 by

$$\mathcal{E}_0(u) = \sum_{i<j} c_{ij}(u(p_i) - u(p_j))^2$$

for any function u on V_0. We wish to construct graph energies $\mathcal{E}_m$ on Γ_m subject to two conditions.

(E1) For some fixed renormalization factors $\{r_i\}_{i=0}^{k-1}$,

$$\mathcal{E}_m(u) = \sum_{i=0}^{k-1} r_i^{-1}\mathcal{E}_{m-1}(u \circ F_i).$$

(E2) Given u on V_{m-1}, then an extension u' of u to V_m is a function on V_m such that $u'|_{V_{m-1}} = u$. Let $\tilde{u}$ be the extension of u that minimizes $\mathcal{E}_m$. Then

$$\mathcal{E}_m(\tilde{u}) = \mathcal{E}_{m-1}(u).$$

Finding $\{c_{ij}\}$ and $\{r_i\}$ satisfying these conditions for a given self-similar structure is called the renormalization problem, which is in general highly nontrivial. Below, we find a solution for $K^{(k)}$ that is invariant under the full symmetry of V_0.

Theorem 3.5.9. The weights $c_{ij} = 1$, $i < j$, and renormalization factor $r_i = r = \frac{k(k-2)}{k^2-k-1}$ are a solution to the renormalization problem for $(K^{(k)}, \mathsf{X}_k, \{F_i\}_{i\in\mathsf{X}_k})$.

Proof. Let $p_i \in V_0$, $q_i \in V_1 \setminus V_0$. Take $c_{ij} = 1$ and, for now, $r_i = 1$. For a function u on V_0 defined by $u(p_i) = a_i$,

$$\mathcal{E}_0(u) = \sum_{i<j}(a_i - a_j)^2.$$

An extension u' of u to V_1 is determined by its values on $V_1 \setminus V_0 = \{q_i\}$; let $u'(q_i) = x_i$. Each edge of Γ_1 connecting q_i and p_j, $i \neq j$, appears in one of the k subgraphs $F_l(\Gamma_0)$ of Γ_1, while each edge connecting q_i and q_j, $i \neq j$, appears in $k-2$ of them. Thus by (E1),

$$\mathcal{E}_1(u') = (k-2)\sum_{i<j}(x_i - x_j)^2 + \sum_{i<j}(x_i - a_j)^2.$$

The values of x_i minimizing this determine $\tilde{u}$ on V_m. If $\mathcal{E}_1(\tilde{u})/\mathcal{E}_0(u) = \lambda$ for all u, then replacing r_i by r_i/λ makes (E2) hold for $m = 1$.

Setting $\frac{1}{2}\frac{\partial\mathcal{E}_1}{\partial x_i} = 0$ yields

$$(k-2)\sum_{j:j\neq i}(x_i - x_j) + \sum_{j:j\neq i}(x_i - a_j) = 0$$
$$[(k-2)(k-1) + (k-1)]x_i = (k-2)\sum_{j:j\neq i} x_j + \sum_{j:j\neq i} a_j$$

for each i. Summing k such equations, one for each $i \in \mathsf{X}_k$, we get $(k-1)^2X = (k-1)(k-2)X + (k-1)X$ or $X = A$, where $X = \sum x_i$ and $A = \sum a_i$. So adding $(k-2)x_i$ to both sides to the previous equation gives

$$[(k-2)(k-1) + (k-1) + (k-2)]x_i = (k-2)X + A - a_i$$
$$(k^2-k-1)x_i = (k-1)X - a_i.$$

Then $a_i - a_j = (k^2-k-1)(x_j - x_i)$, so

$$\mathcal{E}_0(u) = \sum_{i<j}(a_i - a_j)^2 = (k^2-k-1)^2\sum_{i<j}(x_i - x_j)^2.$$

Using $a_i = (k-1)X - (k^2-k-1)x_i$ to write $\mathcal{E}_1(\tilde{u})$ in terms of k and symmetric sums $\sum_i x_i^2$ and $\sum_{i<j} x_i x_j$, we arrive at

$$\mathcal{E}_1(\tilde{u}) = k(k-2)(k^2-k-1)\sum_{i<j}(x_i - x_j)^2$$

$$\Rightarrow \lambda = \frac{\mathcal{E}_1(\tilde{u})}{\mathcal{E}_0(u)} = \frac{k^2-k-1}{k(k-2)}.$$

Hence (E2) holds for $m=1$ with $r_i = \frac{k(k-2)}{k^2-k-1}$.

For the extension from $\mathcal{E}_{m-1}$ to $\mathcal{E}_m$, note that each point in $V_m \setminus V_{m-1}$ lies in a unique m-cell, and that within each m-cell the minimization problem is what we just solved. Since $\mathcal{E}_m$ is the sum of the energy contributions from each cell, (E1) and (E2) hold for any m. ***Qed***

Because $\mathcal{E}_m$ is nondecreasing by (E2), we define $\mathcal{E}(u) = \lim_{n\to\infty} \mathcal{E}_m(u)$, allowing values of $+\infty$. The effective resistance R is then defined on $V_* = \bigcup_{m\geq 0} V_m$ by

$$R(x,y)^{-1} = \min\{\mathcal{E}(u) : u(x) = 0 \text{ and } u(y) = 1\}.$$

This is independent of m. By construction V_* is dense in K and $R(x,y)$ is uniformly continuous in x and y, so R extends to $K \times K$ to a metric on K.

Proposition 3.5.10. Let R be the effective resistance metric on $K^{(k)}$, and $r = \frac{k(k-2)}{k^2-k-1}$ as in Theorem 3.5.9. There exist constants c_1', c_2' such that
(a) if x and y are in the same or adjacent m-cell, then $R(x,y) \leq c_1' r^m$;
(b) otherwise $R(x,y) \geq c_2' r^m$.

Proof. Lemma 1.6.1 in [74] proves this for the Sierpiński gasket. Section 4.4 of the same reference argues why this holds for any p.c.f. self-similar set. ***Qed***

For self-similar Euclidean sets generated by contractive similitudes of ratio r_i, the Hausdorff dimension d_H under the Euclidean metric satisfies Moran's formula [60], $\sum_{i=0}^{k-1} r_i^{d_H} = 1$. The above Proposition says that the contraction maps have ratio roughly r. Here, we need a generalization from Kigami (Theorem 1.5.7 in [43]). We use a special case.

Theorem 3.5.11. (Corollary 1.3 in [41]) Let (X,d) be a complete metric space, and let K be the self-similar invariant set defined by contractions $\{f_i\}_{i\in S}$. Suppose there exist constants $0 < r < 1$, $0 < c_1, c_2$ and $M > 0$ such that
(1) for all $w \in \mathsf{X}^n$,

$$\operatorname{diam}(K_w) \leq c_1 r^n;$$

(2) for all $x \in K$ and $n \geq 0$,

$$\#\{w : w \in \mathsf{X}^n, d(x, K_w) \leq c_2 r^n\} \leq M.$$

Then the Hausdorff dimension of K with respect to d is $-\log|S|/\log r$.

Corollary 3.5.12. The space $K^{(k)}$ has Hausdorff dimension $\frac{\log k}{\log(k^2-k-1)-\log(k(k-2))}$ with respect to the effective resistance metric.

Proof. Let c_1' and c_2' be as in Proposition 3.5.10, and take $c_1 = c_1'$, $c_2 = c_2' r$, $M = k+1$. By (a) in the same proposition, $\operatorname{diam}(K_w) \le c_1 r^n$ for $w \in \mathsf{X}^n$. Take any $x \in K = K^{(k)}$ and $n \ge 0$, and consider $w \in \mathsf{X}_k^n$. If K_w is not one of the $M = k+1$ n-cells that either contain x or is adjacent to the n-cell containing x, then by (b), $R(x, K_w) \ge c_2' r^n > c_2 r^n$. Hence Theorem 3.5.11 applies. ***Qed***

The renormalization problem is often stated through the terminology of harmonic structure. Write $l(V_0)$ for the space of functions on V_0. The quadratic form $-\mathcal{E}_0$ can be written $-\mathcal{E}_0(u) = u^T D u$ for some symmetric linear operator $D : l(V_0) \to l(V_0)$. For $\mathcal{E}_0$, constructed above, D has the k-by-k matrix representation

$$D = \begin{pmatrix} -(k-1) & 1 & \cdots & 1 \\ 1 & -(k-1) & \cdots & 1 \\ \vdots & \vdots & \ddots & \vdots \\ 1 & 1 & \cdots & -(k-1) \end{pmatrix}$$

with respect to the standard function basis. Given $\{r_i\}_{i \in \mathsf{X}_k}$, define linear operators $H_m : l(V_m) \to l(V_m)$ inductively by $H_0 = D$ and

$$H_m = \sum_{i \in \mathsf{X}_k} r_i^{-1} R_i^{-1} H_{m-1} R_i,$$

where $R_i : l(V_m) \to l(V_{m-1})$ is the natural restriction defined by $R_i(u) = u \circ F_i$. Then condition (E2) for energy together with $-\mathcal{E}_0 = u^T D u$ implies that $-\mathcal{E}_m(u) = u^T H_m u$ for all $m \ge 0$. Decompose H_1 as

$$H_1 = \left(\begin{array}{c|c} T & J^T \\ \hline J & X \end{array}\right),$$

where T acts on $l(V_0)$ and X acts on $l(V_1 \setminus V_0)$. In the terminology of [46], $(D, \{r_i\}_{i \in \mathsf{X}_k})$, with suitable additional conditions on D, is called a harmonic structure on $(K^{(k)}, \mathsf{X}_k, \{F_i\}_{i \in \mathsf{X}_k})$ if

$$D = \lambda(T - J^T X^{-1} J) \tag{3.5.2}$$

for some constant λ. A harmonic structure is said to be regular if $\lambda > r_i$ for all $i \in \mathsf{X}_k$.

Corollary 3.5.13. The pair $(D, \{r, \ldots, r\})$ for D defined above and $r = \frac{k(k-2)}{k^2-k-1}$ is a regular harmonic structure on $(K^{(k)}, \mathsf{X}_k, \{F_i\}_{i \in \mathsf{X}_k})$ with $\lambda = 1$.

Proof. Minimizing $\mathcal{E}_1(\tilde{u}) = \tilde{u}^T H_1 \tilde{u}$ as in the proof of Theorem 3.5.9 shows that (3.5.2) is equivalent to $\mathcal{E}_1(\tilde{u}) = \lambda \mathcal{E}_0(u)$. Recall that in Theorem 3.5.9 we replaced r_i by r_i/λ to satisfy condition (E2), which is just the above condition with $\lambda = 1$. Here we instead leave λ apart from $\{r_i\}$. Therefore, finding D, $\{r_i\}$, and λ under these conditions is an equivalent reformulation of the renormalization problem, differing merely in the choice of the fundamental analytic structure (harmonic structure instead of a self-similar energy form). Hence the result of Theorem 3.5.9 carries over. The harmonic structure is regular since $\lambda = 1 > r_i$. ***Qed***

By further specifying the standard Bernoulli (self-similar) measure on $K^{(k)}$, the standard Laplacian on $K^{(k)}$ can be defined as the limit of the operators H_m on Γ_m. The spectral dimension of the harmonic structure describes the spectral asymptotics of this Laplacian.

Theorem 3.5.14. The spectral dimension d_S of $K^{(k)}$ with the harmonic structure $(D, \{r, \ldots, r\})$ defined above is $\frac{2\log k}{\log(k^2-k-1)-\log(k-2)}$.

Proof. By Theorem A.2 in [46],

$$\sum_{i=0}^{k-1} \gamma_i^{d_S} = 1,$$

where $\gamma_i = \sqrt{\frac{r_i \mu_i}{\lambda}}$, with $\mu_i = \frac{1}{k}$ for the standard Bernoulli measure. We omit the computation. ***Qed***

As a remark, since this self-similar structure is fully symmetric on V_0, by Proposition 3.1 in [6], the spectral decimation method allows the explicit computation of the spectrum of the associated Laplacian to this energy form with multiplicities. As was done in the previous chapter

3.6 Symmetric Contracting Hanoi Groups

The pegs of the original Hanoi Towers game are indistinguishable in the sense that the same type of legal move exists between any two pegs. By placing symmetry conditions on the Hanoi groups, we obtain corresponding Hanoi games that preserve this aspect of the game.

The permutation group on X_k, $\mathrm{Sym}(\mathsf{X}_k)$, has a natural action on S_k; for $\phi \in \mathrm{Sym}(\mathsf{X}_k)$ and $a \in S_k$, define $\phi \cdot a$ as the Hanoi automorphism with inactive pegs $\phi(Q_a)$ and root permutation $\phi \sigma_a \phi^{-1}$ on the active pegs $\phi(\mathsf{X}_k \setminus Q_a)$. In the game, this corresponds to re-representing the same move by relabeling each peg i as $\phi(i)$.

Definition 3.6.1. A k-peg Hanoi group G with generating set S is said to be fully symmetric if S is closed under $\mathrm{Sym}(\mathsf{X}_k)$; that is, $\phi \cdot S \subset S$ for all $\phi \in \mathrm{Sym}(\mathsf{X}_k)$.

In fact, since S is finite and the action faithful, $\phi \cdot S = S$. More concretely, if $g \in S$, then S contains every k-peg Hanoi automorphism with the same number of inactive pegs and the same cycle type of the root permutation as g.

Theorem 3.6.2. For any $k \geq 3$, every fully symmetric and contracting k-peg Hanoi group is a subgroup of $H_c^{(k)}$.

Proof. The claim is trivial for $k = 3$ since $H_c^{(3)}$ is the only fully symmetric nontrivial 3-peg Hanoi group. Assume $k \geq 4$, and let G be a fully symmetric k-peg Hanoi group generated by S that is not a subgroup of $H_c^{(k)}$. Then S contains some $a \in S_k$ with two or more inactive pegs and nontrivial σ_a. We will show that G is not contracting.

Let $p = |P_a|$. Relabel the pegs so that $Q_a = \{p, p+1, \ldots, k-1\}$. Further relabel pegs within P_a so that σ_a has the form $(0\ 1\ \cdots\ m)c_2 \ldots c_n$, a product of disjoint cycles. That is,

$$a = (0\ 1\ \cdots\ m)c_2 \ldots c_n(1, 1, \cdots, 1, a, a, \cdots, a),$$

where $a|_i = a$ for $i \geq p$. Take $b = (0\ p) \cdot a$, which is in S by the symmetry assumption. Since each c_i, $2 \leq i \leq n$, is disjoint from $(0\ p)$,

$$\begin{aligned} b &= (p\ 1\ 2\ \ldots\ m)c_2 \ldots c_n(b, 1, \ldots, 1, 1, b, \ldots, b) \\ b^{-1} &= (m\ \ldots\ 2\ 1\ p)c_n^{-1} \ldots c_2^{-1}(b^{-1}, 1, \ldots, 1, 1, b^{-1}, \ldots, b^{-1}), \end{aligned}$$

where $b^{-1}|_i = b^{-1}$ for $i \in (0\ p)Q_a = \{0, p+1, \ldots, k-1\}$. Then G contains

$$ab^{-1} = (0\ 1\ p)(b^{-1}, a, 1, \ldots, 1, 1, ab^{-1}, \ldots, ab^{-1}),$$

where $ab^{-1}|_i = ab^{-1}$ for $i \geq p+1$. Then $(ab^{-1})^3|_{p+1} = (ab^{-1})^3$ and $(ab^{-1})^3|_0 = ab^{-1}$, so Lemma 3.3.5 applies. ***Qed***

Under weaker symmetry conditions, we obtain more contracting Hanoi groups. Identifying X_k with the vertices of a regular k-gon in the order 0 through $k-1$, we say that a Hanoi group is rotationally or dihedrally symmetric if its generating set is closed under the action of the corresponding symmetry group of X_k. We do not have analogues of Theorem 3.6.2 for these symmetries. We state one partial result.

Definition 3.6.3. Let $\underline{R}_{k,n} \subset S_k$, $2n+1 \leq k$, be the union of the identity automorphism and all automorphisms $a \in S_k$ for which

1. $Q_a \subset \{m+1, m+2, \ldots, m+n\}$ for some m, and
2. whenever $i \in Q_a$, σ_a also fixes every element of $\{i-1, i-2, \ldots, i-(n-1)\}$,

where addition is performed modulo k.

In the cyclic arrangement, each peg has an increasing and a decreasing side. Condition 1 of Definition 3.6.3 says that the set of inactive pegs lie among n adjacent pegs. Condition 2 says that σ_a fixes the $n-1$ adjacent pegs on the decreasing side of each inactive peg.

Proposition 3.6.4. Every Hanoi group (G, X_k) generated by $S \subset \underline{R}_{k,n}$ is contracting.

Proof. We verify condition $(*)$ from Theorem 3.4.8. Take an arbitrary subset $T = \{s_i\}_{i=1}^{M}$ of S with nonempty essential set Q, and consider any $j \notin \mathrm{Fix}(T)$. As usual, let σ_i and Q_i be the root permutation and the set of inactive pegs, respectively, of s_i.

Without loss of generality, assume $n-1 \in Q$. Then by the first condition on elements of $\underline{R}_{n,k}$, $Q_i \subset [0, 2n-2]$ for each i. Let M_i be the largest element of Q_i, and choose s_{min} so that $M_{min} \leq M_i$ for all i. Note that $n-1 \leq M_{min} \leq M_i \leq 2n-2$. Then $M_i + 1 \in Q_i$ and $M_i + 1 - (n-1) \leq n$, so by the second condition on elements of $\underline{R}_{n,k}$ each σ_i fixes every element of $[n, M_{min}]$. Furthermore, since $n-1 \in Q_i$, each σ_i fixes every element of $[0, n-1]$.

Since $j \notin \mathrm{Fix}(T)$, by the above we have $j \in [M_{min}+1, k-1]$ and so $\mathrm{Orb}_T(j) \subset [M_{min}+1, k-1]$. Thus $\mathrm{Orb}_T(j) \cap Q_{min} = \emptyset$, as desired. ***Qed***

Define $\overline{R}_{k,n}$ by replacing the set in the second condition of Definition 3.6.3 by $\{i+1, i+2, i+(n-1)\}$. The over line indicates that we now take the adjacent pegs on the increasing side. The analogue of Proposition 3.6.4 also holds with $\overline{R}_{k,n}$ instead of $\underline{R}_{k,n}$.

For example, Hanoi groups generated by the following sets are contracting by Proposition 3.6.4:

$$\{1\} \cup \left\{ \begin{array}{ll} a = (0\ 1)(1,1,1,a,a) & d = (3\ 4)(1,d,d,1,1) \\ b = (1\ 2)(b,1,1,1,b) & e = (4\ 0)(1,1,e,e,1) \\ c = (2\ 3)(c,c,1,1,1) & \end{array} \right\}$$

$$\{1\} \cup \left\{ \begin{array}{ll} a = (0\ 1)(1,1,1,a,a,1) & d = (3\ 4)(d,d,1,1,1,1) \\ b = (1\ 2)(1,1,1,1,b,b) & e = (4\ 5)(1,e,e,1,1,1) \\ c = (2\ 3)(c,1,1,1,1,c) & f = (5\ 0)(1,1,f,f,1,1) \end{array} \right\}.$$

The first is a contracting 5-peg Hanoi group with rotational symmetry, while the second is a contracting 6-peg Hanoi group with dihedral symmetry. Moreover, unlike contracting k-peg Hanoi groups generated by subsets of $S_{k,k-2}$, $k > 3$ (recall Proposition 3.3.4), these groups correspond to meaningful Hanoi games in the following sense.

Proposition 3.6.5. Let G be a k-peg Hanoi group generated by S. The group generated by the set of all root permutations of the generators acts by permutation on X_k. The Schreier graphs Γ_n, $n \geq 1$ are connected if and only if the action of G on X_k is transitive.

Proof. Vertices $x, y \in \Gamma_n$ are connected if and only if $s_m \dots s_2 s_1(x) = y$ for some $s_i \in S \cup S^{-1}$. Since each s_i has finite order, we can write this product without inverses. Thus Γ_n is connected if and only if the legal moves of the associated Hanoi game allow us to change any legal n-disk configuration into any other legal n-disk configuration.

Suppose the action is not transitive, so that there exist i, $j \in \mathsf{X}_k$ such that no product $\sigma = \sigma_m \cdots \sigma_2 \sigma_1$ of root permutations satisfies $\sigma(i) = j$. Then any configuration with the smallest disk on peg j cannot be reached from any configuration with the smallest disk on peg i.

Now assume the action is transitive. The case $n = 1$ is immediate. Assume the claim for $n - 1$, and consider any two legal n-disk configurations. Suppose the largest disk needs to move from peg i to peg j. By transitivity, $\sigma_m \dots \sigma_2 \sigma_1(i) = j$ for some product of root permutations. Let s_i be some generator with root permutation σ_i. Repeat the following for $1 \leq i \leq m$: *Use the $n-1$ case to move the $n-1$ smaller disks onto an inactive peg of s_i. Then use s_i to move the largest disk.* After the m-th step, the largest disk will be on peg j. We then use the $n-1$ case to move the smaller disks to their desired pegs. ***Qed***

We end with several open questions and thoughts.

- Theorem 3.6.2 holds with the alternating group on X_k; since $(0\ p\ p+1) \cdot a = (0\ p) \cdot a$, the proof only requires 3-cycles. Is there a weaker or more natural set of constraints under which $H_c^{(k)}$ remains the unique maximal contracting group?

- There are non-Hanoi automorphisms that may still be interpreted in terms of the Hanoi Towers game. For example, consider

$$a = (0\ 1\ 2)(1, 1, 1, b) \quad b = (0\ 2\ 1)(1, 1, 1, a).$$

  Then $ab = (1, 1, 1, ba)$ and $ba = (1, 1, 1, ab)$, so $ab = 1$. In terms of the game, both a and b start from the smallest disk and keep track of parity the number of disks on peg 3 until it encounters a disk on pegs 0, 1, or 2. If the parity is odd, a applies (0 1 2); if even, (0 2 1). b does the same with the permutations exchanged. How can we characterize all automorphisms that correspond to legal moves of the game in some reasonably defined sense? Which groups with such generators are contracting?

- Can we apply similar symmetry conditions to other self-similar groups to obtain criteria on their contraction or non-contraction?

3.7 Hanoi Tower Networks

This chapter began by examining existing variations of the Hanoi Towers game. Two such modifications were the Hanoi Networks, HN3 and HN4, which were introduced in the physics literature [18] as examples of regular networks with small-world properties. The physical motivation for the small-world property is the notion of a space where particles have the option to very quickly jump a large distance. For more on networks with this small-world property, see [19,63,76]. We will show that while HN3 can be related peripherally to the automaton representing the Hanoi Towers game, these networks have no direct connection to the original Hanoi Towers game.

3.7.1 Construction of HN3/HN4

The construction of both networks is only partially inspired by the traditional 3-peg Hanoi Towers game.

Definition 3.7.1. Define S_n as the sequence of disks moved in the optimal solution of the n-disk game, where disks numbered 1 through n from smallest to largest. That is if you move disk 1 on the first move, the first element in the sequence is 1.

For example, the optimal solution for the 1-disk game simply moves disk 1 to the desired peg, so that

$$S_1 = (1).$$

For two disks, we first move disk 1 to the third peg, disk 2 to the goal peg, then disk 1 above disk 2:

$$S_2 = (1, 2, 1).$$

It is well known (see, for example, [17]) that the optimal solution is given recursively; to move n disks from peg 1 to peg 2, we first move the $n-1$ smaller disks to peg 3, move disk n to peg 2, and finally move the $n-1$ smaller disks from peg 3 to peg 2. This means that S_{n+1} is obtained by concatenating two copies of S_n, with a $n+1$ term between them. We can therefore define the following:

Definition 3.7.2. Define S as the unique infinite sequence having each S_n as a prefix:

$$S = (1, 2, 1, 3, 1, 2, 1, 4, 1, 2, 1, 3, 1, 2, 1, 5, \ldots)$$

A network is a graph with a length assigned to each edge. Vertices of a network are called nodes. We use S to construct two networks that incorporate this model of the Hanoi Towers game and also have small-world properties.

Definition 3.7.3. The HN3 network has nodes that are identified with the positive integers. Nodes corresponding to adjacent integers are connected; these edges form the backbone of this network. Label node n by the n-th element of S, called the disk number of the node. Nodes with the same disk number i are connected if and only if there exists a node labeled $i+1$ in between and there does not exist a node labeled j, where $j \geq i+2$, in between. We call these connections long-distance jumps. An edge connecting nodes n and m is given length $|n-m|$. See Figure 3.3.

Each node is thus connected at least to its adjacent nodes on the backbone by edges of length 1. In addition, certain nodes with disk number i are connected by long-distance jumps of length 2^i. For example, nodes 1 and 3, the first two nodes with disk number 1, are connected, as are 5 and 7, 9 and 11, etc; among nodes with disk number 2, nodes 2 and 6 are connected, then 10 and 14, etc.; and so on for every disk number.

Definition 3.7.4. The network HN4 is the network HN3 with additional connections made between a node labeled i and the first nodes labeled i to its left and to its right. In addition, the backbone is extended to all integers, and the network is made symmetric over 0. The special point 0 is connected to itself by a loop. See Figure 3.3.

For example, for disk number 1, HN4 retains all the long-distance jumps in HN3, and in addition connects $n = 3$ to $n = 5$, $n = 7$ to $n = 9$, etc. to create a 4-regular network. In both HN3 and HN4, the metric is given by the distance along the backbone (not using any long-distance jumps).

Hanoi Towers Automata

The Hanoi Towers game also gives rise to a series of finite networks corresponding to the finite state automata of the n-disk game, as discussed earlier.

Definition 3.7.5. The network H_n is constructed to represent the n-disk game so that each vertex of the automaton is associated to an n-letter word $x_1x_2x_3\ldots\ x_n$, $x_i \in \{0,1,2\}$. This word indicates the peg number of each disk, starting from the smallest disk. Two vertices are connected by an edge if a legal move allows the player to move between the corresponding states. Every edge is given the same length, chosen so that the shortest path between 0^n and 1^n has length 1.

For notational simplicity, we write i^n for the n-letter word $i\ldots ii$. Note that the vertices of H_n correspond to the possible states of the game, i.e. the configuration of n disks. While each H_n has a natural metric independent of the ambient space, it is useful to have an embedding of these networks, both as a visualization and in order to obtain some limiting object. We find that a particular recursive

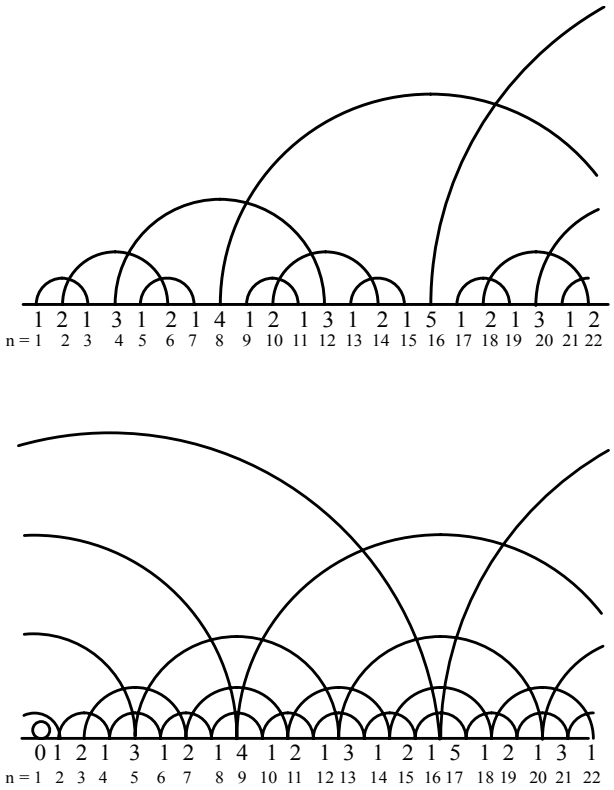

Fig. 3.3: The networks HN3 and HN4

construction allows us to embed each H_n in the plane so that every edge has the same length.

The network H_1 has three states: 0, 1, and 2. We arrange these in an equal triangle; place 0 at the bottom left, 1 at the bottom right, and 2 at the top. Every H_n will contain a triangle with vertices 0^n, 1^n, and 2^n in this same orientation. For the n-disk game represented by H_n, $n \geq 2$, ignoring the largest disk results in the Hanoi Towers game for the $n-1$ smaller disks. As a result, H_n contains three transformed copies of H_{n-1}, each representing the $(n-1)$-disk game with the largest disk on one of the three pegs. The three copies are transformed in the following way. For the copy of H_{n-1} corresponding to the largest disk being on peg i, where $i = 0, 1, 2$, reflect H_{n-1} with its labels across the line through i^{n-1} and the midpoint of the other two vertices, and append i to each label. Now, translate these three copies apart so that the new labels 0^n, 1^n, and 2^n form the vertices of a larger triangle. The only missing edges of H_n are those that correspond to moving the largest disk. This is only possible when the $n-1$ smaller disks are on the same peg, different from the one with the largest disk. It easily follows that there are three more edges: between $1^{n-1}2$ and $1^{n-1}0$; $2^{n-1}0$ and $2^{n-1}1$; $0^{n-1}1$

and $0^{n-1}2$. With appropriate translations of the smaller networks, these three edges connect the three triangles to complete the outer edge of the larger triangle. Moreover, their lengths can be chosen to be the same as the edges in each copy of H_{n-1}See Figure 3.4 for H_3.

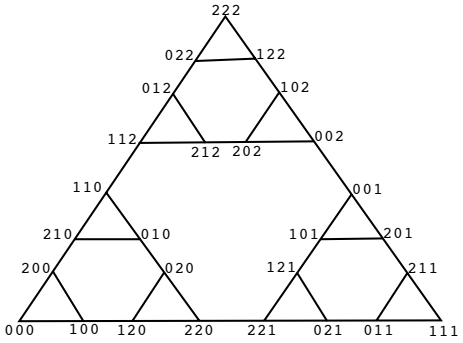

Fig. 3.4: H_3

3.7.2 Relation between HN3 and Hanoi Towers Automaton

In the definitions of HN3 and HN4 the long-distance jumps were added to create a small-world property and as such have no direct relation to the Hanoi Towers game, there is no reason to expect a connection between these and H_n. However, the recursive nature of HN3 allows us to obtain it as a subnetwork of the automaton network.

Theorem 3.7.6. Let $\mathrm{HN3}_n$ be the subnetwork of HN3 consisting of the first $|S_n|$ vertices and edges connecting them. Then $\mathrm{HN3}_n$ can be obtained as a graph minor H'_n of H_n.

Proof. For $n = 1$, set $H'_1 = H_1$. Then $\mathrm{HN3}_1$ is clearly isomorphic to H'_1 as graphs. We develop the isomorphism between $\mathrm{HN3}_n$ and H'_n inductively so that the middle node of $\mathrm{HN3}_n$, with disk number $n+1$, corresponds to 2^n in H_n, and the end nodes with disk number 1 correspond to 0^n and 1^n.

Fix $n \geq 2$. Analogous to the way S_n is obtained from two copies of S_{n-1}, $\mathrm{HN3}_n$ can be obtained from two copies of $\mathrm{HN3}_{n-1}$, an extra node of disk number n, and three new edges: two edges to join the backbone of each copy of $\mathrm{HN3}_{n-1}$ to the new node, and a long-distance jump connecting the two nodes of disk number $n-1$ at the center of each copy of $\mathrm{HN3}_{n-1}$. To construct H'_n, we proceed as in the recursive construction of H_n, but create only two transformed copies of H'_{n-1}, say for $i = 0$ and 1, using the reflections and label appending explained in 3.7.1. These correspond to the two copies of $\mathrm{HN3}_{n-1}$. In place of the third copy of H'_{n-1}, H'_n has the single node 2^n, corresponding to the added middle

node in HN3$_n$ of disk number n. The nodes $1^{n-1}0$ and $0^{n-1}1$ are connected to the node 2^n, corresponding to the two new edges that complete the backbone of HN3$_{n-1}$. The nodes $2^{n-1}0$ and $2^{n-1}1$ are also connected, corresponding to the added long-distance jump in HN3$_n$.

These correspondences show that the isomorphism of HN3$_{n-1}$ and H'_{n-1} implies the isomorphism of HN3$_n$ and H'_n, so by induction, HN3$_n = H'_n$ for all $n \geq 1$. By construction, H'_n can be regarded as a subgraph of H_n in a natural way. Figures 3.5 and 3.6 show the first three levels of $HN3_n$ and H'_n, respectively, with the backbone of $HN3_n$ and the corresponding edges in H'_n thickened. ***Qed***

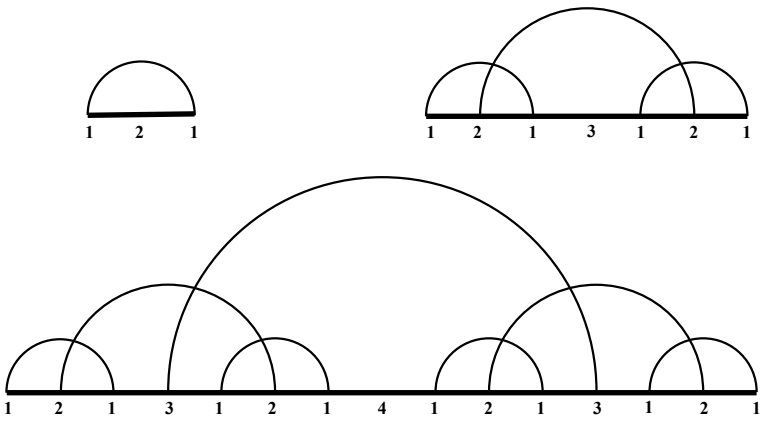

Fig. 3.5: The first three levels of HN3$_n$

In this correspondence, every long-distance jump in HN3 now has length one in any H'_n. All edges of the backbone of HN3 connect a node of disk number 1 to another node, say of disk number k. These edges of length $k-1$ in any H'_n. As a result, the distortion ratio of the metric is unbounded, but only as disk number also goes to infinity. Since higher disk numbers appear further away from the origin in HN3, the distortion is controlled for any finite section of the networks. However, because of difference in metric, it is impossible to extend the correspondence to the limiting space. More precisely, we have the following theorem:

Theorem 3.7.7. There exists a Lipschitz embedding of HN3$_n$ into H_n that is not uniformly bi-Lipschitz in n.

Proof. The subnetwork H'_n is an embedding of HN3$_n$ into H_n that is Lipschitz since all edges in H_n have length less than 1 and all distances in HN3$_n$ are greater than or equal to 1. However, the lower Lipschitz bound is smaller than 2^{-n}. Thus the embedding is bi-Lipschitz for each n, but not uniformly. ***Qed***

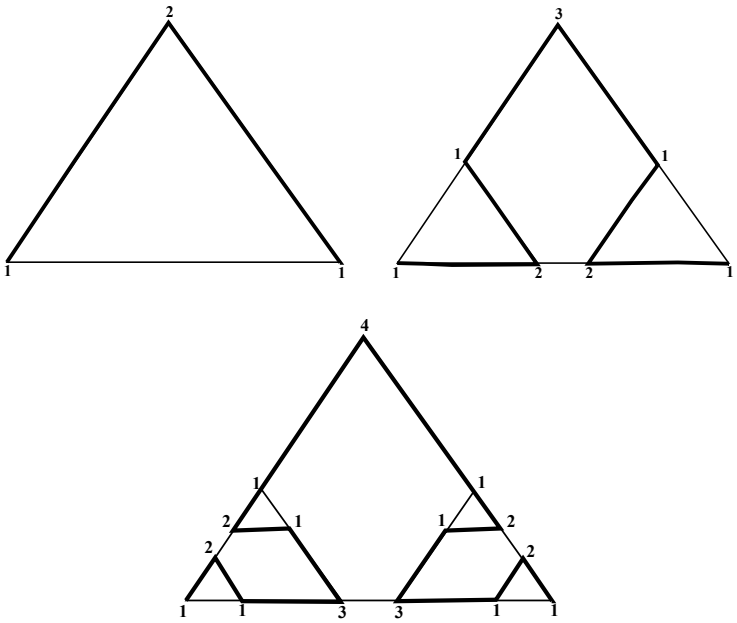

Fig. 3.6: The first three levels of H'_n. The darkened lines correspond to the backbone of HN3$_n$ while the lighter lines correspond to the long-distance jumps.

The network H'_n has an interpretation as an automaton for its own game. Start with the same labeling 0, 1, and 2 for H'_1. At each iteration, follow the usual labeling rule for the two copies of H'_{n-1}, but give the label 2 to the extra node. Then each label in H'_n is, read from right to left, a binary number which ends after n digits or at the first appearance of 2. In terms of the Hanoi Towers game, this corresponds to ignoring disks smaller than the largest disk at peg 2, if there are any. All states in the Hanoi Towers game that agree from the largest disk to the largest disk at peg 2 represent the same state in H'_n, just as we collapsed the copy of H'_{n-1} with the largest disk on peg 2 to a single vertex in the recursive construction. It also follows that the disk number derived from HN3$_n$ has a natural interpretation: a node in H'_n with disk number 1 represents a single state in H_n, and a node with disk number $k > 1$ represents the result of collapsing 3^{k-2} states in H_n.

Part II

Chapter 4

Dirichlet Forms on Laakso and Some Barlow-Evans Fractals of Arbitrary Dimension

This chapter first appeared as [71].

Abstract: In this chapter we explore two constructions of the same family of metric measure spaces. The first construction was introduced by Laakso in 2000 where he used it as an example that Poincaré inequalities can hold on spaces of arbitrary Hausdorff dimension. This was proved using minimal generalized upper gradients. Following Cheeger's work these upper gradients can be used to define a Sobolev space. We show that this leads to a Dirichlet form. The second construction was introduced by Barlow and Evans in 2004 as a way of producing exotic spaces along with Markov processes from simpler spaces and processes. We show, for the correct base process in the Barlow Evans construction, that this Markov process corresponds to the Dirichlet form derived from the minimal generalized upper gradients.

MSC Codes: 31C25 (Primary) 60J45, 28A80, 46A13

4.1 Introduction

There is a sizable literature that considers fractal spaces and operators on them. A common simplification on the fractals to make the study more tractable is to assume that the fractals are finitely ramified, that is they can be disconnected by removing a finite number of points, [75,6]. A stronger but related simplification is to consider fractals that are post-critically finite as done in [43,13,51,58]. There has also been interest in post-critically infinite fractals in [9,10,6]. Often these spaces can be deficient in rectifiable paths between points, which leads to problems in conducting analysis on them [36,68]. The main obstacle this presents is that it prevents the use of capacity and curve modulus arguments to obtain Poincaré inequalities and other related objects.

In [36] there is an excellent survey of the kinds of analysis which can be done on spaces which are not smooth in a classical sense but which do still have a "large supply" of rectifiable curves connecting any two points. One of the notable

results which can come from having enough curves in a space is a $(1,1)-$Poincaré inequality. Unfortunately, many fractals do not have this ample supply of curves, one example is the Sierpinski Gasket. Laakso, in [52], gave a construction of an one-parameter family of metric measure spaces which have sufficient rectifiable curves to support a Poincaré inequality with the advantage that the (continuous) parameter indexing the family of spaces is the Hausdorff dimension. The dimension of the space is determined by the number and dimension of the Cantor sets as well as a sequence $\{j_i\}$ used in the construction. We review this construction in Section 4.3. Moreover, a countable subfamily of these Laakso spaces are self-similar fractals. Laakso's original construction is an elegant one, but is not well suited to studying the properties of operators on these spaces. Examples of other spaces with Ahlfors regularity and probabilistic information such as escape time estimates, as opposed to analytic information, are discussed in [8].

The spaces that Laakso constructed have enough rectifiable curves to allow for the kind of analysis in [68] which uses the capacity of sets as a central tool. We will define a Dirichlet form on each of the Laakso spaces that is derived from the minimal generalized upper gradients of suitable functions. Barlow and Evans [12] have constructed Markov processes that evolve on what they call "vermiculated spaces," and state that Laakso's spaces can be constructed as vermiculated spaces. Starting with the Dirichlet form associated to the minimal generalized upper gradient we identify the Markov process to which it corresponds.

In [12], there are proofs of the existence of Markov processes on Barlow-Evans spaces using a construction which we show can give Laakso spaces, although it can generate a much wider variety of spaces as well. This leads to a natural question: are these Markov processes are symmetric with respect to a reasonable measure on the space? If there are symmetric processes the next question would be to which Dirichlet forms do they correspond? The connection between Dirichlet Forms and Markov processes is well known and we refer to the exposition from [31] for the general theory. Following up on a comment in [12], we offer a proof that Laakso's spaces can also be constructed as projective limits of quantum graphs. We surmise that Barlow and Evans knew this result but did not include it in their paper. This perspective will be used in Section 4.8 to prove the final theorem of the paper. In [75] a similar use of quantum graphs to estimate a Dirichlet form is explored for finitely ramified fractals based on [40,44] however our situation is more complicated.

Both Dirichlet forms and symmetric Markov processes are associated to unbounded, self-adjoint operators. Once we have proved that we can realize Laakso spaces as projective limits of quantum graphs we will be able to show that the operator associated to the minimal generalized upper gradient Dirichlet form is also the limit of the operators on the sequence of approximating quantum graphs that are associated to a particular Markov process taken through the Barlow-Evans construction. In this way we will produce a symmetric Markov process and a

Dirichlet form on any Laakso space which correspond to the same operator, hence are associated themselves. We analyze the spectra of such operators in [66] and [16].

We begin by reviewing the basic theory of Dirichlet forms and Markov processes on general spaces in Section 4.2. Then in Section 4.3 we give in detail Laakso's original construction from [52]. In Sections 4.4 and 4.5 we define a space of functions and then describe explicitly a Dirichlet form and minimal upper gradients on the fractal. The construction offered by Barlow and Evans in [12] is presented in Section 4.6 and sufficient conditions for the existence of Markov processes on the vermiculated spaces are given in Section 4.7. Then in Section 4.8 we link this Dirichlet form to a specific Barlow-Evans Markov process.

4.2 Dirichlet Forms and Markov Processes

In this section we briefly recall some basic facts about the relation between these two approaches and establish notation. The reader can find more details in [31,64]. While our approach is mainly analytic, in much of the previous literature, including [12], probabilistic approaches have been used to great effect.

There is a deep connection between Dirichlet Forms, which are primarily analytic objects, and Markov Processes, which are very much probabilistic objects. This connection is classical and has been explored by many authors including Fukushima, Oshima, and Takeda in [31]. We begin our discussion by recalling basic definitions and stating without proof a theorem that gives the conditions necessary for the correspondence. We assume that all Hilbert spaces mentioned in this paper are real L^2 spaces on the relevant underlying space. Throughout this section we assume a Borel regular measure space (X, μ).

Theorem 4.2.1. There is a one-to-one correspondence between closed symmetric bilinear forms on a Hilbert space and non-positive definite self-adjoint operators on the Hilbert space. The correspondence is given by:

$$\begin{cases} Dom(\mathcal{E}) = Dom(\sqrt{-A}) \\ \mathcal{E}(u,v) = (\sqrt{-A}u, \sqrt{-A}v). \end{cases}$$

The correspondence is between $\mathcal{E}$ and $-A$ where for any $u \in Dom(A)$, $\mathcal{E}(u,u) = (u, -Au)$. And $Dom(A) \subset Dom(\sqrt{-A})$ is a dense, proper subset. See [31] Thm 1.3.1 or [67] for the proof.

This $-A$ is an operator on the underlying Hilbert space which can be viewed as the generator of a semi-group $\{exp(tA)\}_{t\geq 0}$ or alternatively as the generator of a resolvent via $(\alpha - A)^{-1}$, where these expressions are given meaning by a spectral resolution and the functional calculus for self-adjoint operators. Naturally this induces correspondences between closed symmetric forms, operators, semi-groups of operators, and resolvents.

Definition 4.2.2. A Dirichlet Form, $(\mathcal{E}, Dom(\mathcal{E}))$, is a closed bilinear symmetric form on $L^2(X,\mu) = H$ such that if $u \in Dom(\mathcal{E}) \subset H$ then $(u \vee 0) \wedge 1 \in Dom(\mathcal{E})$ and $\mathcal{E}((u \vee 0) \wedge 1, (u \vee 0) \wedge 1) \leq \mathcal{E}(u,u)$. This type of contraction of u is called a unit contraction.

In [31] instead of the $(u \vee 0) \wedge 1$ being again in the domain the authors use a differentiable function $\phi(x)$ being in the domain where $\phi(x) = x$ for $x \in [0,1]$, $\phi(x) \in [-\epsilon, 1+\epsilon]$, $0 \leq \phi'(x) \leq 1$, $\forall x \in \mathbb{R}$. Contraction of $u(x)$ by composition with $\phi(x)$ is just a type of contraction is a normal contraction. However the uit contraction and normal contraction are equivalent when the form is closed.

The adjective Markovian applies to operators, semi-groups of operators, and symmetric forms. Due to the connection between semi-groups and symmetric forms the usages correspond to each other, but before we state that correspondence we set out what those properties are in each case:

- Bounded Linear Operator: An operator, S, is Markovian if for all $0 \leq u \leq 1$ it is the case that $0 \leq Su \leq 1$, where the inequalities hold almost everywhere.
- Semi-group: A semi-group of bounded linear operators, $\{T_t, t \geq 0\}$, is Markovian if for all $t \geq 0$ the operator T_t is Markovian.
- Symmetric Form: A symmetric form, D, is Markovian if for all $\epsilon > 0$ there is a non-decreasing, differentiable function $\phi_\epsilon(t)$ such that $\phi_\epsilon(t) = t$ if $t \in [0,1]$, $-\epsilon < \phi_\epsilon(t) < 1 + \epsilon$, and $\phi_\epsilon(t') - \phi_\epsilon(t) \leq t' - t$, and $u \in Dom(D) \Rightarrow \phi_\epsilon(u) \in Dom(D)$. If $Dom(D)$ is closed this is equivalent to the unit contraction $(u \vee 0) \wedge 1 \in Dom(D)$ and $\mathcal{E}((u \vee 0) \wedge 1, (u \vee 0) \wedge 1) \leq \mathcal{E}(u,u)$ and is defined above.

Notice that a Markovian symmetric form has all the properties of a Dirichlet form except being closed.

Theorem 4.2.3. Let $\mathcal{E}$ be a closed symmetric form on $L^2(X,m)$. Let $\{T_t, t > 0\}$ and $\{G_\alpha, \alpha > 0\}$ be the strongly continuous semigroup and the strongly continuous resolvent on $L^2(X,m)$ which are associated with $\mathcal{E}$. Then the following are equivalent:

1. T_t is Markovian for each $t > 0$.
2. αG_α is Markovian for each $\alpha > 0$.
3. $\mathcal{E}$ is Markovian, i.e. a Dirichlet form.
4. For any $u \in Dom(\mathcal{E})$, $(u \vee 0) \wedge 1 \in Dom(D)$ and $\mathcal{E}((u \vee 0) \wedge 1, (u \vee 0) \wedge 1) \leq \mathcal{E}(u,u)$. This is referred to as the unit contraction "operating" on $\mathcal{E}$.

5. For any $u \in Dom(\mathcal{E})$, $\phi_\epsilon(u) \in Dom(\mathcal{E})$ and $\mathcal{E}(\phi_\epsilon(u), \phi_\epsilon(u)) \leq \mathcal{E}(u, u)$. This is referred to as the normal contraction "operating" on $\mathcal{E}$.

See [31] Thm 1.4.1 for the proof.

This theorem states that the use of the word Markovian in these different settings is an appropriate use of terminology. At the end of the next group of definitions and theorems these contexts will be connected to stochastic processes in which the word Markovian was first used.

We define the basic probabilistic objects and notation that we will need to be able to state which processes the Dirichlet forms will correspond. Denote by Ω a sample space, $\mathcal{F}$ a $\sigma-$field on Ω, X_t a process which is adapted to the filtration $\mathcal{F}_t \subset \mathcal{F}$, P^x is the law of X_t when $X_0 = x$. Denote by S the state space of X_t with Borel field, $\mathcal{B}$. Adjoin a point, Δ, to S to serve as a cemetery point. Let $S_\Delta = S \cup \{\Delta\}$ and $\mathcal{B}_\Delta = \mathcal{B} \cup \{B \cup \Delta : B \in \mathcal{B}\}$. Later in the paper we will use the Laakso fractals and approximations to them as state spaces.

Definition 4.2.4. A quintuplet $(\Omega, \mathcal{F}, \mathcal{F}_t, \{X_t\}, \{P^x\} : t \in [0, \infty], x \in S_\Delta)$ is a Markov process if the following conditions hold:

1. The quintuplet is a progressively measurable stochastic process with t as the time parameter and $(S_\Delta, \mathcal{B}_\Delta)$ as its state space.

2. There exists an admissible filtration $\{\mathcal{M}_t\}_{t \geq 0}$ which has the property that for each $x \in S$,

$$P^x(X_{s+t} \in E | \mathcal{M}_t) = P^{X_t}(X_s \in E) \ a.s.$$

   For any $s, t \geq 0$ and $E \in \mathcal{B}$.

3. $P^x(X_t \in E)$ is $\mathcal{B}$-measurable as a function of x for all $t \geq 0$ and $E \in \mathcal{B}$ and $P^x(X_0 = x) = 1$.

4. $P^\Delta(X_t = \Delta) = 1$ for all $t \geq 0$.

Adjoining the cemetery point compactifies the state space and assures that the associated symmetric form is conservative. However, in our case all of the state spaces will already be compact and we can take the cemetery as an inaccessible state and still have conservative symmetric forms.

To each Markov process, X_t, associate the transition function, $p_t(x, A) = P^x(X_t \in A)$ where A is a Borel subset of S which acts on functions by $p_t u(x) = \int u(y) p_t(x, dy)$. If only a single probability measure is given on the sample space Ω, then one can use a similar definition $p_t(x, A) = \mathbb{P}(X_t(\omega) \in A | X_0(\omega) = x)$ where $\mathbb{P}$ is the given probability measure. For each $t > 0$ $p_t(x, A)$ is a kernel, and a Markovian kernel if $p_s p_t = p_{s+t}$ and $0 \leq p_t(x, A) \leq 1$. Then $\{p_t\}$, integration against which is a symmetric operator, generates a semi-group of symmetric integral operators on

L^2 for each $t > 0$, called T_t. We will need strongly continuous semigroups for the correspondence to Dirichlet forms, so to ensure that T_t is strongly continuous at zero we have the following criterion:

Lemma 4.2.5. If $p_t(x, A)$ is a symmetric Markovian transition function and T_t the associated semi-group of operators. Then T_t is strongly continuous at zero if $\lim_{t\downarrow 0} p_t u(x) = u(x)$ *a.e.* for u that are continuous with compact support in S.

This next theorem gives the next piece of the correspondence. But first we need another definition.

Definition 4.2.6. A Hunt process is a Markov process which almost surely has right continuous and left quasi-continuous sample paths. See [31] for more on quasi-continuity. A diffusion is a Markov process that almost surely has continuous sample paths. A Hunt or diffusion diffusion is symmetric if its infinitesimal generator is a symmetric operator, or equivalently the associated heat kernel is symmetric in the spacial coordinates.

Theorem 4.2.7. There is a one to one, up to equivalence, correspondence between symmetric Markovian transition semi-groups and symmetric Hunt processes.

Proof. This is a combination of Theorems 7.2.5 and 4.2.7 of [31]. ***Qed***

The correspondence between a Hunt process and a Dirichlet form is through the semi-group generated by the process and the associated infinitesimal generator. This generator is the operator defined by the Dirichlet form, the $-A$ in the notation used in the definition of Dirichlet form above. Since we are often interested in looking at processes with continuous sample paths we note that continuity of sample paths translates along the correspondence to the Dirichlet form having the local property.

Definition 4.2.8. A Dirichlet form, $\mathcal{E}$ is regular if the compactly supported continuous functions in $Dom(\mathcal{E})$ are dense in $Dom(\mathcal{E})$ under the $\|u\| = \mathcal{E}(u, u)+(u, u)$ norm, and $Dom(\mathcal{E})$ is sup norm dense in the space of compactly supported continuous functions on the underlying space.

A Dirichlet form, $\mathcal{E}$, possesses the local property if for any $u, v \in Dom(\mathcal{E})$ which have compact, disjoint support then $\mathcal{E}(u, v) = 0$.

We now have all the pieces to be able to state the final and most specific correspondence that we will mention in this section.

Theorem 4.2.9. The following two conditions are equivalent to each other for a regular Dirichlet form $\mathcal{E}$ on $L^2(X, \mu)$:

1. $\mathcal{E}$ possesses the local property.

2. There exists a μ-symmetric diffusion process on $(X, \mathcal{B}(X))$ whose Dirichlet form is the given one, $\mathcal{E}$.

This is Theorem 7.2.2 from [31].

Another property of Markov processes will become important later in the paper so we give the definition of Feller processes here. Let

$$C_\infty(X) = \{f \in C(X) : \forall \epsilon > 0,\ \exists K\ compact, |f(x)| < \epsilon, \forall x \in X \setminus K\}.$$

This is the space of functions vanishing at infinity. When X is itself compact $C_\infty(X) = C(X)$.

Definition 4.2.10. [31] A Markov process is *Feller* if the associated resolvent G_λ has the following property:

$$G_\lambda C_\infty(X) \subset C_\infty(X)$$

That is that the resolvent maps continuous functions vanishing at infinity into continuous functions vanishing at infinity. for all $\lambda > 0$.

There are variations on the definition of Feller processes in the literature. For example in [64] it is the semi-group P_t that is considered and not the resolvent. The Hille-Yosida theorem which gives the relation between resolvents and semi-groups shows that the two approaches yield the same results.

4.3 Laakso Construction

This construction was first presented in [52] as a way to provide examples of metric-measure spaces with nice analytic properties e.g. a Poincaré inequality, of any arbitrary Hausdorff dimension greater than one. The original treatment made no mention of any probabilistic structures associated with the constructed space, though minimal upper gradients were shown to exist. For more on minimal upper gradients see [22]. All of these spaces will have a cell structure, and for a countable collection of Q the cell structure will be self-similar, making these self-similar spaces fractals.

We first mention a few facts about Cantor sets. The standard Cantor set can be constructed with two affine contraction mappings. One, ψ_1, mapping the interval $[0, 1]$ to $[0, \frac{1}{3}]$ and the other, ψ_2, mapping $[0, 1]$ to $[\frac{2}{3}, 1]$. Then the Cantor set can be defined as the unique non-empty compact subset of $\mathbb{R}$, K, such that $K = \psi_1(K) \cup \psi_2(K)$. The Cantor set has Hausdorff dimension $\ln(2)/\ln(3)$ where the two is the number of contraction mappings and the one third the contraction factor, see [28] for more about the dimension of self-similar sets. One can change the Hausdorff dimension by altering the contraction factor to be anything in $(0, \frac{1}{2})$. The cell structure of Cantor sets is defined below. The properties of the cell structure, associated contraction mapping, and exactly calculable Hausdorff dimension extend to products of Cantor sets.

Definition 4.3.1. The zero level cell is K, the entire Cantor set. If ψ_1 and ψ_2 are the contraction mappings that define the Cantor set K by the relation $K = \psi_1(K) \cup \psi_2(K)$ then K is the zero-level cell, $\psi_i(K)$ is a first level cell, $\psi_i(\psi_j(K))$ is a second level cell, and so on. A cell of a Cantor set is a cell of any level. The cell structure of a Cantor set is the set of all the cells of every level.

For a given dimension, $Q > 1$, we begin with two spaces. The first is a Euclidean space, $I = [0, 1]$. The second is a product of cantor sets, K^k where each K has Hausdorff dimension $\frac{Q-1}{k}$ so that the product has dimension $Q - 1$. Consider the product space $I \times K^k$, where the measure is the product of the Lebesgue measure on I and the product Bernoulli measure on K. Note that $I \times K^k$ has total measure one. The fractal, L, will be the quotient space of $I \times K^k$ by an equivalence relation where the identifications will be made on a null set so that there will be a natural, induced measure μ on L that is Borel regular.

To be able to find where the identifications will be made we need a number derived from the desired dimension of K. Let $t \in (0, 1)$ such that $\ln(2)/\ln(1/t) = \frac{Q-1}{k}$ where k is chosen large enough so that $\frac{Q-1}{k} \in (0, 1)$. This gives a t to be used as the contraction factor in the iterative construction of the Cantor set, the fraction of the length of an interval at the mth step that the intervals at the $m + 1$st level are. This gives a natural decomposition of $K = tK \cup (tK + 1 - t)$. When we take the product $I \times K^k$ it will have dimension Q. It is necessary to have a way of describing the location of a point in the Cantor sets with an "address." Call $K_0 := tK$ and $K_1 := tK + 1 - t$ then K_{00} is the left part of the left part of K i.e. t^2K. This naming scheme can be continued and associates to each point $x \in K$ an address $a = a_1a_2a_3 \ldots$ so that $x = K_a$. Finite addresses indicate subsets of K and can be concatenated to produce the addresses of still smaller subsets. If a is a finite address let $|a|$ be its length. This scheme for labeling the points of a self-similar space is heavily used in [43].

For the given t there exists an integer j such that $\frac{1}{j+1} < t \leq \frac{1}{j}$. Then there is a sequence $j_i \in \{j, j + 1\}$ such that

$$\frac{j}{j+1} \prod_{i=1}^{m} j_i^{-1} \leq t^m \leq \frac{j+1}{j} \prod_{i=1}^{m} j_i^{-1}. \tag{4.3.1}$$

Now define a function w which will pinpoint exactly where each level of identifications will occur.

Definition 4.3.2. For $l \geq 1$, define the function

$$w(m_1, \cdots, m_l) = \sum_{i=1}^{l} m_i \prod_{h=1}^{i} j_h^{-1} \tag{4.3.2}$$

Where $0 \leq m_i < j_i$ for $i < l$ and when $i = l$ $0 < m_l < j_l$. The values of $w(m_1, \cdots, m_l)$ give the locations of the lth level wormholes in the I coordinate.

The condition on m_l forces the wormholes to not stack up on each other by forbidding l-level wormholes from being located over any lower level wormholes. Suppose that there are k Cantor sets used in constructing a particular Laakso space, then we consider the set of points in I with coordinates taken from the values of $w(m_1, \cdots, m_l)$ and let $(x_1, x_2, \ldots, x_{k+1})$ be a point with first coordinate in I and the rest of the coordinates in K^k_{a0} where a is an address with length $k-1$. We identify $(x_1, x_2, \ldots, x_{k+1}) \in I \times K^k_{a0}$ with $(y_1, y_2, \ldots, y_{k+1}) \in I \times K^k_{a1}$ if and only if the length of a is $l-1$, $x_1 = y_1$ is a value of $w(m_1, \cdots, m_l)$, and $y_i = x_i + t^{l-1}(1-t)$. We make these identifications iteratively for all l. The points at which these identifications are made are known as wormholes.

Definition 4.3.3. Denote the identification map sending $I \times K^k$ to L by ι.

The space L has, by construction, a cell structure already in the K^k as each one of these Cantor sets has the normal cell structure. If the j_i are also periodic, then there is self-similarity in the I direction as well. Say that the j_i have period p, then let a cell of L be the image under the identification map of the set $[m/d_p, (m+1)/d_p] \times K^k_{a_i}$ where $m = 0, 1, \cdots r$ where $d_p = \prod_{l=1}^{p} j_l$ and the a_i are addresses of length p and there is one (potentially different) address for each copy of K used. Any function defined on L can be defined on $I \times K^k$ as a pullback by the identification map. So a function $f : L \to \mathbb{R}$ can alternatively be worked with as $\hat{f}(x, w) = f \circ \iota : I \times K^k \to \mathbb{R}, x \in I, w \in K^k$ as well.

A simple approach to showing a space metrizable is to construct a metric. The most natural metric on this space is a geodesic metric where the distance between two points is the infimum of lengths of all rectifiable paths connecting the two points. The existence of rectifiable curves connecting any two points in L, which implies that the space is connected and that the geodesic metric is well defined, is shown in [52].

Laakso's construction gives an easy to use measure, namely the product measure on $I \times K^k$ carried down by the identification map. This measure is equivalent the Q-Hausdorff measure on L. We now summarize the basic properties of L before moving onto defining function spaces.

Theorem 4.3.4. The space L is a connected metric measure space which is Ahlfors regular of dimension Q.

This is the central result of [52].

It is worth taking some care in understanding how the geodesic metric behaves on L. The length of a rectifiable path comes entirely from the distance that it travels in the I direction since traversing a wormhole to move from one copy of I to another costs no length. One can then use the arc length parameterization of a path to induce a measure on the image of that path. These measures are the one dimensional Lebesgue-Stieltjes measures associated to the rectifiable paths.

Call these measures dm, but keep in mind that they are dependent on the specific path over which the integral is taken.

Definition 4.3.5. On a metric measure space, $(X, |\cdot|)$, a minimal generalized upper gradient of a function u is a non-negative function p_u with the following property:

$$|u(x) - u(y)| \leq \int_\gamma p_u \, dm$$

For any pair of points $x, y \in X$ and rectifiable curve $\gamma(t) \subset X$ such that $\gamma(0) = x$ and $\gamma(1) = y$ and any other function with this same property is almost everywhere greater than or equal to p_u and the measure dm is the measure induced by γ.

It is a simple matter to note that the function $p = \infty$ is a generalized upper gradient. Thus a generalized upper gradient exists for any function. We follow Cheeger [22] in viewing the set of functions in $L^p(L)$ that have a generalized upper gradient also in $L^p(L)$ as a Sobolev space, $H^{1,p}$. If $p > 1$ then there exists a unique minimal generalized upper gradient. A more complete overview of abstract Sobolev spaces is at the end of the next section. It is more convenient to be able to speak of only one upper gradient, this is fine so long as $p > 1$.

Theorem 4.3.6. [22] For $1 < p < \infty$ if $f \in H^{1,p}$ there exists a minimal generalized upper gradient which is unique up to modification on sets of measure zero.

The intuition behind this theorem is that for $p > 1$ L^p is a convex space, so minimizing sequences of generalized upper gradients actually have a unique limit point. The rest of the proof is checking that the limit is again a generalized upper gradient.

Note that in a Euclidean space for differentiable functions the minimal generalized upper gradient is the norm of the usual gradient, $p_u = |\nabla u|$, so in a sense p_u plays the same role as the absolute value of a more general first derivative. With this generalized minimal upper gradient we have, from [52], a weak $(1,1)-$Poincaré inequality:

$$\int_B |u - u_B| \, d\mu \leq C(diam(B)) \left(\int_{CB} p_u \, d\mu \right).$$

Here $B \subset L$ is a ball, μ is the measure on L, and C is a constant.

4.4 A Space of Smooth Functions

In this section we define a space of functions, $\mathcal{G}$, on L which will serve as a core for the Dirichlet form that is defined in the next section. We then prove that for

these functions the minimal generalized upper gradient is easy to describe. For notational simplicity we assume that $k = 1$, that only one Cantor set is being used in the construction. Finally we define a Sobolev space based on minimal generalized upper gradients.

Definition 4.4.1. For a function $f \in C(L)$ denote by $\hat{f}(x, w) : I \times K \to \mathbb{R}$ the pulled back function $f \circ \iota$ (c.f. Definition 4.3.3).

Definition 4.4.2. If $f \in C(L)$ and for $\hat{f}(x, w)$ there exists an $n \geq 0$ such that when K is decomposed into cells of depth n and these two conditions are met:

- for a fixed $x \in I$ the function $\hat{f}(x, \cdot)$ is constant on each cell of K (see Definition 4.3.1);
- for a fixed $w \in K$ the function $\hat{f}(\cdot, w)$ is continuously differentiable between wormhole locations of depth n or less with finite limits at the wormhole locations;

then we say that $f \in \mathcal{G}_n$. Let $\mathcal{G} = \bigcup_{n=0}^{\infty} \mathcal{G}_n$.

When we pull back to a function $f \circ \iota = \hat{f}(x, w)$ to $I \times K$ the infinitely many identifications are already accounted for by having started with precisely those functions in $f \in C(L)$. The main point of this definition is to be able to analyze $f \in C(L)$ in terms of it's "directional" behavior which doesn't become well defined until f is pulled back to $\hat{f}(x, w) = f \circ \iota$. Also in this definition when we define $\mathcal{G}_n$ and force the functions to be constant on each nth level cell for a given $x \in I$ we are in effect treating the product of an interval between two wormhole locations crossed with cell of K as a single line segment making $I \times K$ look like a quantum graph. Increasing n then increases the complexity of this graph allowing for more functions on L to be included. This intuition will be revisited in Section 4.8.

Lemma 4.4.3. The space $\mathcal{G}$ is dense in the continuous functions on L in the supremum norm.

Proof. To use the Stone-Weierstrass Theorem we need to show that the algebra $\mathcal{G}$ separates points and contains the constant functions. Constant functions are all elements of $\mathcal{G}_0 \subset \mathcal{G}$. Let $p, q \in L$ be distinct points. Then they either have different coordinates in the I direction or they don't. If they do then $\hat{f}(x, w) = x \in \iota^* \mathcal{G}_0$ and will separate the points p and q. The space $\iota^* \mathcal{G}_0$ consists of all of the pull backs of functions in $\mathcal{G}_0$ to functions on $I \times K$, so there exists a function $f \in \mathcal{G}$ such that $\hat{f} = x$ and it will separate p and q. If p and q have the same coordinate in the I direction, say $x_0 \in I$, then they must have different coordinates in the K direction which can be distinguished by cells of some finite level, say $p = \iota(p(x_0, w_1))$ and $q = \iota(q(x_0, w_2))$ where $w_1, w_2 \in K$ are in different nth level cells of K, call them K_1 and K_2. To construct a separating function $\hat{f}(x, w)$ in this case if p and q are

in different nth level cells and not at a wormhole of level n or lower then there are wormholes with locations $y < x_0 < z$ such that they are the closest to x_0. Let

$$\hat{f}(x,w) = \begin{cases} (x-y)(x-z) & x \in (y,z), w \in K_1 \\ -(x-y)(x-z) & x \in (y,z), w \in K_2 \\ 0 & otherwise \end{cases} .$$

Then $\hat{f}(x,w)$ is defined on finite level cells and is piecewise defined from differentiable functions $\hat{f}(x,w) \in \iota^*\mathcal{G}$ and $f(p) = -f(q) \neq 0$. If x_0 is the location of an nth level wormhole simply use the same process with $n+1$ level cells of K. That this function is the pull back of a well defined function on L holds by checking that the first n levels of identifications in the construction of L are respected and that any lower level of identification are as well.

The regions in L defined by $\iota([y,z] \times K_i)$ are actually nth level cells of L because the number of wormholes at each level can be chosen randomly ($\{j_i\}$ need have no pattern) L is not necessarily a self-similar fractal so there aren't analogues to the ψ_i in Definition 4.3.1 to be used in defining a cell structure. We use a notion of cell structure based on Definition 2.1 in [75] that does not rely on self-similarity. In this notion the cells are a family of subsets for each scale of L, $\{F_\alpha\}_{\alpha \in A}$ along with a family of boundaries $\{B_\alpha\}_{\alpha \in A}$, where $F_\alpha \cap F_{\alpha'} = B_\alpha \cap B_{\alpha'}$. This condition states that the intersection of two cells is the intersection of their boundaries. The situation in [75] is one where these boundaries are finite sets of vertices, but each boundary of a cell in a Laakso space is a Cantor set. To see why the cells $\iota([y,z] \times K_i), i = 1,2$ have disjoint interiors in L it becomes necessary to know how a path from a point in $\iota(I \times K_1)$ could reach a point in $\iota(I \times K_2)$. When we defined the identification maps nth level cells could only be connected by nth level and lower (i.e. $n-1$ level) wormholes so if no such wormholes are in the interior of cells then the cells can at most share their boundaries which is no obstacle to defining our function since it is zero on the boundary of the two cells so when these sets are mapped back into L their interiors remain disjoint. ***Qed***

Theorem 4.4.4. For $f \in \mathcal{G}_n \subset \mathcal{G}$ and q not a wormhole i.e. $\iota^{-1}(q) = (x,w)$ and $x \neq w(m_1, m_2, \ldots, m_k)$ for any $k \leq n$ (see Definition 4.3.2 and following for the definition of this function), $p_f(q) = \left|\frac{\partial}{\partial x}\hat{f}(\iota^{-1}(q))\right|$ where x is the I coordinate in $I \times K$ and $q \in L$ for μ-a.e. $q \in L$.

The set of wormholes forms a set of measure zero and are ignored since minimal generalized upper gradients are only defined almost everywhere. As a short hand we denote $\left|\frac{\partial}{\partial x}\hat{f}(\iota^{-1}(q))\right|$ as $|\frac{\partial}{\partial x}f|$.

Proof. First we show that $\left|\frac{\partial}{\partial x}\right|$ is a generalized upper gradient then we show that it is the minimal one. Given the boundedness assured in the definition of $\mathcal{G}$, this upper gradient is also integrable and square integrable. Now take two points

$x, y \in L$ and a rectifiable path connecting them, γ. When γ is pulled back to $\tilde{\gamma}$ on $I \times K$ there is ambiguity at each wormhole that γ goes through so make the choices that make the lifted $\tilde{\gamma}$ right continuous and have left limits in the time parameter. Because $f \in \mathcal{G}$ it is associated to a decomposition of K into cells of some finite level. Then even if $\tilde{\gamma}$ is completely disconnected it must have some length in the I direction in each cell that is passes through. This is because the only way a wormhole can provide a path out of an nth level cell is for the wormhole to be at most of depth $n-1$ which are evenly spaced. Let $x = z_0$ is in one of the cells of K, let z_1 be the point in L when $\tilde{\gamma}$ first leaves this cell, z_2 the point in L when $\tilde{\gamma}$ first leaves that that cell, and so on. Since γ is a rectifiable path it has finite length and γ will only transit finitely many of these cell at most countably many times, with possible repeats. So let z_m be the mth crossing from one cell to another and $z_\infty = y$. It may happen that the path only moves from one cell to another finitely many times, in that case the modification is obvious.

In each nth level cell of K the requirement that $\hat{f}(x, w)$ be constant across the cell for a given $x \in I$ means that in each nth level cell of K $\hat{f}(x, w)$ is a piecewise differentiable function in x. This means that along the path $\tilde{\gamma}$, as it passes through a cell, standard calculus methods can be used to determine an upper gradient in that cell, which will be the usual $\left|\frac{\partial}{\partial x} f\right|$. Since this can be done for each of the countably many transits that $\tilde{\gamma}$ makes through the cells and in fact for any $\tilde{\gamma}$ that we may have chosen we use on all cells the generalized upper gradient $\left|\frac{\partial}{\partial x} f\right|$ on all of L

To show minimality we proceed by contradiction. Suppose that there is another generalized upper gradient, p_f which is less than $\left|\frac{\partial}{\partial x} f\right|$ on a set of positive measure, A. Then there is a subset A' of A with positive measure such that $\frac{\partial}{\partial x} f$ is of one sign and this subset contains open sets by the piece wise continuity of the derivatives of functions in $\mathcal{G}$. There is a subset A'' of A' that is contained in a single cell of K^k crossed with some subinterval of I, without loss of generality assume that $\frac{\partial}{\partial x} f$ is positive. Then for p_f to be less than or equal to $\frac{\partial}{\partial x} f$ on a set of positive measure would imply that on one-dimensional intervals that the absolute value of the first derivative is not the minimal generalized upper gradient which is a contradiction. ***Qed***

Definition 4.4.5. The Sobolev space $H^{1,2} \subset L^2(L)$ is defined to be

$$H^{1,2} = \{u \in L^2(L) | \exists p_u, p_u \in L^2(L)\}$$

Where p_u is the minimal upper gradient of u. $H^{1,2}$ is given the graph norm:

$$\|u\| = \left(\int u^2\right)^{1/2} + \left(\int p_u^2\right)^{1/2}.$$

This definition is from [22] where the following lemma is proved (Theorems 2.7 and 2.10).

Lemma 4.4.6. The space $H^{1,2}$ is a complete Banach space and the minimal generalized gradients are unique up to modification on a set of measure zero.

Lemma 4.4.7. The Sobolev space $H^{1,2}$ contains the closure of $\mathcal{G}$ under the graph norm. That is the set

$$\bar{\mathcal{G}} \subset H^{1,2} = \{u \in L^2(L) | \exists p_u, p_u \in L^2(L)\}.$$

Proof. Since the Sobolev space $H^{1,2}$ is complete the only thing that needs to be checked is that $\mathcal{G} \subset H^{1,2}$. Since all elements of $\mathcal{G}$ have bounded derivatives (see Definition 4.4.2) on a finite measure space we see that $\int u^2 < \infty$ and $\int p_u^2 < \infty$ so $\|u\| < \infty$ hence $\mathcal{G} \subset H^{1,2}$. ***Qed***

Theorem 4.4.8. For any $u \in \overline{\mathcal{G}}$ the map $u \mapsto \frac{\partial}{\partial x} u \in L^2(L)$ is well-defined.

Proof. For any function $u \in \mathcal{G}$ the object $\frac{\partial}{\partial x} u$ exists by passing to the pull back, $\hat{u}(x, w)$ where the definition of $\mathcal{G}$ assure us that $\frac{\partial}{\partial x} u$ exists a.e.. Now let $u_n \in \mathcal{G}$ such that $u_n \to u$ in $H^{1,2}$. This convergence implies that $u_n \to u$ in L^2 and $\frac{\partial}{\partial x} u_n$ is Cauchy in L^2. This means that $\frac{\partial}{\partial x} u_n$ converge to an unique element in $L^2(L)$ which we will call $\frac{\partial}{\partial x} u$. In [22] it is shown that $p_u = \lim_{n\to\infty} \left|\frac{\partial}{\partial x} u_n\right|$ is actually the minimal generalized upper gradient of u so $\left|\frac{\partial}{\partial x} u\right| = \lim_{n\to\infty} \left|\frac{\partial}{\partial x} u_n\right| = p_u$. Thus the relationship between p_u and $\frac{\partial}{\partial x} u$ that was observed for $u \in \mathcal{G}$ extends to $\overline{\mathcal{G}}$. ***Qed***

It seems reasonable that the inclusion $H^{1,2} \subset \overline{\mathcal{G}}$ holds as well, but we do not need this currently. It rests on the consideration of whether $\bar{\mathcal{G}}$ is dense in the Lipschitz functions, [34]. This is still an unresolved issue. We continue by defining our Dirichlet form on $\mathcal{G}$ and then take the closure of $\mathcal{G}$ as the domain.

4.5 A Dirichlet Form and Upper Gradients

In this section we show how to use generalized minimal upper gradients to produce a Dirichlet form. We use the space of functions $\mathcal{G}$, see Definition 4.4.2, on which the generalized minimal upper gradients can explicitly be computed. It would be a natural choice to define a Dirichlet form $\mathcal{E}(u, u) = \int_L p_u^2 \, d\mu$ and then use polarization to extend to a bilinear form that would look like $\mathcal{E}(u, v) = \int_L p_u p_v \, d\mu$. This can't be done because $u \mapsto p_u$ is not a linear operator because p_u is a positive function, so setting $p_u = \sqrt{-A}u$ is not a viable definition. Recalling the notation from Section 4.2, we have another option at our disposal. We have the map $u \mapsto \frac{\partial}{\partial x} u$ that can be used instead and since this map is linear the extension to a bilinear form will hold.

Lemma 4.5.1. Let $u \in \bar{\mathcal{G}} = Dom(\mathcal{E})$, let

$$\mathcal{E}(u, u) = \int_L p_u^2 \, d\mu = \int_L \left(\frac{\partial}{\partial x} u\right)^2 \, d\mu.$$

Then $(\mathcal{E}, Dom(\mathcal{E}))$ is a Dirichlet form.

Remark: If $u \in \mathcal{G}$ is such that $\hat{u}(x,w)$ is piecewise twice-differentiable in the I direction with derivatives vanishing on the boundary and have directional derivatives summing to zero at the wormholes. Integration by parts with suitable boundary conditions imposed indicates that we can also express the Dirichlet form as

$$\mathcal{E}(u,u) = -\int_L u\frac{\partial^2 u}{\partial x^2}\, d\mu.$$

The domain of $-\frac{\partial^2}{\partial x^2} = -A$ is a strict, but dense, subset of $\bar{\mathcal{G}} = Dom(\mathcal{E})$.

Proof. By defining $\mathcal{E}$ through polarization it can be seen that $\mathcal{E}$ is a symmetric, quadratic form on $H^{1,2}(L,\mu)$. That $\mathcal{E}$ is closed is ensured by the general construction of the ambient Sobolev space in [22] which addressed Dirichlet forms constructed from minimal generalized upper gradients. This leaves the Markov property to check. Since $\mathcal{E}$ is a closed form it suffices to check the Markov property on $\mathcal{G}$. We shall use Theorem 4.2.3 to use a normal contraction instead of the unit contraction as in our definition. Since the normal contraction ϕ_ϵ is a differentiable function if $u \in \mathcal{G}$ then $\phi_\epsilon \circ u \in \mathcal{G}$ with p_u being a generalized upper gradient for $\phi_\epsilon \circ u$ so that $\mathcal{E}(\phi_\epsilon \circ u, \phi_\epsilon \circ u) \leq \mathcal{E}(u,u)$. It is worth noting that $p_{\phi_\epsilon \circ u}$ is in general point-wise less than p_u. ***Qed***

By this lemma we see that the Dirichlet form $(\mathcal{E}, Dom(\mathcal{E}))$ is generated by the self-adjoint operator $-A$ whose domain is a dense subspace of $Dom(\mathcal{E})$. At present it is unclear whether $Dom(\mathcal{E}) = H^{1,2}$ since this rests on the density of $\mathcal{G} \subset H^{1,2}$ (see the comments after Lemma 4.4.7). However many Dirichlet forms have smaller domains than the ambient Sobolev space so this is not an unusual situation. Consider the application of boundary conditions to the domain of an operator. One could view $Dom(\sqrt{-A})$ as a sort of first order Sobolev space and $Dom(A)$ as a second order Sobolev space. Care must be taken when using this analogy to remember that these spaces are embedded in, but not equal to $H^{1,2}$. The operator, $-A$, comes back in to consideration at the end of the paper. Now we show two properties of $\mathcal{E}$, locality and regularity.

Theorem 4.5.2. The symmetric form $\mathcal{E}$ is a local, regular Dirichlet form whose domain is contained in the Sobolev space $H^{1,2}$ and is the closure of the function space $\mathcal{G}$ under the graph norm associated to the operator $\sqrt{-A}$. For the function spaces this implies that

$$\overline{\mathcal{G}} = Dom(\sqrt{-A}) = Dom(\mathcal{E}).$$

Proof. The only two things left to check are locality and regularity. Locality holds for $u \in \mathcal{G}$ as an immediate consequence of the definition of $\mathcal{G}$ and Theorems 4.4.4 and 4.4.8. Because $\mathcal{E}$ is closed this can be extended to the entire domain of the form. Regularity is a consequence of Lemma 4.4.3 and the definition of $H^{1,2}$. ***Qed***

Corollary 4.5.3. There is a non-trivial Markov process with continuous sample paths on the fractal L.

Proof. Non-triviality follows from $\mathcal{E}(f,f) \neq 0$ when $\hat{f}(x,w) = x^2$. Continuity of sample paths is from Theorem 4.2.9 which requires both the locality and regularity that we have established. ***Qed***

We end this section with an overview of the various definitions of Sobolev spaces with mention of various equivalencies. Much of this discussion is taken from [36]. We begin with a quick summary of what has already been done in this chapter.

What we've done here has been to find a replacement for the norm of the gradient in building up Sobolev spaces on Laakso spaces. This brings the classical notions of Sobolev spaces which may be stated in terms of the Laplacians associated to Dirichlet forms defining the Sobolev space. In the remark after Lemma 4.5.1 we stated what the Laplacian and its domain are. With these two objects in hand we recall the various notions of Sobolev spaces on Euclidean domains.

Historically Sobolev spaces began with function spaces over domains in $\mathbb{R}^n$, such as $W^{1,2}(\mathbb{R})$ which is the space of square integrable functions with square integrable first derivatives. This forces the members of $W^{1,2}$ to have a desired amount of smoothness. Higher derivatives could be required or p-integrability instead of square integrability to get spaces $W^{1,p}$; the latter only changes the exponent in the integrability condition and nothing else in the definition. In the light of distribution theory we might want to ease the smoothness requirement and require that the distributional derivatives be integrable instead of classical derivatives, these spaces are also known as $H^{1,p}$. These spaces coincide with $W^{1,p}$ when the boundary of the domains is sufficiently smooth, so over all of $\mathbb{R}^n$ or on disks they are the same [35]. These definitions still restrict us to spaces locally reminiscent of $\mathbb{R}^n$ to be able to talk about "derivatives."

Hajłasz [33,30] extended the concept of derivativesinto arbitrary metric measure spaces.He defined a space $M^{1,p}$ which consisted of all functions u for which there existed another function g such that for all x, y in the space

$$|u(x) - u(y))| \leq d(x,y)(g(x) + g(y)).$$

This estimate is valid in the classical Sobolev space setting if g is the maximal function of ∇u. We take the norm $\|u\| = \|u\|_p + \inf \|g\|_p$, where the infimum is taken over all g with the required property. In Euclidean spaces $M^{1,p} = W^{1,p}$ [35]. Using upper gradients there is another definition of a Sobolev space in a metric measure space. Shanmugalingam [69] introduced Newtonian Spaces $N^{1,p}$, where a function u is in $N^{1,p}$ if there exists some p_u such that

$$|u(x) - u(y)| \leq \int_\gamma p_u \, dm,$$

for all but a capacity zero set of paths γ connecting x and y. It is known that if the space supports a $(1,q)$-Poincaré inequality then Shanmugalingam's and Hajłasz's Sobolev spaces coincide [34]. We use in this paper Cheeger's [22] version of this type of space, which also relies on upper gradients.

4.6 Barlow-Evans Construction

In [12], Barlow and Evans commented that their construction can also produce Laakso's spaces. They do not, however, prove this statement. This fact is very useful because it lends itself to providing alternative proofs for the existence of Dirichlet forms and Markov processes on Laakso spaces. Towards this end we describe their construction, prove that the Laakso spaces can be constructed this way, and show that there are many Dirichlet forms on Laakso's spaces. Barlow and Evans' construction is based on Evans' previous work with Sowers in [26].

To construct a vermiculated space, L, one needs three ingredients. The first is a state space, F_0, for the base Markov process. We'll take $F_0 = [0,1]$ to construct Laakso spaces. The second is a family of sets, G_n, which at each step of the construction will index the possible alternate universes or copies of F_{n-1} that the process could evolve in, these sets are taken to be $\{0,1\}$ to construct Laakso spaces with dimension less than two. The last ingredient is another family of sets, B_n, which indicate where the identifications or "wormholes" between the $\#G_n$ copies of F_{n-1} are made. It is the sequence $\{B_n\}_{n=1}^{\infty}$ that will determine the metric and then the dimension of L.

We begin with $F_0 = F$, and the sequences $\{G_n\}_{n=1}^{\infty}$, and $\{B_n\}_{n=1}^{\infty}$. The construction is inductive. Define $E_1 = F_0 \times G_1$, $\hat{E}_1 = F_0$, and $A_1 = B_1 \times G_1 \subset E_1$. Note that $B_1 \subset F_0$. The next two functions are defined so as to perform the identifications that will create the next approximation to L, namely F_1. Define $\psi_1 : E_1 \to \hat{E}_1 = F_0$ by $\psi_1(y,z) = y$. Let $\tilde{E}_1 = (E_1 \setminus A_1) \cup \psi_1(A_1)$ with the topology induced by the function

$$\pi_1(y,z) = \begin{cases} (y,z), & if\ y \in F_0 \setminus B_1, \\ y, & if\ y \in B_1; \end{cases}$$

Let $F_1 := \tilde{E}_1$. There is also a continuous surjection $\phi_1 : F_1 \to F_0$ given by

$$\begin{array}{ll} \phi_1(y,z) = y, & (y,z) \in E_1 \setminus A_1 = (F_0 \setminus B_1) \times G_1 \\ \phi_1(y) = y, & y \in \psi_1(A_1) = B_1. \end{array}$$

This construction can be repeated by using F_1, G_2, B_2 to produce F_2 and so on. The set $\{F_n\}_{n=0}^{\infty}$ along with the surjections $\{\phi_{n,m}\}_{n,m=1}^{\infty} : F_m \to F_n$ form a projective system whose inverse limit is the space $\lim_{\leftarrow} F_i \subset \prod_{n=1}^{\infty} F_n$. Due to basic facts from [37] about projective limit spaces $\lim_{\leftarrow} F_i$ is compact and Hausdorff since all of the F_n are compact and Hausdorff.

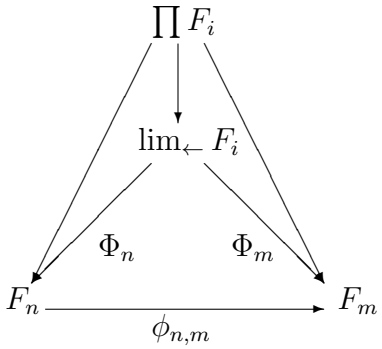

Fig. 4.1: Summary of the Projective System, $n > m \geq 0$

The projective system is summarized in Figure 4.1. In the proof of the following Lemma we describe each of the maps explicitly and then use the Universal Property of Projective Limits to show that the map η in Figure 4.2 is an isometry between the Laakso space and the inverse limit space of the F_n. In our opinion these considerations are best understood in conjunction with the example instead of the abstract terms in the preceding discussion.

The claim of the following Lemma is one of the primary goals of this section, proving that the Barlow-Evans construction can be used to construct Laakso spaces and thus is a more general construction. One of the benefits of using the Barlow-Evans construction is that the existence of Markov processes is also ensured. After this Lemma we will show that there is not one, but many of these Markov processes on L. We believe that Barlow and Evans were aware of a proof of this fact but have not published it.

Lemma 4.6.1. There exists a homeomorphism, η between any Laakso fractal and a vermiculated space.

Proof. First we show that there exists a continuous surjection, η, from a given Laakso space onto a particular Barlow-Evans space which is constructed in the following paragraphs. Then we show that η is also injective with continuous inverse.

This proof is specialized for Laakso spaces with dimension between 1 and 2 to simplify notation. However, for higher dimensions use products of the G_n that we define. Take $F_0 = [0, 1]$ and $G_n = G = \{0, 1\}$. For a given $t \in (0, \frac{1}{2})$ one can find a sequence of $j_m \in \{j, j + 1\}$ where $j \leq t^{-1} < j + 1$. This sequence should be chosen such that

$$\frac{j}{j+1} \prod_{i=1}^{m} j_i^{-1} \leq t^m \leq \frac{j+1}{j} \prod_{i=1}^{m} j_i^{-1}.$$

Note that this is the same sequence of integers that was chosen in the Laakso

construction above, see Equation 4.3.1. Let B_n consist of points of the form

$$w(m_1, m_2, \ldots, m_n) = \sum_{i=1}^{n} m_i \prod_{h=1}^{i} j_h^{-1}$$

Where $0 \leq m_i \leq j_i$ with the additional proviso that $m_n > 0$, and g_n any point in G_n, this is the same function that gave the location of the wormholes in the Laakso construction in Definition 4.3.2 and following. These choices will put wormholes at the same locations in the Barlow Evans construction. This makes $A_n = B_n \times G_n \subset F_{n-1} \times G_n$ as needed. If each $F_{n-1} \times G_n = \hat{E}_n$ is taken to lie in the unit square in $\mathbb{R}^2$ with lower left corner at the origin then then horizontal slices are approaching a Cantor set of the necessary dimension and vertical slices are copies of the unit interval [37, Section 2-14].

Inductively construct the spaces F_i as described above. These spaces come with maps $\phi_{i+1,i} : F_{i+1} \to F_i$. Let $\phi_{i,j} = \phi_{j+1,j} \circ \cdots \circ \phi_{i-1,i} : F_i \to F_j$ for $i > j$. Now consider the space $\prod_{i=0}^{\infty} F_i$, there are projection maps which we will call $\Phi_n : \prod_{i=0}^{\infty} F_i \to F_n$ for all $n \geq 0$. The projective limit space $\lim_{\leftarrow} F_i$ will actually be a subspace of $\prod_{i=0}^{\infty} F_i$ that we can explicitly define. Define $\lim_{\leftarrow} F_i$ to be all elements $\{x_i\}_{i=0}^{\infty} \in \prod_{i=0}^{\infty} F_i$ such that $\phi_{i,j}(x_i) = x_j$ for all $i > j \geq 0$ [37, Page 91]. We can then restrict the maps Φ_n to $\lim_{\leftarrow} F_i$ since it is a subspace of $\prod_{i=0}^{\infty} F_i$ and we will call the restrictions Φ_n as well leaving it to context to make it clear which space they project from. It is important to note how Φ_n and $\phi_{i,j}$ interact since they are all projection operators we have that $\Phi_j = \phi_{i,j} \circ \Phi_i$ for $i > j$. Projective limits are a very general concept that is even treated in Category theory. The most pertinent property of projective limit systems is the universal property. This property is a statement that in a certain sense the projective limit is minimal. Minimality in this sense means that if another topological space L has maps $\tilde{\Phi}_n : L \to F_n$ for all $n \geq 0$ such that $\tilde{\Phi}_j = \phi_{i,j} \circ \tilde{\Phi}_i$ for all $i > j$ that there is an induced a continuous surjection $\eta : L \to \lim_{\leftarrow} F_i$ that factors $\tilde{\Phi}_i$ as $\Phi_i \circ \eta$. The diagram in Figure 4.2. Moreover, this diagram commutes. To show that we can take L to be a given Laakso space we need to construct $\tilde{\Phi}_i$ such that $\tilde{\Phi}_j = \phi_{i,j} \circ \tilde{\Phi}_i$ and then we will know that η is a continuous surjection from a given Laakso space onto the Barlow Evans space constructed to have the same wormholes as the Laakso space.

Let L be a Laakso space, then define $\tilde{\Phi}_i : L \to F_i$ to be given by $\iota_i \circ (id, \pi_i) \circ \iota^{-1}$ where ι is the identification map sending $I \times K$ in the Laakso construction, $(id, \pi_i) : I \times K \to I \times \mathcal{K}$, $\mathcal{K}$ is the collection of cells of the depth i cells of the Cantor set K (a finite set), there is only one copy of K since we have restricted ourselves to spaces with dimension less than two. And ι_i is the identification map that only identifies the wormholes of level i or less. Refer to Section 4.3 for the original discussion of the Laakso space's construction. The composition of these maps is continuous and surjects onto a quantum graph that can be identified with F_i.

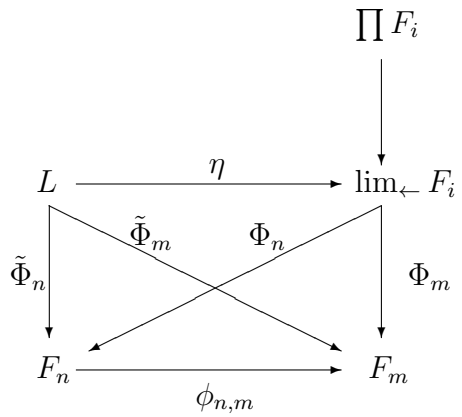

Fig. 4.2: Use of the Universal Property

Since $\pi_i \circ \pi_j = \pi_i$ we will have that $\tilde{\Phi}_j = \phi_{i,j} \circ \tilde{\Phi}_i$ for $i > j \geq 0$. By the universal property of projective limits then map $\eta : L \to \lim_{\leftarrow} F_i$ exists and is a continuous surjection.

It remains to be proved that η is injective and has continuous inverse. Both families Φ_i and $\tilde{\Phi}_i$ separate points. For Φ_i this is because if they didn't separate two points the construction of the projective limit would have made them the same point. For the $\tilde{\Phi}_i$ it is because any two points in L can eventually be distinguished by cells in the Cantor set of some finite level or by I-coordinate. Suppose that η is not injective then there exists distinct $p, q \in L$ such that $\eta(p) = \eta(q)$. Thus $\Phi_i(\eta(p)) = \Phi_i(\eta(q))$ for all $i \geq 0$. But $\tilde{\Phi}_i(p) \neq \tilde{\Phi}_i(q)$ for some i since $p \neq q$. Since the diagram in Figure 4.2 is a commutative diagram $\Phi_i \circ \eta = \tilde{\Phi}_i$ and we have a contradiction to the commutativity of the diagram. Thus η is bijective. Since η is a continuous bijection from a compact Hausdorff space into a Hausdorff space, it is a homeomorphism. ***Qed***

We have shown that $\eta(L) = \lim_{\leftarrow} F_i$ and that η is a homeomorphism so for the rest of the paper we will simply say that $L = \lim_{\leftarrow} F_i$ and identify the function spaces as well.

Since we are interested in processes on the limit space we need to also consider a projective system of measures as well. Recall that $\Phi_n : L \to F_n$ is a projection from the limit space to the *nth* approximating space, then $\Phi_n^* : B(F_n) \to B(L)$ maps the functions spaces by composition i.e. $\Phi_n^*(f) = f \circ \Phi_n^*$. If we use Φ_n^* to map indicator functions we can use Φ_n^* to map sets from the finite approximation spaces to the limit space. In our example on each F_n there is a measure, μ_n, that is a weighted one-dimensional Lebesgue measure on the Quantum graph with total mass one. Alternatively it can be viewed as the measure induced in the quotient space F_n by Lebesgue measure on $F_{n-1} \times G_n$. To be a projective system

of measures the collection $\{\mu_n\}$ must be compatible

$$\mu_{n+1}(\phi^*_{n+1,n}A) = \mu_n(A)$$

For $A \in B(F_n)$ and $\phi^*_{n+1,n} : B(F_n) \to B(F_{n+1})$ defined the same way as Φ^*_n. The μ_n have bounded total mass so by [21, Prop 8, III.50] there is a unique limit measure such that $\mu_\infty(\Phi^*_n U) = \mu_n(U)$ if U is a measurable subset of F_n. The concern will be if this measure μ_∞ can be given in concrete terms adapted to our situation. That is represent it in a way such that it can be worked with. Here we show it to be the same measure as obtained from the Laakso construction.

Lemma 4.6.2. Let μ be the measure obtained in the Laakso construction and μ_∞ the measure obtained from the Barlow-Evans construction. Then $\mu = \mu_\infty$.

Proof. Since we know that the spaces $\lim_{\leftarrow} F_i$ and L are topologically the same and we have a subbasis for the topology in both, which generates the $\sigma-$algebra on which the measures are defined. Since the measures are finite, as long as they agree on the algebra generated by the basis elements the measures will agree on all measurable sets. We take as subbasis elements $(r,s) \times K_{a_1} \times \cdots \times Ka_n$ where r, s are *not* wormholes and the a_i are finite length addresses. The intersection of two elements of this subbasis is again an element of the subbasis. Call the measure on the Laakso construction μ to distinguish it from μ_∞. Then $\mu((r,s) \times K_{a_1} \times \cdots \times Ka_n) = |r-s|2^{-|a_1|} \cdots 2^{-|a_n|}$, where $|a_i|$ is the length of the address a_i. If the maximum length of the a_i is M then $(r,s) \times K_{a_1} \times \cdots \times Ka_n$ is the image under Φ^*_M of some rectangle-like set in F_M which has μ_M measure $|r-s| \times 2^{-|a_i|} \cdots 2^{-|a_n|}$. Since μ_M is the product measure with identifications on a set of measure zero it agrees with μ. Since these sets generate the Borel $\sigma-$algebra both μ and μ_∞ are extensions of the same finite pre-measure and so are equal. Thus the the map η from the proof of the previous theorem is a measure preserving homeomorphism. ***Qed***

Before moving onto considering random processes on these two spaces we take advantage of the measure preserving isometry η. It is a recapitulation of the preceding results.

Remark: The spaces L and $\lim_{\leftarrow} F_i$ are identified through the map η. The Sobolev space $H^{1,2}(L)$ is naturally identified with a function space on $\lim_{\leftarrow} F_i$ via composition with the map $\eta^{-1} : \lim_{\leftarrow} F_i \mapsto L$ which is also called $H^{1,2}$. Similarly with any function space, such as L^2, $Dom(A)$, or $Dom(\mathcal{E})$, on either L and $\lim_{\leftarrow} F_i$ are identified. Since η is an isometry between L and $\lim_{\leftarrow} F_i$ then for $f : L \to \mathbb{R}$ we have $f \circ \eta : \lim_{\leftarrow} F_i \to \mathbb{R}$ and for $g : \lim_{\leftarrow} F_i \to \mathbb{R}$ we have $g \circ \eta^{-1} : L \to \mathbb{R}$. Because η is itself a continuous bijection pre-composing with η or η^{-1} a function space on either L or $\lim_{\leftarrow} F_i$ can be viewed as a function space on the other.

The Sobolev space $H^{1,2}$ is defined in Definition 4.4.5. In Lemma 4.5.1, the spaces $Dom(\mathcal{E})$ and $Dom(A)$ are defined as the domains of the Dirichlet Form on

the Laakso construction and the domain of the associated Laplacian. Note that this is not yet enough to show that any of the function spaces, other than the continuous functions, defined via the Laakso construction or the Barlow Evans construction coincide this is addressed in the remaining sections.

4.7 Processes on Barlow-Evans Spaces

In [12], Barlow and Evans present not only a construction of state spaces using projective limits but also sufficient conditions on a base Markov process on F_0 so that a Markov process on the limit space can be constructed. They show this process to be a Hunt process. We maintain the notation from the previous section concerning the names of sets involved in the Barlow-Evans construction, but from now on we'll only consider the process on F_0 to be reflected Brownian motion on the unit interval.

Assumption: Write $\mathcal{C}$ for the collection consisting of the empty set and finite unions of sets drawn from $B_1, B_2, \ldots$. Assume that for each $C \in \mathcal{C}$ that the resolvent of the process X_t^0 stopped on hitting C maps $C(F_0)$ into itself.

We use this assumption in the context where X_t^0 is the Markov process on F_0 that we wish to extend. This assumption is much stronger than saying that X_t^0 is a Feller process and will allow us to show that X_t^n is Feller as well. We note that standard Brownian motion on a line fits the assumption but Brownian motion on the plane does not [12] if the sets in $\mathcal{C}$ are finite sets of singletons.

Proposition 4.7.1. One-dimensional reflected Brownian motion on the unit interval satisfies the assumption with the B_i being finite point subsets of the unit interval.

Proof. Given any finite set of points in the unit interval, B, and a Brownian motion starting at any point and stopped at B the Brownian motion will behave, including its resolvent, like Brownian motion on an interval of finite, and possibly zero, length where the endpoints stop the process. Since Brownian motion has continuous sample paths it cannot escape from between which ever two points of B it started between. Thus as long as Brownian motion stopped at end points has a resolvent that maps continuous functions to continuous functions this assumption will be satisfied.

The resolvent map as defined by $f \mapsto (\alpha - \Delta)^{-1} f = g$ with Dirichlet boundary conditions to describe the absorbing boundaries of the process on this interval is an ODE which has a differentiable solution. So $(\alpha - \Delta)^{-1} C(F_0) \subset C(F_0)$. ***Qed***

The process of constructing a sequence of Markov processes on the space F_n is a repeated use of the method set forth in [26] whereby the process X_t^{n+1} on F_{n+1} is constructed from X_t^n by extending the resolvents U_α^n associated to X_t^n to be resolvents U_α^{n+1} on F_{n+1}. These resolvents U_α^{n+1} are then associated to a Markov

process which is called X_t^{n+1} which evolves on F_{n+1}. The limiting process which gives U_α^∞, the resolvent for the limit process, is described by Barlow and Evans in [12]. We are going to use Theorem 4.2.9 to link the limit process, X_t^∞, to a Dirichlet form, $\tilde{\mathcal{E}}$, that can be compared to the Dirichlet form, $\mathcal{E}$, from Section 4.5. The hypotheses of Theorem 4.2.9 must be checked, the first of which is symmetry of the process.

Lemma 4.7.2. The Markov process on L built from a Markov process X_t on F_0 is symmetric with respect to the measure μ_∞ if X_t^0 is symmetric on F_0 with respect to Lebesgue measure on the unit interval.

Proof. It follows by construction that $\bigcup_n \Phi_n^* C(F_n)$ is dense in $C(L)$ [12], where $C(F_n)$ are the continuous functions on F_n. So to talk about the symmetry of U_α^∞ it is sufficient to consider only functions from $\bigcup_n \Phi_n^* C(F_n)$. Then if $f, g \in \bigcup_n \Phi_n^* C(F_n)$ we have $f = \Phi_N^* \tilde{f}$ and $g = \Phi_N^* \phi_{M,N}^* \tilde{g}' = \Phi_N^* \tilde{g}$ where $\tilde{f}, \tilde{g} \in C(F_N)$. The value of N is simply indicating at which level of approximation both f and g are describable without loss of information. Let U_α^n be the resolvent associated to the process X_t^n on F_n and U_α^∞ be the resolvent associated to the process X_t on L. The relation that defines U_α^∞ on $\bigcup_n \Phi_n^* C(F_n)$ is

$$U_\alpha^\infty \Phi_n^* f = \Phi_n^* U_\alpha^n f \qquad \forall f \in C(F_n),\ \forall n \geq 0. \tag{4.7.1}$$

This relation defines U_α^∞ on $\Phi^* C(F_n)$ for every n which since $\bigcup_n \Phi_n^* C(F_n)$ is dense in $C(L)$ U_α^∞ can be extended by continuity to all of $C(L)$. This relationship between U_α^∞ and U_α^n is called the Dynkin Intertwining relationship. Then by the Dynkin Intertwining relationship that holds for these resolvents we have:

$$\begin{aligned}
(f, U_\alpha^\infty g)_L &= (U_\alpha^\infty f, g)_L \ iff \\
(\Phi_N^* \tilde{f}, U_\alpha^\infty \Phi_N^* \tilde{g})_L &= (U_\alpha^\infty \Phi_N^* \tilde{f}, \Phi_N^* \tilde{g})_L \ iff \\
(\Phi_N^* \tilde{f}, \Phi_N^* U_\alpha^N \tilde{g})_L &= (\Phi_N^* U_\alpha^N \tilde{f}, \Phi_N^* \tilde{g})_L \ iff \\
(\tilde{f}, U_\alpha^N \tilde{g})_{F_N} &= (U_\alpha^N \tilde{f}, \tilde{g})_{F_N}
\end{aligned}$$

That is U_α^∞ is symmetric if all of the U_α^N are symmetric. Note that to get the last line in the calculation we used the fact that Φ_n^* is an isometry from $\mathcal{B}(F_n)$ to $\mathcal{B}(L)$, which is a consequence of how the measures, μ_n, are related to each other and to μ_∞.

Now it remains to show that from U_α^0 being symmetric that U_α^N are all also symmetric. Already we have that U_α^∞ being symmetric implies that U_α^0 is symmetric. The symmetry of operators on collections of finite line segments is a well studied topic in Quantum Graph theory [49,50,2]. By the way that the U_α^N were constructed inductively from U_α^0 it is seen that all of the U_α^N are symmetric resolvents. Here we use the fact that B_n consists of isolated points. ***Qed***

It is worth noting that the only facts that were used in proving this lemma were that we had a projective system of measure spaces, a family of resolvents satisfying Equation 4.7.1, and facts about self-adjoint operators on quantum graphs. None of these things intrinsically are related to the production of a Laakso space and so this lemma is applicable in a much broader context than just this paper [73].

Lemma 4.7.3. If the sequence of spaces, F_n, are all quantum graphs and X_t^0 is Feller process then X_t is a Feller process.

Proof. That X_t^n is Feller follows from the assumptions made on X_t^0 as part of the Barlow-Evans construction and from the fact that the F_n are all quantum graphs. Since X_t^n are Feller processes $U_\lambda^n : C(F_n) \to C(F_n)$. Now we use Equation 4.7.1 to say that $U_\lambda^\infty \Phi_n^* f \in C(L)$ for all $f \in C(F_n)$ for any $n \geq 0$. But in $C(L)$ the functions $\Phi_n^* C(F_n)$ are a dense subset so by taking uniform limits, because the resolvents are Markov, we get that $U_\lambda^\infty C(L) \subset C(L)$. ***Qed***

Lemma 4.7.4. If a process is Feller, then the associated Dirichlet form is regular.

This is Lemma 2.8 from [11]. We note this fact because we will be defining a Dirichlet form at the beginning of Section 4.8 and proceed to show that certain continuous functions are dense in its domain. If the Dirichlet form were not already known to be regular the argument would be more delicate.

It will be useful to fix some notation for function spaces that will be used to describe the domains of the operator and Dirichlet form associated to the process X_t.

Definition 4.7.5. Recall that $\Phi_n : L \to F_n$ is the projection from the space L to the nth level quantum graph from the Barlow Evans construction, and Φ_n^* is the pull back operator sending a function on F_n to a function on L.

1. Let $\tilde{A}_0 = \frac{\partial^2}{\partial x^2}$ on $[0, 1]$ with Neumann boundary conditions.

2. Let $\tilde{A}_n$ be the infinitesimal generator of the resolvent U_α^n that is associated to the process X_t^n on F_n, which is by the construction in [12] and [26] has the same action as $\tilde{A}_0$ on each line segment. Denote by $Dom(\tilde{A}_n) \subset L^2(F_n, \mu_n)$ domain of $\tilde{A}_n$.

3. Let $G_n \subset C(F_n)$ be functions on the quantum graph, F_n, that are twice differentiable on each line segment of the graph, have continuous first and second derivatives on each line segment, and satisfy the Kirchoff matching conditions at each vertex. The Kirchoff matching condition states that the directional first derivatives along all the line segments meeting at a vertex sum to zero, see [49]. The continuity condition implies that elements of G_n are bounded as are their first and second derivatives over all of F_n.

4. Let $\mathcal{D}_n = \Phi_n^* Dom(\tilde{A}_n) \subset L^2(L, \mu_\infty)$ be the pull back of the domain of $\tilde{A}_n$ to a function space on L. This is so that the domains are subspaces of the same L^2 space.

5. Let $\tilde{\mathcal{G}}_n$ be the set of continuous functions on F_n that are continuously differentiable on each line segment in F_n and the derivatives have finite limits at the vertices. Set $\tilde{\mathcal{G}} = \bigcup_{n=0}^{\infty} \Phi_n^* \tilde{\mathcal{G}}_n$.

Remark: There is a non-trivial Dirichlet form on the fractal L. Since there is a non-trivial symmetric Markov process, namely standard Brownian motion, which can be used in the Barlow-Evans construction there is a non-trivial symmetric Markov process on the fractal L by the previous lemma. Which by Theorem 4.2.9 yields a Dirichlet form which will be generated by a non-trivial self-adjoint linear operator, $\tilde{A}$. This operator is the generator of the resolvent U_α^∞.

Remark: The spaces $\mathcal{G}$ and $\tilde{\mathcal{G}}$ are the same function space on L. This is easily seem by tracing Definition 4.7.5 through the homeomorphism, η, to Definition 4.4.2. It is straight forward to see that the definitions are equivalent.

In Proposition 4.7.1 and the last remark we know that there is a Laplacian on L defined as the infinitesimal generator of the Markov process through Barlow and Evans' construction, i.e. $-\tilde{A}$. We also know that negative second differentiation with Neumann boundary conditions is the operator associated to one dimensional reflecting Brownian motion on the unit interval and that this is reminiscent of the operator $-A$ defined in the remark on 70 which generates the Dirichlet form for the Laakso construction using minimal generalized upper gradients. To begin the process of showing that these are the same operators we look into the domain of $\tilde{A}$ with the intention of showing it is the same as the domain of A.

We will shortly be considering the closure of function spaces and of self-adjoint operators. For both of these the graph norm $\|u\|_{L^2(L,\mu_\infty)} + \|\tilde{A}u\|_{L^2(L,\mu_\infty)}$ gives the relevant topology.

Proposition 4.7.6. Let $\tilde{A}_n$ as above, then

1. For $f \in G_n$ $\tilde{A}_n f = \frac{\partial^2}{\partial x^2} f$ where $\frac{\partial^2}{\partial x^2} f$ is the second derivative of f at each point in the interior of the line segments and not defined at the vertices, which are a set of measure zero, and $Dom(\tilde{A}_n) = \overline{G_n}$ (closure taken in the graph norm),

2. For $n \geq 0$, $\Phi_n^* G_n \subset \Phi_{n+1}^* G_{n+1}$,

3. For $n \geq 0$ and $f \in G_n$, $\tilde{A}\Phi_n^* f = \Phi_n^* \tilde{A}_n f$.

Proof. We take each claim separately.

1. By Definition 4.7.5 part 2, $\tilde{A}_n$ acts on each line segment in F_n in the same manner as $\tilde{A}_0$, which is the standard Laplacian on the line. For $f \in G_n$ when restricted to a line segment in F_n is in the domain of the standard Laplacian and mapped to $\frac{\partial^2}{\partial x^2} f$ restricted to that line segment. The self-adjointness is given by the general theory in [49] but can also be seen by using integration by parts on each line segment in F_n and using the matching conditions built into the definition of G_n to make the boundary terms vanish. So taken together we get the claim on all of F_n.

2. It is sufficient to show that $\phi^*_{n+1,n} f \in G_{n+1}$ for $f \in G_n$. As a pullback through a map as constructed in Section 4.6 it can been seen that $\phi^*_{n+1,n} f$ meets the criteria for membership in G_n.

3. This follows from the defining relationship of U^∞_α that was given in Lemma 4.7.2 and the strong continuity of the resolvent of a Dirichlet form that makes it possible to relate U^∞_α to its generator by a limit in the strong topology.

Qed

Proposition 4.7.7. Let U^n_λ be the resolvent associated to $\tilde{A}_n$ then $U^n_\lambda(\tilde{\mathcal{G}}_n) \subset \tilde{\mathcal{G}}_n$.

Proof. Since X^n_t is a Feller process we already have that $U^n_\lambda(\tilde{\mathcal{G}}_n) \subset C(F_n)$. Let $f \in \tilde{\mathcal{G}}_n$. Then $U^n_\lambda f = g$ for some $g \in Dom(\tilde{A}_n)$. But this is the same as saying that $f = \tilde{A}_n g + \lambda g$. Due to Proposition 4.7.6 we know that $\tilde{A}_n$ is a local operator that on each line segment of the graph F_n acts as second differentiation. With this locality we can look to see what properties g has on each line segment individually. For g to be an element of $\tilde{\mathcal{G}}_n$ is has to be continuous on F_n which we already have and it also has to be continuously differentiable on each line segment with finite limits at the ends of the line segments. Compare with the comments in the proof of Theorem 17 in [49]. The question now is if $f \in C^1([a,b])$ with bounded derivative the question is if g is as well when we have the relationship $f = g'' + \lambda g$. But this is a standard question in the theory of ordinary differential equations and is known to be true. Thus $g \in \tilde{\mathcal{G}}_n$. ***Qed***

The Laplacian $\tilde{A}$ is defined as the projective limit of the operators $\tilde{A}_n$, as a consequence of the fact that

$$\bigcup_{n=0}^{\infty} \mathcal{D}_n \subset Dom(\tilde{A})$$

is a dense subset in the graph norm $\|u\|_{L^2(L,\mu_\infty)} + \|\tilde{A}u\|_{L^2(L,\mu_\infty)}$. We distinguish the projective limit of $\tilde{A}_n$ from the closure of an increasing family of self-adjoint operators because in themselves the domains of $\tilde{A}_n$ are in $C(F_n)$, see [56] for closing self-adjoint operators. We call $\tilde{A}$ the projective limit of $\tilde{A}_n$ if $(\tilde{A}, \mathcal{D}_n) = (\tilde{A}_n, \mathcal{D}_n)$ for all $n \geq 0$ and the operator $(\tilde{A}, \overline{\cup_n \mathcal{D}_n})$ is self-adjoint.

Theorem 4.7.8. Using the graph norm $\|u\|_{L^2(L,\mu_\infty)} + \|\tilde{A}u\|_{L^2(L,\mu_\infty)}$ on the space $Dom(\tilde{A})$ to define a topology, we have that $\Phi_n^* G_n \subset \mathcal{D}_n \subset Dom(\tilde{A})$, and

$$Dom(\tilde{A}) = \overline{\bigcup_{n=0}^{\infty} \Phi_n^* G_n}.$$

Proof. The first claim is $\Phi_n^* G_n \subset \mathcal{D}_n \subset Dom(\tilde{A})$, which reduces to showing $G_n \subset Dom(\tilde{A}_n)$. On F_n the boundary consists of vertices of degree one so the Kirchoff matching condition that elements of G_n satisfy force the directional derivatives at all boundary points to be zero, so elements of G_n satisfy the boundary conditions of $Dom(\tilde{A}_n)$. The action of $\tilde{A}_n$ is second differentiation on each line segment, the vertices being a null set can be set aside, so for $f \in G_n$ the function $\frac{\partial^2 f}{\partial x^2}$ where x is a coordinate in any of the line segments is well defined and in $L^2(F_n, \mu_n)$ by the boundedness of the second derivatives imposed by the definition of G_n.

The second claim $\mathcal{D}_n = \overline{\Phi_n^* G_n}$, reduces to $Dom(\tilde{A}_n) = \overline{G_n}$ by the first part of Proposition 4.7.6. The last claim that $Dom(\tilde{A}) = \overline{\bigcup_{n=0}^{\infty} \Phi_n^* G_n}$ holds because the associated Dirichlet form is regular by Lemma 4.7.4. ***Qed***

4.8 A Shared Markov Process

We have shown that the Laakso construction of L guarantees that there is a Dirichlet form linked to the minimal generalized upper gradients which corresponds to some Markov process. We have seen from the Barlow-Evans construction that a Markov process is guaranteed to exist as well. The choice of base process as reflected Brownian motion was not the only possible decision. Other processes on L could be built from Markov processes on the base space F_0 satisfying the assumption at the beginning on Section 4.7. These Markov processes give rise to generators which then give rise to Dirichlet forms. But as we have chosen a particular one let us stay with it and complete the comparison between the process X_t^∞ and the Dirichlet form $(\mathcal{E}, Dom(\mathcal{E}))$.

Definition 4.8.1. Let $\tilde{\mathcal{E}}$ be the Dirichlet form associated to the Markov process considered in Section 4.7 via the self-adjoint operator, $\tilde{A}$, by the formula

$$\tilde{\mathcal{E}}(u,u) = -\int_L u(\tilde{A}u)\, d\mu$$

For $u \in Dom(\tilde{A})$. The domain of $\tilde{\mathcal{E}}$ is $Dom(\sqrt{-\tilde{A}})$ as defined by the functional calculus for self-adjoint operators.

This way of associating a Dirichlet form and operator is the same as in Theorems 4.2.1 and 4.2.3. It is worth noting that since the self-adjoint operator in question

is the infinitesimal generator of a Markov process it is Markovian itself hence $\tilde{\mathcal{E}}$ is a Dirichlet form by Theorems 4.2.3 and 4.2.7. Recall the Dirichlet form $\mathcal{E}$ defined in Lemma 4.5.1, these two Dirichlet forms have their domains contained in $L^2(L)$ and to check whether they are the same we have to first check that their domains have a common dense subset and then that they agree on this dense subset.

Before continuing to show that $\mathcal{E}$ and $\tilde{\mathcal{E}}$ are the same Dirichlet form we need a lemma to describe the domain of $\tilde{\mathcal{E}}$ in a manner that will be comparable to the description of the domain of $\mathcal{E}$ using the functions in $\mathcal{G}$ in Lemma 4.5.1.

Lemma 4.8.2. Given $\tilde{\mathcal{E}}$, $\mathcal{G}$ is a dense subset of $Dom(\tilde{\mathcal{E}})$ in the norm $\|u\|_{L^2} + \tilde{\mathcal{E}}(u,u)$.

Proof. With a similar argument as in Lemma 4.4.3 we can see that $\mathcal{G}$ is a dense subset of $C(L)$ in the uniform norm, but L is a finite measure space so $C(L) \subset L^2(L)$ and by standard results is a dense subset in the L^2 norm. Because of this $U_\lambda^\infty(\mathcal{G})$ is a dense subset of $Dom(\tilde{A})$ in it's topology because the resolvents are continuous maps. It is also known that $Dom(\tilde{A})$ embeds continuously as a dense subset of $Dom(\sqrt{-\tilde{A}})$. This leaves only whether or not $U_\lambda^\infty(\mathcal{G}) \subset \mathcal{G}$ but this has been shown in Proposition 4.7.7. ***Qed***

Now we are ready to state and prove the main result of the paper.

Theorem 4.8.3. The two Dirichlet forms, $\mathcal{E}$ and $\tilde{\mathcal{E}}$, are equal.

Proof. In order to show that the two Dirichlet forms, $\mathcal{E}$ and $\tilde{\mathcal{E}}$, are equal we show that they agree on a dense subset of their domains. Since we already know this subset is dense in the domains of $\mathcal{E}$ and $\tilde{\mathcal{E}}$ this agreement will extend to their full domains by continuity in the *same* metric. Hence the two Dirichlet forms will have the same domains and give the same values to functions in their common domain.

The subset of $Dom(\mathcal{E})$ and $Dom(\tilde{\mathcal{E}})$ that we will consider is $\mathcal{G}$. As remarked after Definition 4.7.5, $\mathcal{G} = \tilde{\mathcal{G}}$ is dense in both domains. Both $\mathcal{E}$ and $\tilde{\mathcal{E}}$ are the integrals of first derivatives squared on functions in $\mathcal{G}$. By Theorem 4.4.8 we give meaning to this in the language of Laakso's construction. At the beginning of this Section we defined $\tilde{\mathcal{E}}$ in terms of the self-adjoint operator $\tilde{A}$ and said that it's domain is $Dom\left(\sqrt{-\tilde{A}}\right)$ without saying what was in that domain. However using the results in [49] we see that $\sqrt{-\tilde{A}_n}$ on F_n has domain $\overline{\mathcal{G}_n}$ where the closure taken in the metric given by

$$\|\cdot\|_2 + \left\|\sqrt{-\tilde{A}_n}\cdot\right\|_2 = \|\cdot\|_2 + \tilde{\mathcal{E}}(\cdot,\cdot).$$

By Definitions 4.4.2 and 4.7.5.5 and the definitions of $\mathcal{E}$ and $\tilde{\mathcal{E}}$ we can see that for $f \in \mathcal{G}$ that $\mathcal{E}(f,f) = \tilde{\mathcal{E}}(f,f)$. Since the two Dirichlet forms have the same domains and agree on a dense subset they are the same. ***Qed***

Corollary 4.8.4. The Dirichlet form from Theorem 4.5.1 associated to the minimal generalized upper gradients on the fractal L corresponds to the Markov process from the Barlow-Evans construction with X_t^0 the standard Brownian motion on the unit interval.

Proof. By Theorem 4.8.3 the Dirichlet forms generated by the minimal generalized upper gradients and to the Markov processes built from Brownian motion on the unit interval are associated to the same Dirichlet form. Then by Theorem 4.2.3 the Dirichlet forms, Markov processes, and self-adjoint operators from both constructions are the same, $A = \tilde{A}$. ***Qed***

Remark: It is unlikely that this sort of result would hold for a general space constructed by Barlow and Evan's construction. What makes it possible in this situation is the well defined cell structure where the interior and complement of a cell are disjoint, approximating 1-dimensional spaces. These properties ensure that the processes are relatively accessible objects with which to work. It seems reasonable that as long as a cell structure is available this type of method should be possible for other families of Barlow-Evans spaces.

Chapter 5

Eigenmodes of the Laplacian on some Laakso Spaces

This chapter first appeared as [66] with co-author Kevin Romeo who worked as a REU student under the author's supervision.

Abstract: We analyze the spectrum of a self-adjoint operator on a Laakso space using the projective limit construction originally given by Barlow and Evans. We will use the hierarchical cell structure induced by the choice of approximating quantum graphs to calculate the spectrum with multiplicities. We also extend the method for using the hierarchical cell structure to more general projective limits beyond Laakso spaces.

MCS: 34L40 (primary); 34L16; 54B30

5.1 Introduction

Laakso's spaces were first introduced in [52] to give examples of spaces that have nice analytic properties of any arbitrary dimension greater than one. Among these properties is having a sufficient supply of rectifiable curves connecting pairs of points to not give positive capacity to single points. In [12], Barlow and Evans present a construction of a projective limit space with sufficient conditions that Markov processes can be constructed on the limit space, and mention that their construction should be able to create Laakso's spaces as well. In the previous chapter that assertion was proved in detail, and a Laplacian operator was constructed from both the minimal generalized upper gradients provided in [52] and from a Markov process constructed as in [12]. In this chapter we work in terms of Barlow and Evans construction as the projective limit of quantum graphs (Sections 5.2 and 5.3) because it makes describing the action of the Laplacian simpler (Section 5.5).

Working on the approximating graphs allows us to numerically compute eigenvalues and eigenfunctions of the Laplacian on each graph. From the projective system of graphs (Section 5.3) an eigenfunction on one approximating graph can be lifted to a corresponding eigenfunction on a more detailed approximating graph. It follows that the spectra of the approximating Laplacians are building up towards the spectrum of the Laplacian on the limit space. This is proved in Sections

5.3 and 5.6. An account of how the numerical calculations are performed is given in Sections 5.4 and 5.5. We begin with a few words on quantum graphs in Section 5.2.

As fractals, Laakso spaces are an interesting class to study because they are infinitely ramified but not generated as the fixed space of an iterated function system. In addition, Laakso spaces cannot be bi-Lipschitz embedded into $\mathbb{R}^n$ for any n [52]. However, these spaces can be given a cell structure that is similar to that of a Sierpinski carpet. In this situation it might be hoped that the kind of analysis done in [3] can be done on Laakso spaces as well. Moreover the similarity of the cell structure to that used in [11] for showing the existence of, and bounds on, heat kernels on Sierpinski carpets suggests that it might also be possible to estimate heat kernels in this setting. A specific question is whether these spaces have a spectral dimension. Based on our numerical data and theoretical results on the high multiplicities it is natural to conjecture that the spectral dimension is larger than one and quite possibly equal to the Hausdorff dimension of the Laakso space.

5.2 Quantum Graphs

A metric graph is a graph which not only has a metric giving the distance between vertices but can also give distances between points along the edges. Such a graph consist of a set of vertices and a set of edges connecting vertices. A pair of vertices can have more than one edge connecting them, and any vertex not connected to an edge can be ignored. Each edge is given a length, and the distance between any two points is the infimum of the lengths of the paths connecting the two points. Such graphs are best visualized as a series of wires connected together at the vertices where interesting phenomena can occur not just at the vertices but along the "wires" as well. If a Hamiltonian operator is defined on the metric graph as well it can then be called a quantum graph, the simplest Hamiltonian is the standard Laplacian. A good survey of quantum graphs, their properties, and the properties of the Hamiltonians on them is [49], followed up in [50].

The Hamiltonian need not be an exotic operator, since a quantum graph is primarily a collection of intervals operators can be built out of one dimensional operators and have their action remain intuitive. A simple operator, and the one used throughout, is the negative second derivative,

$$Af(\cdot) = -\frac{d^2 f}{dx^2}(\cdot),$$

The domain of this operator contains all the functions on the graph that are twice differentiable on each line segment and such that the directional first derivatives at a vertex sum to zero. This vertex condition is known as (Neumann-)Kerchoff

matching conditions and force the boundary terms to vanish when using integration by parts to check the self-adjointness of the operator. If the degree of the vertex is one then it is a boundary vertex and the matching condition reduces to a Neumann boundary condition. We will consider this Laplacian on a series of quantum graph approximations to Laakso spaces where the Laplacians also approximate the Laplacian on the limit space.

Hamiltonians are self-adjoint operators not merely symmetric ones, see [2] for examples in the physics literature. This means that care has to be taken in identifying their domains. For instance, second differentiation on the unit interval is a common Hamiltonian but the domain has to be restricted by boundary conditions, classical ones being Dirichlet and Neumann. However on a quantum graph there are vertices with many line segments meeting. At these points there are more choices for boundary conditions, zero (Dirichlet), zero derivative (Neumann), one sided derivatives summing to zero (Kirchoff), and so on [49,50]. In Section 5.5 we discuss which vertex conditions are most appropriate to Laakso spaces.

5.3 Projective Limits

The Laakso spaces that we will be analyzing Laplacians on are constructed as projective limits. The original construction was given in [12], shown to produce Laakso spaces in [71], and background for projective limits in the category of topological spaces is given in [37] and [21]. We start with the definitions of a projective system and the projective limit space and then move on to giving the spectrum of an operator on the projective limit space.

Definition 5.3.1. A projective system of topological spaces, $(F_i, \phi_{i+1,i})_{i=0}^{\infty}$, is a family of spaces and surjective maps where the F_i are topological spaces and $\phi_{i+1,i} : F_{i+1} \to F_i$ are continuous.

Definition 5.3.2. The projective limit of a projective system, $\lim_{\leftarrow} F_i \subset \prod_{i=0}^{\infty} F_i$ is a topological space. An element $\{x_i\} \in \lim_{\leftarrow} F_i$ if and only if $x_i \in F_i$ and $\phi_{i,i-1}x_i = x_{i-1}$ for all $i \geq 1$ and the maps $\Phi_j : \lim_{\leftarrow} F_i \to F_j$ are all continuous surjections.

Projective limits possess a version of the "universal property." This means that if another space L was another topological space satisfying the diagram in Figure 4.1 then all of the maps "factor" through $\lim_{\leftarrow} F_i$ inducing a continuous surjection from L to $\lim_{\leftarrow} F_i$. This gives a sense in which the projective limit space is minimal because it is the smallest space which has all of the Φ_j surjective. The diagram showing this is Figure 4.2, where L is the other candidate for a limit space and $\tilde{\Phi}_j$ the set of surjections belonging to L. By the universal property of the projective limit space we have that $\tilde{\Phi}_j = \Phi_j \circ \eta$ for all $J \geq 0$ and some $\eta : L \to \lim_{\leftarrow} F_i$ a continuous surjection.

We need not only a topology on the limit space, $\lim_{\leftarrow} F_i$, but also a measure. In [21] sufficient conditions for the existence of a measure on the limit space are given. They are:

1. If $A \subset F_i$ is μ_i-measurable that $\int_{F_i} \mathbb{I}_A \, d\mu_i = \int_{F_{i+1}} \mathbb{I}_A \circ \phi_{i+1,i} \, d\mu_{i+1}$.

2. The total masses of the measures μ_i are bounded.

Given these two conditions there exists a limit measure μ_∞ with the property

$$\int_{F_i} \mathbb{I}_A \, d\mu_i = \int_{\lim_{\leftarrow} F_i} \mathbb{I}_A \circ \Phi_i \, d\mu_\infty.$$

This condition forces the sequence of measures μ_i to be mutually compatible so that the sequence of measures $\Phi_i^* \mu_i(A) := \int \mathbb{I}_A \circ \Phi_i \, d\mu_\infty$, with the integral taken over $\lim_{\leftarrow} F_i$, converge to the measure μ_∞.

Fix a projective system of quantum graphs, $\{F_n\}_{n=o}^{\infty}$ with measures, μ_n that are weighted Lebesgue measure on each line segment with total mass one. Let $\Phi_n : \lim_{\leftarrow} F_i \to F_n$ where $\lim_{\leftarrow} F_i$ is projective limit of F_n. It is possible to pull back functions on F_n to functions on $\lim_{\leftarrow} F_i$ by pre-composing with Φ_n. I.e. if $f : F_n \to \mathbb{R}$ then $\Phi_n^* f := f \circ \Phi_n : \lim_{\leftarrow} F_i \to \mathbb{R}$.

Definition 5.3.3. Let A_n be a self-adjoint operator on F_n acting by

$$A_n f = -\frac{\partial^2}{\partial x^2} f$$

where the differentiation is along each line segment and undefined at the vertices. Then A_n has domain $Dom(A_n)$ containing as a dense subset in the graph norm the functions on F_n that are twice differentiable on each line segment and also have the property that at each vertex the one-sided first derivatives along each edge incident to the vertex sum to zero. These are the Kirchoff matching conditions.

Definition 5.3.4. A family of self-adjoint operators, $(B_n, Dom(B_n))$ acting on the same space is *increasing* if $Dom(B_n) \subset Dom(B_{n+1})$ and $B_{n+1} f = B_n f$ for all $f \in Dom(B_n)$ and all $n \geq 0$.

Fix a projective system where the F_i are quantum graphs constructed as multiple copies of F_{i-1} identified at "wormholes," $q \in F_{i-1}$ across all copies of F_{i-1} so that F_i is a connected space also the locations of the wormholes are chosen so that the wormholes at step n do not occur at the same location as those of any step earlier than n. In this situation the maps $\phi_{i,i-1}$ are simply projection of the copies of F_{i-1} onto a single copy of F_{i-1}.

Theorem 5.3.5. Given such a projective system the operators, A_n, with domains

$$\mathcal{D}_n = \{f \circ \Phi_n | f \in Dom(A_n)\} \subset L^2(\lim_{\leftarrow} F_i, \mu_\infty)$$

Acting by $A_n \tilde{f} = (A_n f) \circ \Phi_n$ for $\tilde{f} \in \mathcal{D}_n$ are an increasing family of self-adjoint operators and the operator A is the minimal self-adjoint extension of the A_n with domain

$$Dom(A) = \overline{\bigcup_{n=0}^{\infty} \mathcal{D}_n}.$$

Moreover, if $\mathcal{D'}_n$ is the orthogonalization of $\mathcal{D}_n$ then

$$\sigma(A) = \bigcup_{n=0}^{\infty} \sigma(A_n|_{\mathcal{D'}_n}).$$

Where multiplicities of the eigenvalues add.

Proof. We will refer to the self-adjoint operator, A, as the projective limit of the operators A_n. The proof of the first half of the theorem is rather involved using Dirichlet forms and is proved in [71]. From that proof we have

$$\bigcup_{n=0}^{\infty} \mathcal{D}_n = \bigcup_{n=0}^{\infty} \Phi_n^* Dom(A_n) \subset Dom(A)$$

Densely in the graph norm, $\|u\| = \|u\|_{L^2} + \|Au\|_{L^2}$, because of the projective limit construction which defines $Dom(A)$ as the minimal domain containing $\mathcal{D}_n$ for all $n \geq 0$ such that $(A, Dom(A))$ is self-adjoint. It can be checked that the graph norm closure of $\bigcup_{n=0}^{\infty} \mathcal{D}_n$ is that domain. To ease the calculations that follow in the last section we orthogonalize the spaces $\mathcal{D}_n$ as follows:

$$\begin{aligned} \mathcal{D}'_0 &= Dom(A_0) \\ \mathcal{D}'_1 &= \mathcal{D'}_0^{\perp} \cap \mathcal{D}_1 \\ \mathcal{D}'_n &= \mathcal{D'}_{n-1}^{\perp} \cap \mathcal{D}_n. \end{aligned}$$

Where $\mathcal{D}_{n-1}^{\perp}$ is the orthogonal complement of $\mathcal{D}_{n-1}$ in $\mathcal{H} = L^2(L, \mu)$ and $\oplus_{n=0}^{\infty} \mathcal{D'}_n = \bigcup_{n=0}^{\infty} \mathcal{D}_n$ and one can write

$$A = \oplus_{n=0}^{\infty} A_n|_{\mathcal{D'}_n}.$$

If one can find the spectrum of the Laplacian, $-A$, when restricted to each $\mathcal{D'}_n$ then the spectrum of $-A$ when acting on its entire domain is the union of its spectrum on the $\mathcal{D'}_n$ with multiplicities adding.

If the union, $\bigcup_{n=0}^{\infty} \sigma(A_n|_{\mathcal{D}'_n})$, did not account for all of the eigenvalues of A then this would imply that that there was at least a one dimensional subspace of $Dom(A)$ which is orthogonal to every $\mathcal{D}_n$ which is not true because A is defined as the projective limit of the operators, A_n. Thus a complete set of eigenfunctions for $Dom(A)$ can be found in $\oplus_{n=0}^{\infty} \mathcal{D'}_n$. ***Qed***

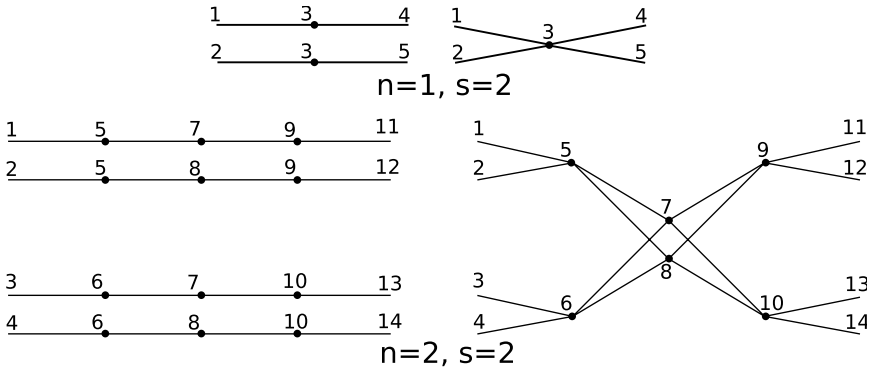

Fig. 5.1: Constructions of the simplest case, $j = s = 2$.

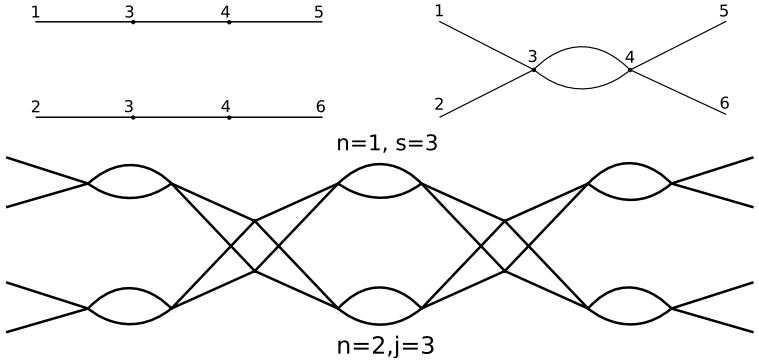

Fig. 5.2: Constructions of a more general case, $j = s = 3$.

If the geometry of a projective limit space is well understood then it is possible to explicitly determine the orthogonalization, $\mathcal{D}'_n$. This is done in Section 5.6 in the case of Laakso spaces.

5.4 Laakso Spaces

Laakso originally described these spaces in [52] with emphasis on showing there was a large supply of rectifiable curves and a tunable dimension. Later Barlow and Evans created a projective limit construction that could be specialized to use quantum graphs that would also produce Laakso spaces. This was verified in [71] see also Chapter 4 of this thesis. We consider only a few examples of these spaces to calculate spectra of Laplacians, however we take advantage of two ways of visualizing the process. One of the factors in determining the dimension of Laakso spaces is how many subintervals the new identifications made at each level of approximation make, we consider only the cases when this number, j, is fixed from one level to the next and work with $j = 2, 3, 4, 5, 6, 7$.

The first visualization of the projective limit construction of approximating

quantum graphs is the account that Barlow and Evans give in [12]. In this account the first graph is a unit interval, call it F_0. To construct F_n from F_{n-1} take two copies of F_{n-1} (if the dimension is larger than two more copies are needed, see [71] for details of how many). With those two copies, identify pairs of points, i.e. wormholes, from both spaces to create a single space this will be F_n. It is important that the locations of the wormholes are chosen so that wormholes used for different n do not occur at the same horizontal coordinate. In Figures 5.1 and 5.2 one can see the first few steps for when $j = 2$ and $j = 3$. This visualization is very convenient for drawing pictures but not for the numerical approximations needed to describe a Laplacian and then to calculate its spectrum.

Another way to visualize the construction of the approximating graphs to the Laakso spaces is to think in terms of their cell structure. In general a Laakso space's cell structure is not self-similar but in the cases that we consider, where at each step we split every horizontal interval into the same number, j, of subintervals, the Laakso spaces do have a self-similar cell structure. Again we begin with F_0 being the unit interval. Now take $2j$ copies of F_{n-1} arrange them in two horizontal lines of j copies each. Figure 5.3 shows an example of how this is done. To start with we have two copies of F_0 identified together at their mid-points (they are left as separated to keep the figure easier to understand), this is shown by the dots, to form F_1. To construct F_2 we take four copies of F_1 with the endpoints labeled so as to glue the graphs together as one would expect from the picture, but the extra step is to say that in the last part of the Figure that the points labeled "1" are identified together and the points labeled "2" are identified together. The process would then be continued to generate F_3. This example is when $j = 2$ but in other cases one just has more instances of this process. This may seem like an inelegant mode of thought but it leads to simpler labeling schemes for the nodes when building the incidence matrices.

To describe each of the approximating graphs for the numerical computations we use incidence matrices. The incidence matrix of a graph is a simple representation of how the nodes in space are connected. An entry of 0 indicates no connection while a 1 in row 1, column 2, would represent a connection between node 1 and node 2. This would also require node 2 to be connected to node 1, as the incidence matrix must be symmetric. An entry of 2 means that there are two separate edges connecting those two vertices. Many different incidence matrices are possible since the labeling of nodes is arbitrary. We assume a labeling natural from the second visualization of the construction process in the previous paragraph. The incidence matrix according to the vertex labeling scheme we use for the $n = 1$, $j = 2$ space

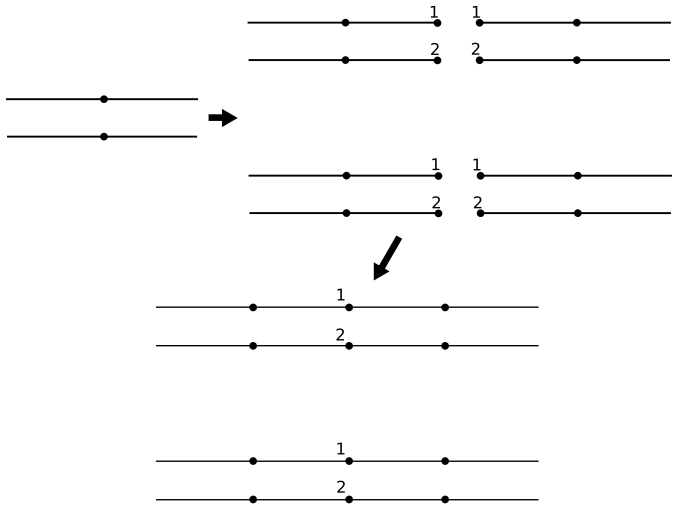

Fig. 5.3: Method of constructing the space when $j = 2$

is

$$\begin{bmatrix} 0 & 0 & 1 & 0 & 0 \\ 0 & 0 & 1 & 0 & 0 \\ 1 & 1 & 0 & 1 & 1 \\ 0 & 0 & 1 & 0 & 0 \\ 0 & 0 & 1 & 0 & 0 \end{bmatrix}.$$

The incidence matrix for the $n = 1$, $j = 3$ case is

$$\begin{bmatrix} 0 & 0 & 1 & 0 & 0 & 0 \\ 0 & 0 & 1 & 0 & 0 & 0 \\ 1 & 1 & 0 & 2 & 0 & 0 \\ 0 & 0 & 2 & 0 & 1 & 1 \\ 0 & 0 & 0 & 1 & 0 & 0 \\ 0 & 0 & 0 & 1 & 0 & 0 \end{bmatrix}.$$

The numbering scheme used for these matrices started in the top left node and went down columns of nodes, left to right across the space. It is the same scheme as shown in Figures 5.1 and 5.2. These matrices are needed to create the Laplacian matrices in the next section.

From [52] we know that our space has a Hausdorff dimension Q given by

$$1 + \ln(2)/\ln(j) = Q.$$

Since j is an integer larger than one the set of dimensions we deal with are contained in $[1, 2]$. The more general construction given in [71] allows for different values of j at each step. This is necessary to get all possible dimensions possible according to [52]. In these cases we deal with the sequence $\{j_i\}_{i=0}^{\infty}$ listing the choice of j at the ith step in the construction.

$j=2$		$j=3$		$j=4$		$j=5$		$j=6$		$j=7$		*Expected*
λ	m	λ	m	λ	m	λ	m	λ	m	λ	m	λ
0	1	0	1	0	1	0	1	0	1	0	1	0
9.87	3	9.87	1	9.87	1	9.87	1	9.87	1	9.87	1	π^2
		22.21	2									$(1.5\pi)^2$
39.48	3	39.48	1	39.48	3	39.48	1	39.48	1	39.48	1	$(2\pi)^2$
						61.68	2					$(2.5\pi)^2$
88.82	3	88.83	2	88.83	1	88.83	1	88.83	3	88.83	1	$(3\pi)^2$
										120.90	2	$(3.5\pi)^2$
157.88	18	157.91	1	157.91	3	157.91	1	157.91	1	157.91	1	$(4\pi)^2$
		199.86	8									$(4.5\pi)^2$
246.66	3	246.74	1	246.74	1	246.74	4	246.74	1	246.74	1	$(5\pi)^2$
355.15	6	355.30	2	35.31	3	355.30	1	355.31	5	355.30	1	$(6\pi)^2$
483.31	3	483.61	1	483.61	1	483.61	1	483.61	1	483.61	6	$(7\pi)^2$
						555.16	2					$(7.5\pi)^2$
631.15	66			621.65	10			631.65	1	631.65	1	$(8\pi)^2$
798.63	3			799.43	1			799.44	3			$(9\pi)^2$

Table 5.1: Calculated values of the first 10 eigenvalues for $j = 2, 3, 4, 5, 6, 7$ with multiplicity, m, and the theoretical value, λ.

5.5 Laplacian

In this section we describe how we numerically approximate the Laplacian in Definition 5.3.3. On each approximating graph an operator acts on a finite dimensional space of functions and so can be given a matrix representation. The matrix of the Laplacian is generated by simple manipulations of the incidence matrix and is constructed to follow the second difference quotient formula,

$$u''(x) = \lim_{h \to 0} \frac{u(x+h) - 2u(x) + u(x-h)}{h^2}.$$

However, as most nodes are connected to two nodes on each side, we took the average of the second derivative along the two paths. To construct the Laplacian's matrix representation from the incidence matrix, scale each row so that the row sum is -2 and then set all diagonal entries to 2. Now the row sum is always zero. If one considers functions depending only on the horizontal coordinate, i.e. a function on the unit interval, this Laplacian coincides with the negative second derivative on the unit interval. This representation also imposes Neumann boundary conditions at the endpoints by reflecting the value at the points just inside the boundary of the space to the points just outside. This makes the "first derivative" zero on all boundary points of the space and allows the second derivative to be approximated there. The entire matrix is then scaled by $1/h^2$, where h is the distance between nodes or wormholes in the space. This distance

decreases with increasing n such that the total width of the graph is 1 and h is given by $h(n) = 1/j^n$. The algorithmic description is described here to indicate how the calculations were actually performed.

The Laplacian matrix for the $n = 1$, $j = 2$ space is

$$M_{1,2} = \begin{bmatrix} 8 & 0 & -8 & 0 & 0 \\ 0 & 8 & -8 & 0 & 0 \\ -2 & -2 & 8 & -2 & -2 \\ 0 & 0 & -8 & 8 & 0 \\ 0 & 0 & -8 & 0 & 8 \end{bmatrix}.$$

The Laplacian matrix for the $n = 1$, $j = 3$ space is

$$M_{1,3} = \begin{bmatrix} 18 & 0 & -18 & 0 & 0 & 0 \\ 0 & 18 & -18 & 0 & 0 & 0 \\ -4.5 & -4.5 & 18 & -9 & 0 & 0 \\ 0 & 0 & -9 & 18 & -4.5 & -4.5 \\ 0 & 0 & 0 & -18 & 18 & 0 \\ 0 & 0 & 0 & -18 & 0 & 18 \end{bmatrix}.$$

Denoting by $M_{n,j}$ is the Laplacian matrix for the nth level approximating graph to the Laakso space constructing using the value of j.

This algorithm was implemented in MATLAB. It first produces the incidence matrix from recursive patterns emerging from the labeling scheme for the nodes. Then the Laplacian matrix is constructed using the process outlined above. Since these matrices are well structured and very sparse, no row has more than five entries compared to thousands of zeroes, we were able to find the thousand smallest eigenvalues numerically using the MATLAB *eigs* command which is based on ARPACK, a package that implements an Implicitly Restarted Arnoldi Method. More information on ARPACK can be found in its users guide, [57]. Even using sparse storage techniques the computations are impractical on a personal computer past $n = 9$ when $j = 2$. The ten lowest eigenvalues for each of the spaces with $j = 2, 3, 4, 5, 6, 7$ are listed in Table 5.1 along with their observed multiplicities, and histograms given in Figure 5.4. In the next section we give a theoretical account of how these spectrums with multiplicities arise and the calculations to show the exact details for $j = 2, 3$ is the last result of this chapter. Figure 5.5 show two eigenfunctions labeled with eigenvalues for the Laakso space with $j = 2$. These two pictures show how high multiplicity can be obtained since the eigenfunctions are only obeying the Kirchoff matching condition at the vertices of the graph. These matching conditions are weak enough so that functions which do not appear smooth at the vertices are still in the domain of the Laplacian.

Lastly, for the given Laakso space, L, where j is the number of subintervals in the construction. The action of the operator $M_n\phi^*_{n,m}, n > m$, on $f \in C(F_m)$ needs

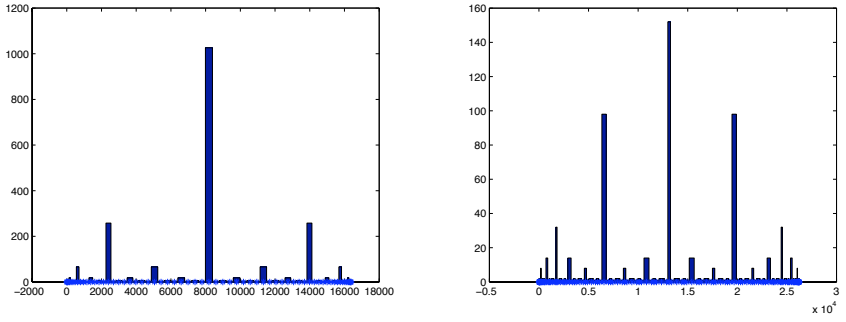

(a) $j = 2$ (b) $j = 3$

(c) $j = 4$ (d) $j = 5$

Fig. 5.4: Multiplicities of eigenvalues when j is $2, 3, 4$, and 5 respectively, $n = 4$ except for the (a) where $n = 6$

to be related to the action of A_m to justify approximating A by M_n instead of A_n. Recall that $\phi_{n,m} : F_n \to F_m$ is a surjection, so $\phi^*_{n,m} : C(F_m) \to C(F_n)$ by $\phi^*_{n,m} f = f \circ \phi_{n,m}$. Since M_n is a second finite difference operator on the graph of F_n it is seen that $M_n \phi^*_{n,m}$ for $n > m$ are the standard second finite difference operators on each line segment of F_m which converge to second differentiation as n goes to infinity. Then this holds for functions on any F_m so the M_n can be taken as suitable approximations to second differentiation. The operator A_n (Definition 5.3.3) acts by second differentiation on each line segment of the quantum graph F_m. Then for fixed j and m and $f \in Dom(A_m)$

$$\lim_{n \to \infty} M_n \phi^*_{n,m} f = A_m f.$$

The proof of this statement is standard and is essentially a statement about approximating derivatives with finite difference operators.

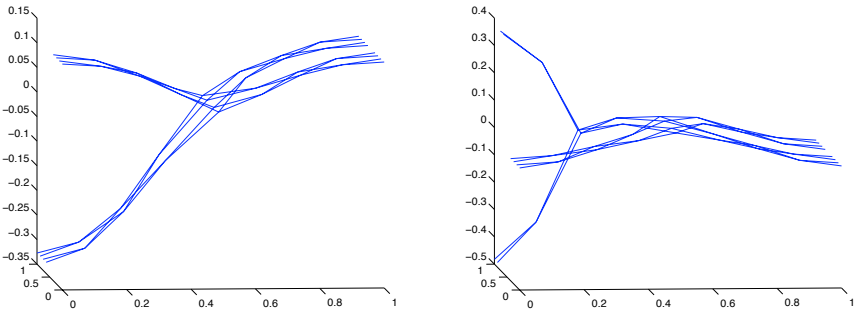

(a) $\lambda = 9.74$ (b) $\lambda = 37.49$

Fig. 5.5: Eigenfunctions on the $n = 3$, $j = 2$ space

5.6 Spectrum of The Laplacian

In this section we use the framework from Theorem 5.3.5 to verify that the calculations in the previous section are valid. Fix a Laakso space $L_j = L$, and the sequence of quantum graphs of which it is the projective limit, $\{F_n\}_{n=0}^{\infty}$, [12,71]. Let $\Phi_n : L \to F_n$ where L is a Laakso space and F_n one of the approximating quantum graphs be a projection map. It is possible to pull back function on F_n to functions on L by pre-composing with Φ_n. I.e. if $f : F_n \to \mathbb{R}$ then $\Phi_n^* f := f \circ \Phi_n : L \to \mathbb{R}$. We can then take $A = A_j$ to be the self-adjoint operator with it's domain $Dom(A)$ where this operator is the projective limit of A_n which acts by second differentiation on each line segment of F_n with domain $Dom(A_n)$ as given in Definition 5.3.3. Recall also the orthogonalization of the domains of A_n as $\mathcal{D}'_n$ from Theorem 5.3.5.

In the case of the Laakso spaces it will be useful to have a clear picture of what the projection maps ϕ_n do to a function from $C(F_{n-1})$ as it is being pulled back to an element of $C(F_n)$ to better understand what the orthogonal space is. Since F_n is constructed from copies of F_{n-1} modulo identifications, we can think of $F_n = F_{n-1} \times G_n$ so a function from $C(F_{n-1})$ when pulled back to $C(F_n)$ will be constant across G_n for a given coordinate in F_{n-1}. However, at wormholes G_n is identified to a single point so the pull back of a $C(F_{n-1})$ function will just have its value there. If we want to describe $\mathcal{D}'_n = \mathcal{D}'^{\perp}_{n-1} \cap \mathcal{D}_n$. we have to describe the functions on F_n that are orthogonal to those on F_{n-1}. The functions pulled back from $C(F_{n-1})$ to $C(F_n)$ are constant across G_n so the orthogonal functions would be those that average to zero across G_n and at the nth level wormholes where G_n is identified to a single point the orthogonal functions must be equal to zero.

In [52] a sequence of integers $\{j_i\}$ is associated to each Laakso space in the examples we calculated we have taken $j = j_i$ but we use the Laakso's notation for the generality since nowhere in the following proof do we use the fact that the j_i are equal. Let A be the self-adjoint operator for the Laakso space with $j_i = j$,

and A_n the self-adjoint operators on the approximating quantum graphs.

Theorem 5.6.1. Let the sequence $d_n = \prod_{j=1}^{n} j_i^{-1}$ $n \geq 1$ be associated to a given Laakso space, with Hausdorff dimension, Q, between one and two. Set $d_0 = 1$. Then the spectrum of A on this Laakso space is

$$\sigma(A) = \bigcup_{n=0}^{\infty}\bigcup_{k=1}^{\infty}\left\{\frac{k^2\pi^2}{d_n^2}\right\} \cup \bigcup_{n=2}^{\infty}\bigcup_{k=1}^{\infty}\left\{\frac{k^2\pi^2}{4d_n^2}\right\} \cup \bigcup_{n=1}^{\infty}\bigcup_{k=0}^{\infty}\left\{\frac{(2k+1)^2\pi^2}{4d_n^2}\right\}.$$

Proof. The proof falls naturally into two parts. The first is to show that A_n restricted to $\mathcal{D}'_n$ has the claimed spectrum. The second is to show that the union of $\sigma(A_n)$ contains all of $\sigma(A)$. Calculating exact multiplicities is left for the following proposition.

The approximating graphs for Laakso spaces are introduced in [71] and have been reviewed Section 5.4. For example if $j_i = 3$ then we have the graph in Figure 5.2 as the second approximating quantum graph. The structure that we exploit to calculate the spectrum is that the graph can be broken down into simple configurations of line segments on which the behavior of A_n is the usual second differentiation. All of the operators, A_n, have Kirchoff matching conditions which imposes Neumann boundary conditions since the boundary consists of degree one vertices.

The functions in $\mathcal{D}'_n$ are those functions in the domain of the operator A that are expressible as $\Phi_n^* f$ where $f \in Dom(A_n)$ where the values of f summed over the copies of F_{n-1} that F_n is built from are all zero, especially at the nth level wormholes where all the copies of F_{n-1} have been collapsed to single points f must be equal to zero at these wormholes. Referring back to Figure 5.2, if one considers the two most upper left line segments forming the sideways "V". An element of $\mathcal{D}'_2$ would have to equal zero at the second level wormhole, i.e. the apex of the V. It must also sum to zero over the copies of F_1 from which this graph is made meaning that the value of f on the upper branch of the V must be opposite to the value of f on the lower branch. On this "V," the part of the function that is symmetric across the two branches is in $\mathcal{D}'_1$, while the anti-symmetric part is in $\mathcal{D}'_2 \subset \mathcal{D}_2$.

The zeros at the nth level wormholes break the graph F_n into three kinds of pieces. The first are those segments at the boundary which have length d_n, Neumann boundary conditions on the boundary end and Dirichlet boundary conditions on the interior end. If $j_n > 2$ then we have interior intervals, such as those that form the loops in Figure 5.2, which again have length d_n but these have Dirichlet boundary conditions at each end. The third configuration is a cross, four segments of length d_n joined at a common point and Dirichlet boundary conditions at the four outer vertices. These three configurations can be seen in Figure 5.6. In the cross we must note that the upper and lower branches are from different copies of F_{n-1} so f is not forced to equal $-g$ for functions in $\mathcal{D}'_n$ but we

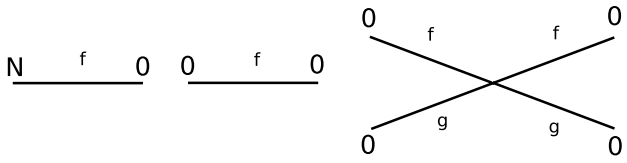

Fig. 5.6: The three types of pieces that the orthogonality condition creates in F_n.

will consider the symmetric and anti-symmetric cases where $f = g$ and $f = -g$ from which any function on the cross is a combination. If $f = g$ then the cross is essentially just an interval of length $2d_n$ with Dirichlet boundary condition and if $f = -g$ then at the intersection $f = 0$ and we have two intervals of length d_n with Dirichlet boundary conditions.

Note that the crosses do not appear for $n = 0$ or $n = 1$ for any j_0 or j_1. The intervals with Dirichlet conditions do not appear in $n = 0$ or when $j_n = 2$. The intervals with mixed boundary conditions do not appear when $n = 0$ either. What does appear when $n = 0$ is an interval of unit length and both ends having Neumann boundary conditions. When all of these are put together and their spectra found by the usual methods we get the claimed spectra where the contributions towards multiplicity from each of the pieces may be zero occasionally, i.e. $j_i = 2$ so there are no intervals of length d_n and Dirichlet boundaries except those which are part of the crosses.

The last claim that these are all of the eigenvalues of A on L follows from the fact that $\bigcup_{n=0}^{\infty} \mathcal{D}'_n$ is dense in $Dom(A_j)$ by the projective limit construction of the operator A. So if there were another eigenvalue unaccounted for there would be at least a one dimensional subspace of $Dom(A)$ orthogonal to a dense subset of $Dom(A)$ which is not the case. ***Qed***

There is a more general statement for higher dimension that replaces the crosses with 2^{k+1} line segments of length d_n on each side of a central vertex where k is the number of Cantor sets in the construction of the Laakso space as in [52]. The spectrum given in these higher dimensions is given by the same expression but the multiplicity counting as in the following Proposition has to be redone for each k.

Proposition 5.6.2. Denote by A the Laplacian on the Laakso space that has the sequence $j_i = j$ for all $i \geq 0$. The first ten eigenvalues of A and their multiplicity for the $j = 2$ and $j = 3$ constructions determined from Theorem 5.6.1 agree with the computed values in Table 5.1.

Proof. It is immediate from the spectrum of A_n on a given Laakso space as determined in Theorem 5.6.1 that the lowest eigenvalue is increasing with n, so to

find the first ten eigenvalues only a small number of approximating graphs are necessary.

Let us establish some notation. Let $\sigma^N[0,d]^N$ be the spectrum of the usual second derivative on an interval of length d with Neumann boundary conditions. If either, or both, of the N's are replaced by 0 then Dirichlet boundary conditions are indicated instead. Denote by $\sigma_0^0[X,d]_0^0$ the spectrum of second differentiation on a cross where the four intervals have length d and Dirichlet boundary conditions at the four ends points. If we write $2\times\sigma_0^0[X,d]_0^0$ the two denotes the multiplicity of these eigenvalues.

1. For $j=2$, we get from drawing the first few approximating graphs and forming the function spaces $\mathcal{D}'_n$ and calculating the spectrum of A_n on each of these spaces we get the following table. Let σ_n be the spectrum of the A_n operator on the function space $\mathcal{D}'_n$.

$$\begin{aligned}
\sigma_0 &= 1\times\sigma^N[0,1]^N \\
\sigma_1 &= 2\times\sigma^N[0,\frac{1}{2}]^0 \\
\sigma_2 &= 4\times\sigma^N[0,\frac{1}{4}]^0+1\times\sigma_0^0[X,\frac{1}{4}]_0^0 \\
\sigma_3 &= 8\times\sigma^N[0,\frac{1}{8}]^0+6\times\sigma_0^0[X,\frac{1}{8}]_0^0 \\
\sigma_4 &= 16\times\sigma^N[0,\frac{1}{16}]^0+28\times\sigma_0^0[X,\frac{1}{16}]_0^0
\end{aligned}$$

   It is easy to check that $1\times\sigma_0^0[X,d]_0^0=1\times^0[0,2d]^0+2\times\sigma^0[0,d]^0$. Using the known spectra for second differentiation on intervals the first ten eigenvalues are readily computed along with their multiplicities which do match those found in Table 5.1.

2. In the case where $j=3$ we need fewer approximating graphs to account for the first ten eigenvalues. The spectra of the Laplacian on the first few functions spaces $\mathcal{D}'_n$ are:

$$\begin{aligned}
\sigma_0 &= 1\times\sigma^N[0,1]^N \\
\sigma_1 &= 2\times\sigma^N[0,\frac{1}{3}]^0+1\times\sigma^0[0,\frac{1}{3}]^0 \\
\sigma_2 &= 4\times\sigma N[0,\frac{1}{9}]^0+3\times\sigma^0[0,\frac{1}{9}]^0+2\times\sigma_0^0[X,\frac{1}{9}]_0^0
\end{aligned}$$

   When these spectra are written out with the indicated multiplicities and compiled into a single list we get the same eigenvalues and multiplicities listed in Table 5.1.

Qed

Chapter 6

Spectrum and Heat Kernel Asymptotics on General Laakso Spaces

This chapter first appeared as [16] with co-authors Matthew Begue, Levi DeValve, and David Miller who worked as REU students under the author's supervision.

Abstract: We introduce a method of constructing a general Laakso space while calculating the spectrum and multiplicities of the Laplacian operator on it. Using this information, we find the leading term of the trace of the heat kernel and the spectral dimension of an arbitrary Laakso space.

6.1 Introduction

Much work has been done on the analysis of fractals, specifically concentrating on the spectrum of the Laplacian operator on irregular domains. One such topic are drums with Koch snowflake boundary, see for example [55]. This paper will be concerned instead with the irregular domain being a fractal itself. Some notable works with this type of domain include [3,29,39,66,71,74]. Laakso's spaces were introduced in [52]. They are a family of fractals with an arbitrary Hausdorff dimension greater than one and were considered originally for their nice analytic properties. Constructions of the Laakso spaces are given in [52,66,71] as well as in Section 6.2 of this chapter. Theorem 6.1 in [66] gives the spectrum of the Laplacian operator on any given Laakso space, in Theorem 6.3.1 we give the multiplicities.

An important part of the analysis of Laplacians is the heat equation and associated heat kernel, which can reveal significant information about the operator and underlying space. The information gained from studying heat kernels can be applied in other areas of analysis as well as other fields such as physics. The papers [2,74] are devoted to finding and analyzing the heat kernel and the trace of the heat kernel. The notion of complex valued fractal dimensions and the accompanying oscillating behavior of the heat kernel were studied in [2,3].

We begin by reviewing the construction of the Laakso spaces as presented in [52,66,71] in Section 6.2. This section also contains background information on the Hausdorff dimension, it's calculation for Laakso spaces, and some specific values for certain Laakso spaces. In subsection 6.2.3 we define the Laplacian operator

that will be used throughout the rest of this chapter which is the same as defined in the previous two chapters.

In Section 6.3 we begin by stating the spectrum of the Laplacian and the multiplicities of each eigenvalue (Theorem 6.3.1), while the rest of the section is devoted to the proof of this result. In Section 6.3.1 we provide an analytical proof by examining, as in [66], the different "shapes" that make up the space. Since each shape has a unique contribution to the spectrum counting the number of shapes allows us to calculate the spectrum with multiplicities. In Section 6.3.2 we verify the results computationally using MATLAB. Finally in Sections 6.4 and 6.5 we use the spectrum and multiplicities obtained in Sections 6.2.2 and 6.3.1 to calculate the trace of the heat kernel using the same method outlined for diamond fractals in [2].

6.2 Laakso Spaces

The spaces that will be analyzed were first defined by Laakso in [52]. Laakso's spaces form an uncountable family of metric-measure spaces indexed by sequences $\{j_n\}_{n=1}^{\infty}$. An equivalent construction using projective limits was hinted at in [12] and fully developed in [71]. Then in [66], a more in depth description of the projective limit construction was used to calculate the spectrum of the Laplacian constructed in [71]. We will be using the construction in [66] as it is also well-suited for our calculations.

A Laakso space can be visualized with a sequence of quantum graphs, denoted $F_n, n \geq 0$, each an increasingly fine approximation of a Laakso space. The first of these graphs is the unit interval, denoted F_0. Laakso spaces are defined by a sequence $\{j_n\}_{n=1}^{\infty}$ of integers $j_n \geq 2$, where each j_n described the number of identifications at step n of the construction. To construct the graph F_{n+1}, first every cell, or interval between two nodes, of the F_n graph is split evenly into j_n segments by adding nodes. This graph is then duplicated and connected at the newly-added notes. In this visualization, all nodes are arranged in columns.

We describe a simple case, where $j_n = 2$, $n \geq 1$. To obtain F_1, bisect F_0 with a node. Then make a copy of this graph. Identify the new nodes "glueing" the two graphs together, represented by the arrow in Figure 6.1. This glueing process is the identification process described in [12]. This yields the graph F_1, an X-shape with five nodes as seen in Figure 6.1.

This procedure is repeated to obtain F_2 from F_1. Nodes bisect each cell of F_1 as seen in Figure 6.2. A duplicate copy of F_1 is created and the two graphs are "glued" together at the newly added nodes. This is shown in Figure 6.2 where the solid line represents F_1 and the dashed lines represent the copy of F_1. The $j_n = 2$ Laakso space is the projective limit of the sequence of graphs $\{F_n\}_{n=0}^{\infty}$ all produced in this manner.

As another simple example consider $j_n = 3$, for all $n \in \mathbb{N}$. Again starting

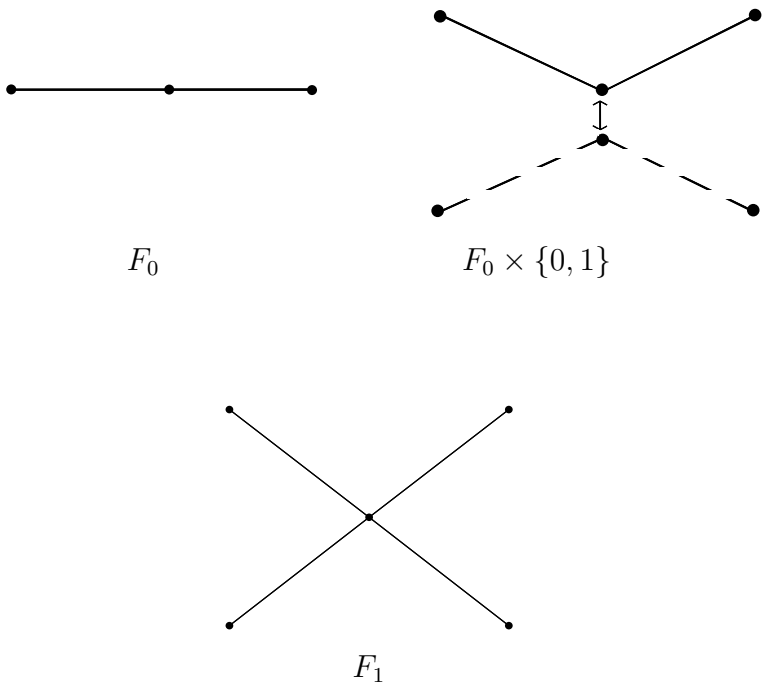

Fig. 6.1: Construction of F_1 from F_0 with $j_1 = 2$.

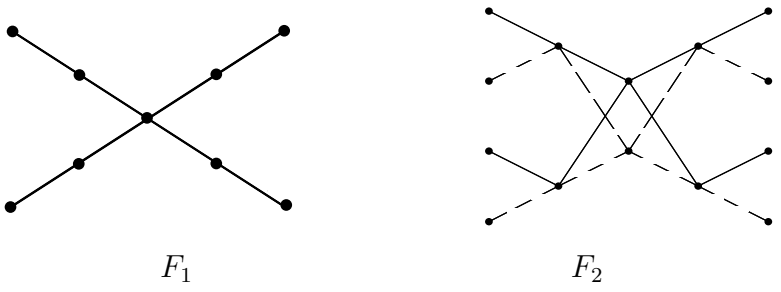

Fig. 6.2: Construction of F_2 from F_1 where $j_2 = 2$. The dashed lines represent the second copy of F_1 with the added nodes.

with the unit interval, F_0, F_1 is constructed by splitting F_0 into three subintervals and placing a node between each interval as shown in Figure 6.3. This graph is duplicated and is glued to the original graph at the newly added nodes. The two nodes in the middle of the figure are connected by the middle interval and its copy, thus creating a loop shape that is not seen in the case where $j = 2$. The outer thirds of the figure create a "V" shape, also seen in the $j = 2$ construction. These shapes, loop and "V", will be two of those considered in Section 6.3.

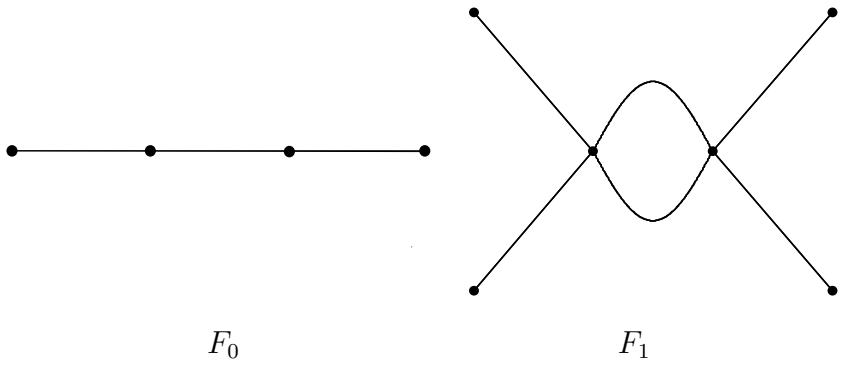

Fig. 6.3: Construction of F_1 from F_0 with $j_1 = 3$.

In this chapter, we deal with the general case where j_n may vary at each approximation level n. The sequence $\{j_n\}_{n=1}^{\infty}$ may be a constant integer, as seen in the previous examples. Or the sequence may alternate regularly between two integers. Figure 6.4 shows the construction of F_2 and F_3 when $\{j_n\}_{n=1}^{\infty} = \{2, 3, 2, 3, ...\}$. The sequence $\{j_n\}_{n=1}^{\infty}$ could even be a completely random sequence of integers. In any case, it is $\{j_n\}_{n=1}^{\infty}$ which defines the Laakso space and from which the properties are derived.

6.2.1 Cell Structure of a Laakso Space

Recall that as an inverse limit system the pair $(L, \{F_n\})$ come with continuous projection $\Phi_n : L \to F_n$.

Definition 6.2.1. The cell structure in a Laakso space, L, is determined by the pre-images under the map Φ_n of the cells in the graph F_n which approximates L

Given a space as defined by Laakso in [52], and the construction of the space as given in [66], and the level of approximation, n, the cell structure has specific properties, including number of cells, N_n, and the interval length, d_n^{-1}. Both the number of cells and the interval length are dependent on the choice of j_i for all $i \leq n$.

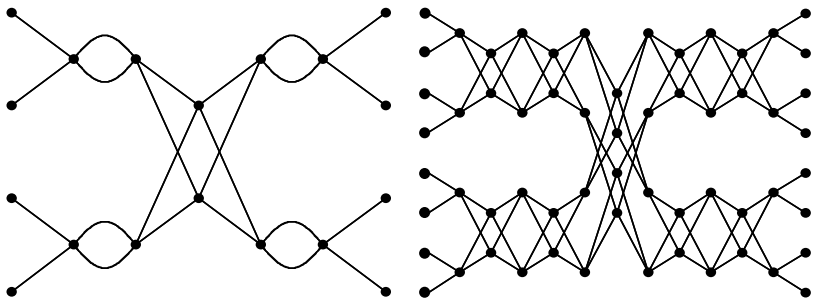

Fig. 6.4: Construction of the Laakso space for $\{j_n\}_{n=1}^{\infty} = \{2, 3, 2, 3, ...\}$

Proposition 6.2.2. Each cell in F_n has metric diameter

$$d_n^{-1} = \prod_{i=1}^{n} j_i^{-1} \tag{6.2.1}$$

where $d_0 = 1$. In addition the number of cells is

$$N_n = 2^n \prod_{i=1}^{n} j_i. \tag{6.2.2}$$

Proof. In F_0 there is a single cell, the unit interval, with metric diameter equal to 1. At each step in the construction the diameter of each cell in F_n is j_n^{-1} times that of a cell in F_{n-1}. By induction the diameter of the cells in F_n is d_n^{-1}.

There is a single cell in F_0. At each step of the construction there are $2 \times j_n$ cells in F_n for every cell in F_{n-1}. Thus the number of cells in F_n is $2^n d_n$. ***Qed***

6.2.2 Hausdorff dimension of the Laakso Space

In order to discuss the Hausdorff dimension of Laakso spaces we fix our choice of metric and measure. We use the path length metric. The measure used is the probability measure that gives equal mass to all cells of a given depth. Implicitly in the given construction, we have restricted the Hausdorff dimension to $1 \leq Q \leq 2$. In [66] the Hausdorff dimension Q of the Laakso Space associated with a constant j_n at every level n is shown to be

$$Q = 1 + \frac{log(2)}{log(j)}$$

Here we give the Hausdorff dimension of a Laakso space associated with a general sequence $\{j_n\}_{n=1}^{\infty}$. The measure used in calculating the Hausdorff dimension is

the projective limit of Lebesgue measure on F_n scaled to have total mass one for all n.

Lemma 6.2.3. Given sequence $\{j_i\}_{i=1}^{\infty}$ the Hausdorff Dimension, Q, of the corresponding Laakso space is given by

$$Q_{j_i} = \lim_{n\to\infty} \frac{log\left(2^n \prod_{i=1}^{n} j_i\right)}{log\left(\prod_{i=1}^{n} j_i\right)} = \lim_{n\to\infty} \frac{log(2^n d_n)}{log(d_n)} = \lim_{n\to\infty} 1 + \frac{log(2^n)}{log(d_n)}, \tag{6.2.3}$$

if the limit exists.

Proof. Laakso spaces are lacunary self-similar sets as defined in [38] where the contraction ratios at any n are equal. The number of identifications for each cell at the i'th iteration is j_i and the formula that Igudesman gives in [38] can be given in terms of n and j_i. This formula uses the number of cells, N_n and the cell diameter, which is simply d_n^{-1}. In the geodesic metric, the cell length is also the diameter of the cell. ***Qed***

While there are many sequences $\{j_n\}$ for which Q will not exist it is more relevant to our interests that for every Q there exist sequence $\{j_n\}$ yielding a Hausdorff dimension of Q. Different sequences $\{j_n\}$ can yield the same dimension, as shown in Table 6.1. These values agree with the dimensions given implicitly in [52].

j_i	Q_{j_i}
2	2
3	$\frac{log(6)}{log(4)}$
$[2,3,2,3,...]$	$\frac{log(24)}{log(6)}$
$[3,2,3,2,...]$	$\frac{log(24)}{log(6)}$

Table 6.1: Hausdorff Dimension for Laakso Space associated with given sequence of $\{j_i\}_{i=1}^{\infty}$

6.2.3 Laplacian

In [66,71] Laakso spaces are described as projective limits of quantum graphs and it is shown how to extend a compatible family of self-adjoint operators on the approximating quantum graphs to a self-adjoint operator on the limit space, i.e. the Laakso space. It was also shown how to use the spectrum with multiplicities of the operators on each quantum graph to determine the spectrum with multiplicities of the operator on the limit space. A quantum graph is a metric graph

with a Hamiltonian operator, as described in [49,50], the simplest of which would be the Laplacian operator, i.e. a Hamiltonian without a potential.

On each metric graph, F_n, consider the space of functions defined on the collection of edges each treated as a line segment. Define an operator on these function by $\Delta_n = -\frac{d^2}{dx^2}$. To make this a self-adjoint operator we need to also specify a suitable domain. A function is in $Dom(\Delta_n)$ if it is continuous everywhere, continuously twice differentiable on each line segment, and has Kirchhoff matching conditions at the nodes. Kirchhoff conditions require a function's with directional first derivatives summing to zero at nodes.

Definition 6.2.4. A Laakso space, L, is a projective limit of the F_n. Also there exist projection maps $\Phi_n : L \to F_n$ for all n. Thus any function on F_n can be pulled back to a function on L by writing $f \circ \Phi_n = \tilde{f} : L \to \mathbb{R}$. The pulling back is under the projections Φ_n.

By Theorem 4.7.8 those functions in $Dom(\Delta)$ that are pull backs are dense. so a complete set of eigenfunctions can be taken from this set. A consequence of this is that we can numerically approximate the spectrum of the Laplacian on the Laakso spaces working on some F_n. Computations of these approximations are described in Section 6.3.2 along with calculations described in Section 6.3.1. Tables 6.2 and 6.3 show calculated values of the spectrum of the Laplacian for Laakso space.

6.3 The Spectrum of Δ

Theorem 6.3.1 gives the spectrum and associated multiplicities of the Laplacian operator by considering Δ_n on F_n and on any Laakso space. We devote the rest of the section to proving the theorem. Following the analytic arguments are details of computational experiments carried out before the analytic results were available. We use an iterative, computer-assisted process to find the bottom end of the spectrum on a number of specific Laakso spaces. In all cases the computed results and analytic results agree within the precision of the computations.

Theorem 6.3.1. Given any Laakso space, L, with associated sequence $\{j_i\}_{i=1}^n$, the spectrum of Δ on $Dom(\Delta)$ is

$$\bigcup_{k=0}^{\infty}\{\pi^2k^2\} \cup \bigcup_{n=1}^{\infty}\bigcup_{k=0}^{\infty}\{(k+1/2)^2\pi^2d_n^2\} \cup \bigcup_{n=1}^{\infty}\bigcup_{k=1}^{\infty}\{k^2\pi^2d_n^2\} \cup \bigcup_{n=2}^{\infty}\bigcup_{k=1}^{\infty}\{k^2\pi^2d_n^2\} \cup \bigcup_{n=2}^{\infty}\bigcup_{k=1}^{\infty}\left\{\frac{k^2\pi^2d_n^2}{4}\right\} \tag{6.3.1}$$

$n=3$		$n=4$		$n=5$		$n=6$		$n=7$		*Expected*
λ	m	λ	m	λ	m	λ	m	λ	m	
0	1	0	1	0	1	0	1	0	1	0
9.87	3	9.87	3	9.87	3	9.87	3	9.87	3	$\pi^2 = 9.87$
39.58	1	39.38	1	39.45	1	39.48	1	39.48	1	$(2\pi)^2 = 39.48$
84.35	8	88.32	8	88.70	8	88.81	8	88.82	8	$(3\pi)^2 = 88.83$
144	1	156.32	1	157.51	1	157.87	1	157.90	1	$(4\pi)^2 = 157.91$
213.46	3	242.85	3	245.76	3	246.63	3	246.71	3	$(5\pi)^2 = 246.74$
288	26	347.26	26	353.28	26	355.08	26	355.25	26	$(6\pi)^2 = 355.31$
		468.78	3	479.86	3	483.19	3	483.51	3	$(7\pi)^2 = 483.61$
		606.41	1	625.27	1	630.94	1	631.48	1	$(8\pi)^2 = 631.65$
		759.18	8	789.22	8	798.30	8	799.15	8	$(9\pi)^2 = 799.44$
		925.89	1	971.40	1	985.22	1	986.53	1	$(10\pi)^2 = 986.96$
		1105.3	3	1171.5	3	1191.7	3	1193.6	3	$(11\pi)^2 = 1194.2$
		1296	38	1389.0	38	1417.6	38	1420.3	38	$(12\pi)^2 = 1421.2$
		1496.6	3	1623.7	3	1663.0	3	1666.7	3	$(13\pi)^2 = 1668.0$
		1705.5	1	1875.0	1	1927.8	1	1932.8	1	$(14\pi)^2 = 1934.4$
		1921.1	8	2142.5	8	2211.9	8	2218.5	8	$(15\pi)^2 = 2220.7$
		2141.9	1	2425.7	1	2515.2	1	2523.8	1	$(16\pi)^2 = 2526.6$
		2366.1	3	2723.9	3	2837.8	3	2848.7	3	$(17\pi)^2 = 2852.3$
		2592	86	3036.7	86	3179.5	86	3193.2	86	$(18\pi)^2 = 3197.8$
		2817.9	3	3363.5	3	3540.3	3	3557.3	3	$(19\pi)^2 = 3562.9$

Table 6.2: Calculated Values of the first 20 Eigenvalues for $\{j_n\}_{n=1}^{\infty} = \{2, 3, 2, 3, ...\}$ with multiplicity, m, the iteration value, n, and the expected value, λ. As n increases, the observed eigenvalues converge to the expected result.

with associated multiplicities:

$$1, \quad 2^n, \quad 2^{n-1}(j_n - 2)d_{n-1}, \quad 2^{n-1}(d_{n-1} - 1), \quad 2^{n-2}(d_{n-1} - 1) \tag{6.3.2}$$

respectively.

This does correct a typographical error in the similar statement given in [66].

6.3.1 Counts of Eigenvalues and Multiplicities

In order to determine the spectrum of the Laplacian on the Laakso space, the approximating quantum graph is considered as a collection of simpler parts. In [66] it was determined that three distinct shapes with appropriate boundary conditions could be used to construct any quantum graph representations of Laakso spaces, save F_0, which is treated as a special case. Definition 6.3.2 defines these three shapes shown in Figure 6.5 with their respective boundary conditions which are

A		B		C		D		*Expected*
λ	m	λ	m	λ	m	λ	m	
0	1	0	1	0	1	0	1	0
9.87	3	9.87	1	9.87	1	9.87	1	π^2
		22.2	2	22.2	2			$(1.5\pi)^2$
39.48	1	39.48	1	39.48	1	39.48	3	$(2\pi)^2$
88.82	8	88.82	8	88.82	2	88.82	1	$(3\pi)^2$
157.91	1	157.91	1	157.91	1	157.91	3	$(4\pi)^2$
		199.85.3	2	199.85	2			$(4.5\pi)^2$
246.71	3	246.71	1	246.71	1	246.71	1	$(5\pi)^2$
355.25	26	355.25	8	355.25	8	355.25	10	$(6\pi)^2$
483.51	3	483.51	1	483.51	1	483.51	1	$(7\pi)^2$
		555.1	2	555.1	2			$(7.5\pi)^2$
631.48	1	631.48	1	631.48	1	631.48	3	$(8\pi)^2$
799.15	8	799.15	36	799.15	2	799.15	1	$(9\pi)^2$
986.53	1	986.53	1	986.53	1	986.53	3	$(10\pi)^2$
		1087.9	2	1087.9	2			$(10.5\pi)^2$
1193.6	3	1193.3	1	1193.3	1	1193.3	1	$(11\pi)^2$
1420.3	38	1420.3	8	1420	2	1420	20	$(12\pi)^2$
1666.7	3	1666.7	4	1666.7	1	1666.7	1	$(13\pi)^2$
		1798.1	2	1798.1	2			$(13.5\pi)^2$
1932.8	1	1932.8	1	1932.8	1	1932.8	3	$(14\pi)^2$
2218.5	8					2218.5	1	$(15\pi)^2$
2523.8	1					2523.8	3	$(16\pi)^2$
2848.7	3					2848.7	1	$(17\pi)^2$
3193.2	86					3139.2	10	$(18\pi)^2$
3557.3	3					3557.3	1	$(19\pi)^2$

Table 6.3: Calculated Values of the first 20 eigenvalues for given sequences of j_i's with multiplicity, m and the expected value, λ.
A={2,3,2,3,...} B={3,2,3,2,...} C={3,4,3,4,...} D={4,3,4,3,...}

forced by the Kirchhoff matching conditions and the orthogonality requirements that assign an eigenfunction to a given representation level. These orthogonality conditions were discussed in detail in the previous chapter. In short they allow the counting arguments to count an eigenfunction only once. The shapes in Chapter 5 are shown as only the top half of those here

Definition 6.3.2. (a) A shape is a connected quantum sub-graph, as shown in Figure 6.5. In that figure the "D" denotes a Dirichlet boundary condition at that node and an "N" the Neumann condition.

(b) A V is the shape consisting of three nodes: two nodes in a column and the third node a second. The two nodes in the first column are degree one and the node in the second column is degree two. When a V is in F_n, it shares its degree

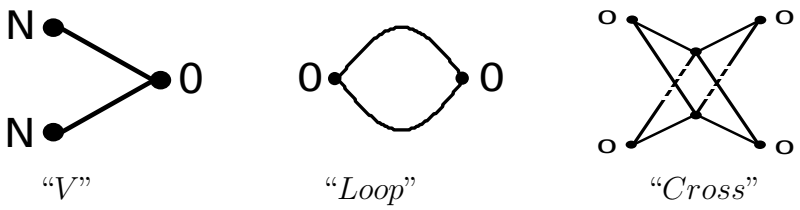

Fig. 6.5: Construction of V's, loops, and crosses along with associated boundary conditions

two node with another shape thus making it a degree four node, as seen in Figure 6.4.

(c) A loop is the shape that consists of two nodes each of degree two. The nodes are connected to each other by two cells, creating a loop. When a loop is in F_n, both degree two nodes are shared as degree two nodes for another shape thus making them degree-four nodes, Figure 6.4.

(d) A cross is the shape consisting of six nodes four of degree two and two of degree four. The degree two nodes each have a cell connecting the node to each of the degree four nodes. Notice the cross is the only shape containing nodes of degree four in the subgraph. When a cross is in F_n the degree two nodes are shared with degree two nodes of another shape thus making them degree four nodes, as in Figure 6.4.

Before determining the spectrum of Δ_n on the three shapes, we must first establish the following proposition which describes how these three shapes are involved in the construction of F_n and L.

Proposition 6.3.3. (a) Any node in any quantum graph approximating a Laakso space is either of degree one or degree four.

(b) For any degree one node in F_n, a V is produced in F_{n+1}.

(c) For any degree four node in F_n, a cross is produced in the construction of F_{n+1}.

(d) Any cell in F_n produces $j_{n+1} - 2$ loops in F_{n+1} between the V's or crosses produced by the nodes in F_n.

(e) For $n \geq 0$ the number of nodes in F_n is $N_n = 2^{n-1}(d_n + 3)$.

Proof. (a) A degree one node in F_{n-1} gives rise to two degree one nodes in F_n as an immediate consequence of the construction. Similarly a degree four node gives rise to a single degree four node in F_n. The new nodes in F_n that are not nodes in a copy of F_{n-1} are the identification of two degree two nodes, hence of degree four.

(b) In the construction of F_{n+1}, the cell connected to a degree one node is split into j_{n+1} intervals by adding $(j_{n+1}-1)$ nodes. Then the graph is duplicated yielding two rows of cells connected between j_{n+1} columns with two nodes in each, all of degree two except for the nodes at the end of the cell. The original and duplicated cells are connected at the newly added nodes. Thus the original node of degree one from F_n remains degree one in F_{n+1}. The graph around the original node and it's duplicate is a V.

(c) In the construction of F_{n+1}, the four cells connected to the degree four node in F_n will be split into j_{n+1} intervals. To construct F_{n+1}, F_n is duplicated, new nodes inserted, and connected at the newly added nodes. Thus the original degree-four node remains degree four and is duplicated, creating two degree-four nodes. The graph around the original node and it's duplicate is a cross.

(d) Parts b and c account for two of the j_{n+1} intervals. The rest produce loops. So, there are $j_{n+1}-2$ loops in F_{n+1} for every cell in F_n.

(e) We will induct on n. The unit interval, F_0, has two nodes. Suppose that F_{n-1} has $N_{n-1} = 2^{n-2}(d_{n-1}+3)$ nodes. Then $N_n = 2 \times N_{n-1} + 2^{n-1}(j_n - 1)d_{n-1}$, the nodes from the two copies of F_{n-1} plus the new nodes of which there are $j_n - 1$ new nodes per cell in F_{n-1} and there are $2^{n-1}d_{n-1}$ cells in F_{n-1}. This simplifies to the claimed formula.

Qed

We now generalize the results from [66] in three lemmas that give the eigenvalues and multiplicites (counts) for each of the three shapes.

Lemma 6.3.4. For any $n \geq 1$, the number of V's in F_n is 2^n. The eigenvalues for this shape at this level are:

$$\{[d_n(k+1/2)\pi]^2 : k = 0, 1, \ldots\}. \tag{6.3.3}$$

Proof. We prove the count by induction. The graph F_1 is constructed out of F_0, which is a single cell connecting two degree one nodes. This implies by Proposition 6.3.3 that F_1 will have 2 V's. Now assume that for some arbitrary $n \geq 1$, the number of V's in F_n is 2^n. From Definition 6.3.2, the V is the only shape that has a degree one node. Furthermore, it has two degree one nodes. From Proposition 6.3.3 we know that each degree one node in F_n produces a V in F_{n+1}. From [66] the shapes defined in Definition 6.3.2 are all the possible shapes in the graphs, so there cannot be any degree one nodes from any other shape. So the number of V's in F_{n+1} is twice the number of V's in F_n. So F_{n+1} has 2^{n+1} V's.

In order to get the spectrum of Δ_n restricted to a V we look at the functions in this domain that are orthogonal to the functions expressible on an interval.

These functions have the property that the values on the top branch are the negative of the values on the lower. We therefore need only consider the top branch, as it fully determines the behavior on the bottom branch. This top branch is one interval, and has Neumann boundary conditions at one end and Dirichlet boundary conditions at the other. The length of the cell is d_n^{-1}. So we are looking for eigenfunctions on intervals of length d_n^{-1} with zero derivative at one end and zero value at the other. These come in the form $\cos(d_n(k+1/2)\pi x)$ where $k = 0, 1, \ldots$ and $x \in [0, d_n^{-1}]$. The eigenvalues in (6.3.3) are now obtained in the usual way. ***Qed***

Lemma 6.3.5. For any $n \geq 1$, the number of loops in F_n is

$$2^{n-1}(j_n - 2)(d_{n-1}). \tag{6.3.4}$$

The eigenvalues for this shape at this level are

$$\{[d_n k\pi]^2 : k = 1, 2, \ldots\}. \tag{6.3.5}$$

Proof. By Proposition 6.3.3 every cell in F_{n-1} produces $j_n - 2$ loops in F_n. In order to know how many loops are in F_n, the number of cells in F_{n-1} are counted and multiplied by $j_n - 2$. The number of cells in F_n were already counted in Proposition 6.2.2 and shown to be $2^n(d_n)$. Substituting in $n-1$ for n in this expression and multiplying by $j_n - 2$ gives (6.3.4).

In order to get the spectrum of Δ_n restricted to a loop we look at the functions in this domain that are orthogonal to the functions expressible on an interval. Again, these functions have the property that the vales on the top branch are the negative of those on the lower. As was the case with the V above, the orthogonality condition imposed on the functions reduces the question to only considering the top interval of length d_n^{-1} with Dirichlet boundary conditions. The eigenfunctions that fit these conditions are $\sin(d_n k\pi x)$ with $k = 1, 2, \ldots$ and $x \in [0, d_n^{-1}]$. These result in the set defined in (6.3.5).

Qed

Lemma 6.3.6. For any $n \geq 2$, the number of crosses in F_n is

$$2^{n-2}(d_{n-1} - 1). \tag{6.3.6}$$

There are two sets of eigenvalues for this shape at this level. They are

$$\left\{ \left[\frac{1}{2}(d_n k\pi) \right]^2 : k = 1, 2, \ldots \right\} \tag{6.3.7}$$

with multiplicity one and

$$\{[d_n k\pi]^2 : k = 1, 2, \ldots\} \tag{6.3.8}$$

with multiplicity two.

Proof. From Proposition 6.3.3 crosses in F_n appear only where there were degree four nodes in F_{n-1}. Therefore, to find the number of crosses in F_n, we will count the number of degree four nodes in F_{n-1}. By Proposition 6.3.3 every node in a quantum graph approximating a Laakso space is either of degree one or degree four. Therefore, subtracting the number of degree one nodes from the total number of nodes will give the number of degree four nodes. From the same proposition, the total number of nodes is $2^{n-1}(d_n+3)$. We have seen already that in F_n degree one nodes only occur in V's and that for every v there are two degree one nodes. From Lemma 6.3.4 that there are 2^n V's in F_n. Therefore, there are 2^{n+1} degree one nodes in F_n and $2^{n-1}(d_n+3)-2^{n+1} = 2^{n-1}(d_n+3-2^2) = 2^{n-1}(d_n-1)$ degree four nodes. Substituting $n-1$ for n in this last expression gives (6.3.6). We note that this lemma is stated only for $n \geq 2$ because F_1 never has a cross since there are only degree one nodes in F_0.

To obtain the spectrum of Δ_n restricted to the cross, we must consider the functions in the domain of the Laplacian on the cross. We can think of the cross as two X-shapes, (such as F_1 in Figure 6.1) connected at their four outer nodes. The orthogonality conditions from [66] force the function on the bottom X to equal the negative of the function on the top X. The value of the function on the top of the X determines the value of the function on the bottom. The width of the X shape is $2d_n^{-1}$ and will have Dirichlet boundary conditions at the degree two nodes. Any function can be decomposed as symmetric and anti-symmetric with respect to the upper and lower branches of the X. We consider the two cases in turn.

In the symmetric case, the function is the same along the top and bottom branches of the X. Therefore we need only to look at the top branch as it fully determines the bottom branch. Here we are looking for eigenfunctions on an interval of length $2d_n^{-1}$ and zero at the boundaries. These are $\sin(\frac{1}{2}d_n k\pi x)$ with $k = 1, 2, \ldots$ and $x \in [0, 2d_n^{-1}]$. The associated eigenvalues to these functions are those given in (6.3.7).

In the antisymmetric case, the function value horizontally along the bottom branch of the X is the negative of the value along the top branch. At the central node, where the two branches meet, these two values must equal, so they must be zero. We then effectively have the X broken up into two V's of length d_n^{-1} but with Dirichlet boundary conditions at either end. Looking at one of these V's, we still have the value along the bottom branch equal to the negative of the value along the top, so we consider only the top branch. Here we look for functions of length d_n^{-1} with Dirichlet boundary conditions at both ends. This has already been done in Lemma 6.3.5 for the loop shape. There we got $\sin(d_n k\pi x)$ with $k = 1, 2, \ldots$ and $x \in [0, d_n^{-1}]$ as the eigenfunctions and $\{[d_n k\pi]^2 : k = 1, 2, \ldots\}$ as the spectrum. This spectrum has multiplicity two because there are two halves of in the cross. ***Qed***

Shape	Count	Spectrum	n Value
F_0	1	$\{[k\pi]^2 : k = 0, 1, \ldots\}$	$n = 0$
V	2^n	$\{[d_n(k + \frac{1}{2})\pi]^2 : k = 0, 1, \ldots\}$	$n \geq 1$
Loop	$2^{n-1}(j_n - 2)(d_{n-1})$	$\{[d_n k\pi]^2 : k = 1, 2, \ldots\}$	$n \geq 1$
Cross	$2^{n-2}(d_{n-1} - 1)$	$\{[\frac{1}{2}(d_n k\pi)]^2 : k = 1, 2, \ldots\}$ $\{[d_n k\pi]^2 : k = 1, 2, \ldots\}^{\times 2}$	$n \geq 2$

Table 6.4: Summary of Lemmas 6.3.4 through 6.3.6

Now we must consider the graph F_0 and the eigenvalues it contributes to the spectrum. This graph is just the unit interval, and has Neumann boundary conditions forced by the Kerchoff matching conditions. So we are looking for eigenfunctions on intervals with length one and zero derivative at either end. These come in the form $\cos(k\pi x)$ where $k = 0, 1, \ldots$. This results in the following spectrum with multiplicity one:

$$\{[k\pi]^2 : k = 0, 1, \ldots\} \tag{6.3.9}$$

Table 6.4 we summarizes the results of these lemmas. In order to obtain the full spectrum with multiplicities, these sets must be combined with the multiplicities over all $n \geq 0$. Hence, Theorem 6.3.1 holds.

6.3.2 Numerical Computations of the Spectrum

A MATLAB script described in [66] calculated the spectrum of the Laplacian for constant j_n for all $n \in \mathbb{N}$ by producing the incidence matrices of the approximating graphs. We modified this script to handle general Laakso spaces. As in the original script, the eigenvalues are calculated using the *eigs* function, which is based on ARPACK (see users guide [57]).

Quantum graphs approximating the Laakso space associated with the sequence j_i=[2,3,2,3,...] is shown in Figure 6.4 and the first twenty eigenvalues of the Laplacian on this space are shown in Table 6.2. The first twenty eigenvalues of Laplacians on other Laakso spaces are shown in Table 6.3. These computations agree with the calculations found in Lemmas 6.3.4 through 6.3.6.

6.4 Heat Kernel

Given a Laplacian on a Laakso space, the trace of its heat kernel will be obtained following the same procedure used in [2] where the heat kernel's trace was found for the diamond fractal. From [74] the heat kernel of the Laplacian is

$$p(t, x, y) = \sum_{k,l,m} \psi_{k,l}(y)\psi_{k,m}(x)e^{-tE_k}$$

where $\psi_{k,l}$ and $\psi_{k,m}$ are L^2-normalized eigenfunctions of Δ. The heat kernel on Laakso spaces will be further studied in [72] where continuity and bounds will be proved. The trace of the heat kernel $Z(t)$ is defined in [2] as

$$Z(t) = \int p(t,x,x)dx = \sum_k g_k e^{-E_k t}, \tag{6.4.1}$$

where E_k are the eigenvalues of the Laplacian on the fractal and g_k are the respective multiplicities associated with those eigenvalues. Associated with the heat kernel is the spectral zeta function also defined in [2] from the heat kernel as

$$\zeta(s,\gamma) = \frac{1}{\Gamma(s)} \int_0^\infty t^{s-1} Z(t) e^{-\gamma t} dt \tag{6.4.2}$$

where $\Gamma(s) = \int_0^\infty t^{s-1} e^{-t} dt$ is the gamma function. We set $\gamma = 0$ throughout the rest of this paper. Substitute (6.4.1) into (6.4.2) to obtain

$$\begin{aligned} \zeta(s,\gamma) &= \frac{1}{\Gamma(s)} \int_0^\infty t^{s-1} \sum_k g_k e^{-E_k t} e^{-\gamma t} dt \\ &= \sum_k \frac{g_k}{(E_k+\gamma)^s}. \end{aligned} \tag{6.4.3}$$

The next step in any specific example is to simplify the spectral zeta function by recognizing Riemann zeta functions, $\zeta_R(s) = \sum_{n=0}^{\infty} \frac{1}{n^s}$, and identifying the other terms as geometric series.

Definition 6.4.1. Define $r = \lim_{n\to\infty} (d_n)^{1/n}$ when this limit exists. In the case of self-similar spaces r is the contraction ratio since d_n^{-1} is the diameter of each cell. There is for any value of r a sequence j_n that will produce that value.

Once all of the series are simplified, the poles of $\zeta(s,0)$ in the complex plane can be calculated. The poles of $\zeta(s)$ for the diamond fractals are given in [2] as

$$s_m = \frac{d_h}{d_w} + \frac{2i\pi m}{d_w \ln r}, \qquad m \in \mathbb{Z}, \tag{6.4.4}$$

where d_h and d_s are the Hausdorff and walk dimensions respectively.

Since the spectral zeta function was expressed as an integral of $Z(t)$, applying an inverse Mellin transform [5] allows the heat kernel to be expressed as

$$Z_D(t) = \frac{1}{2\pi i} \int_{a-i\infty}^{a+i\infty} \zeta_D(s)\Gamma(s) t^{-s} ds. \tag{6.4.5}$$

By the Residue Theorem, $Z_D(t)$ is the sum of the residues of $\zeta_D(s)\Gamma(s)t^{-s}$. The residue must also be calculated at $s = 0$ (a pole for $\Gamma(s)$) and at $s = 1/2$ (a pole for the $\zeta_R(2s)$ term in $\zeta(s, \gamma)$).

It is known that $\overline{\zeta_R(s)} = \zeta_R(\overline{s})$ and $\overline{\Gamma(s)} = \Gamma(\overline{s})$ for all complex s. Thus, the residues from s_m and s_{-m} are complex conjugates of one another; therefore their sums equal twice the real part of the residue of s_m. The complex values of the trace of the heat kernel yield oscillatory behavior in the heat kernel. We shall observe what happens to the heat kernel as $t \to 0$. Therefore, only the leading term with the most negative real power of t as well as any constants are included. For example, a result of [2] shows that for the diamond fractals, the trace of the heat kernel is

$$Z_D(t) \sim \zeta_D(0) + \frac{r^{d_h-1}-1}{\log r^{d_w}} \frac{1}{t^{d_s/2}} (a_0 + 2Re(a_1 t^{-2i\pi/(d_w \log r)})) + ... \tag{6.4.6}$$

This shows that the dominating power of t in the leading term as $t \to 0$ is $-d_s/2$. This incidentally is the complex dimension introduced in [53]. We shall now perform the same calculation for general Laakso spaces.

6.5 The Trace of the Heat Kernel on Laakso Spaces

In Laakso spaces the dimensions and value of r are not always known by other means. Therefore the poles will be calculated analytically and the results will provide information about the Hausdorff, walk, and spectral dimensions. We now give the leading powers of the trace of the heat kernel for the Laplacian on a general Laakso space.

Theorem 6.5.1. For the Laakso space associated to the sequence $\{j_i\}_{i=1}^{\infty}$ the trace of the heat kernel is

$$\begin{aligned} Z(t) &= \sum_{n=2}^{\infty} 2^{n-1}(d_{n-1}-1) \sum_{k=1}^{\infty} e^{-k^2\pi^2 d_n^2 t} \\ &\quad + \sum_{n=2}^{\infty} 2^{n-2}(d_{n-1}-1) \sum_{k=1}^{\infty} e^{-\frac{1}{4}k^2\pi^2 d_n^2 t} + \sum_{n=1}^{\infty} 2^n \sum_{k=0}^{\infty} e^{-(k+1/2)^2\pi^2 d_n^2 t} \\ &\quad + \sum_{n=1}^{\infty} 2^{n-1} d_{n-1}(j_n-2) \sum_{k=1}^{\infty} e^{-k^2\pi^2 d_n^2 t} + \sum_{k=0}^{\infty} e^{-k^2\pi^2 t} \end{aligned} \tag{6.5.1}$$

with an associated spectral zeta function

$$\begin{aligned} \zeta_L(s) = \frac{\zeta_R(2s)}{\pi^{2s}} &\left[\left(\sum_{n=2}^{\infty} \frac{2^{n-1}(d_{n-1})(2^{2s-1}+j_n-1) + 2^{n-1}(\frac{3}{2}2^{2s}-3)}{d_n^{2s}} \right) \right. \\ &\left. + \frac{2^{2s+1}-4+j_1}{j_1^{2s}} + 1 \right]. \end{aligned} \tag{6.5.2}$$

Proof. The spectrum of the Laplacian on various Laakso spaces was given in Table 6.4 as

$$\sigma(\Delta_L) = \bigcup_{n=2}^{\infty}\bigcup_{k=1}^{\infty}\{k^2\pi^2 d_n^2\} \cup \bigcup_{n=2}^{\infty}\bigcup_{k=1}^{\infty}\left\{\frac{k^2\pi^2 d_n^2}{4}\right\} \cup \bigcup_{n=1}^{\infty}\bigcup_{k=0}^{\infty}\{(k+1/2)^2\pi^2 d_n^2\} \cup \bigcup_{n=1}^{\infty}\bigcup_{k=1}^{\infty}\{k^2\pi^2 d_n^2\} \cup \bigcup_{k=0}^{\infty}\pi^2 k^2 \tag{6.5.3}$$

with respective multiplicities

$$2^{n-1}(d_{n-1}-1),\ \ 2^{n-2}(d_{n-1}-1),\ \ 2^n,\ \ 2^{n-1}d_{n-1}(j_n-2),\ \ 1. \tag{6.5.4}$$

Direct substitution of the these values into (6.4.1) gives the heat kernel. By (6.4.3) the associated spectral zeta function is

$$\begin{aligned}\zeta_L(s) = \ & \sum_{n=2}^{\infty}\sum_{k=1}^{\infty}\frac{2^{n-1}(d_{n-1}-1)+2^{n-2+2s}(d_{n-1}-1)}{(d_n^2k^2\pi^2)^s} \\ & +\sum_{n=1}^{\infty}\sum_{k=0}^{\infty}\frac{2^{n+2s}}{(d_n^2(2k+1)^2\pi^2)^s}+\sum_{n=1}^{\infty}\sum_{k=1}^{\infty}\frac{2^{n-1}d_{n-1}(j_n-2)}{(d_n^2k^2\pi^2)^s} \\ & +\sum_{k=1}^{\infty}\frac{1}{(k^2\pi^2)^s}.\end{aligned} \tag{6.5.5}$$

This can be simplified by identifying Riemann zeta functions and, in certain cases, a Dirichlet Lambda function [1]. Then the function can be manipulated in to one sum.

$$\begin{aligned}\zeta_L(s) = \ & \tfrac{\zeta_R(2s)}{\pi^{2s}}\ \left[\left(\sum_{n=2}^{\infty}\frac{2^{n-1}(d_{n-1})(2^{2s-1}+j_n-1)+2^{n-1}(\frac{3}{2}2^{2s}-3)}{d_n^{2s}}\right)\right. \\ & \left.+\frac{2^{2s+1}-4+j_1}{j_1^{2s}}+1\right]\end{aligned} \tag{6.5.6}$$

as claimed in the proposition. ***Qed***

This expression of the spectral zeta function cannot be simplified further for a general Laakso space with an arbitrary sequence of j_i's. However, it provides a common starting point for Laakso spaces in which the sequence of j_i's is known. The next step is to locate the poles of the spectral zeta function. Recall that only poles which yield the most negative real power of t are considered since they produce the dominating behavior as $t \to 0$ in the trace of the heat kernel. There are in general more poles than these.

Proposition 6.5.2. Of all the poles of the spectral zeta function in the complex plane, the poles that yield the most negative real power of t in the leading term of the trace of the heat kernel are located at

$$s_m = \frac{\log 2r + 2\pi i m}{\log r^2} \tag{6.5.7}$$

for integer m.

Proof. The trace of the heat kernel requires the most negative power of t which corresponds to the poles with the greatest real component due to the t^{-s} term in (6.4.5). The proof of the proposition relies on analyzing the series in (6.5.2) to find the poles. Note that the in the series in (6.5.2), the numerator has two terms; values of s will be calculated that will make the denominator grow at the same rate as the numerator. The value of s with the greatest real part are the poles that will be used. First rewrite the denominator of (6.5.2) as $d_n^{s_1} d_n^{s_2}$ where $2s = s_1 + s_2$. Select s to match the rate of growth for the first term in the numerator. To make $d_n^{s_1}$ grow at the same rate as d_{n-1}, s_1 should equal 1. To have $d_n^{s_2}$ grow at the same rate as 2^{n-1} s_2 should equal $\log_r 2$. Therefore, for the first term, $2s = 1 + \log_r 2$. It can be verified that any poles from the second term in (6.5.2) will not have a real component as large as this pole. Therefore, the real part of the poles that will yield the desired leading term in the trace of the heat kernel are $s = \frac{1}{2} + \frac{\log 2}{2 \log r} = \frac{\log 2r}{\log r^2}$. Including $2\pi i m$ in the numerator gives all of the complex values of this pole ***Qed***

Corollary 6.5.3. The dominating t term in the trace of the heat kernel has power $-ds/2 = -Re(s_m)$.

Proof. Recall from Section 6.4 that the dominating power of t in the trace of the heat kernel as $t \to 0$ was $-d_s/2$. A result of Proposition 6.5.2 is that the greatest real component of the poles yield the dominating power of t. Therefore, when calculating the residue of $\zeta_L(s)\Gamma(s)t^{-s}$ at the pole obtained from (6.5.7), the real power of t will be precisely $-Re(s_m)$. But as stated at the beginning of the proof, it is also equal to $-d_s/2$. Thus, $d_s/2 = Re(s_m)$ ***Qed***

Corollary 6.5.4. The spectral dimension of any Laakso space with $\{j_i\}$ such that r exists is

$$d_s = \frac{\log 2r}{\log r}. \tag{6.5.8}$$

The walk dimension, d_w, is 2 for any Laakso space which implies $d_h = d_s$.

Proof. This follows directly from Proposition 6.5.2 and Corollary 6.5.3 since $d_s/2 = Re(s_m) = \frac{\log 2r}{\log r^2}$ which implies $d_s = \frac{\log 2r}{\log r}$. The walk dimension is a result in [72]. It does agree with d_h and d_s via the Einstein relation $2d_h/d_w = d_s$. ***Qed***

The next two subsections give the trace of the heat kernel for two specific Laakso spaces where the sum in the spectral zeta function can be evaluated exactly: $j = 2$, and $j = \{2, 3, 2, 3...\}$.

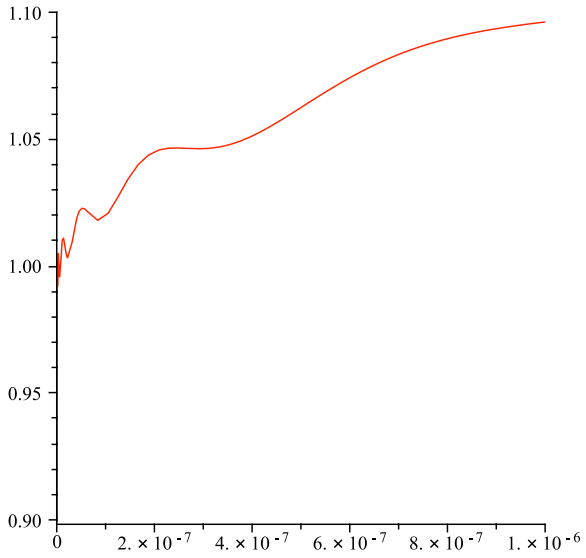

Fig. 6.6: Heat kernel Z_{L_2}, normalized by the leading non-oscillating term for the $j = 2$ Laakso space. The variable s is on the horizontal axis.

6.5.1 Laakso Space with j=2

Proposition 6.5.5. For the Laakso space where at each iteration $j = 2$, written L_2, the trace of the heat kernel is

$$Z_{L_2} \sim \zeta_{L_2}(0) + \frac{1}{16t\log 2}\left(1 + 2Re\left(\frac{6\zeta_R(2+\frac{4\pi i}{\log 4})\Gamma(1+\frac{2\pi i}{\log 4})}{t^{\frac{2\pi i}{\log 4}}\pi^{2+\frac{4\pi i}{\log 4}}}\right) + \ldots\right).$$

Proof. For Laakso spaces with a fixed $j = 2$, $d_n = 2^n$. Substituting these into (6.5.1) and (6.5.2) gives the following two equations

$$\begin{aligned} Z_{L_2}(t) = & \sum_{n=1}^{\infty}\left[2^{2n-2} - 2^{n-1}\right]\sum_{k=1}^{\infty} e^{-t2^{2n}k^2\pi^2} \\ & + \sum_{n=2}^{\infty}\left[2^{2n-3} - 2^{n-2}\right]\sum_{k=1}^{\infty} e^{-tk^2\pi^2 2^{2n-2}} \\ & + \sum_{n=1}^{\infty} 2^n \sum_{k=0}^{\infty} e^{-t(2k+1)^2\pi^2 2^{2n-2}} \end{aligned} \tag{6.5.9}$$

and

$$\zeta_{L_2}(s,0) = \frac{\zeta_R(2s)}{\pi^{2s}}\left(\frac{4(2^{2s-1}+1)}{4^s(4^2-4)} + \frac{6(2^{s2-1}-1)}{4^s(4^s-2)} + \frac{2^{s+1}-2+2^{2s}}{4^s}\right) \tag{6.5.10}$$

which has poles

$$z = \left(\frac{1}{2} + \frac{2\pi i m}{\log 4}\right), z = \left(1 + \frac{2\pi i m}{\log 4}\right), \forall m \in \mathbb{Z}. \tag{6.5.11}$$

By Proposition 6.5.2, only the second term of the above equation with the greatest real part contributes to the leading t term. Then an inverse Mellin transform is applied just as in Theorem 6.5.1. Table 6.5 shows the residues of the integrand after the inverse Mellin transform at the poles given in (6.5.11) as well as $s = 0$ from the $\Gamma(s)$ term. Again we add complex conjugates and take only the most negative powers of t. Notice that when adding the residue from the poles in (6.5.11) only the poles with real part one contribute to the heat kernel, the others with the exception of zero and one half have residue zero. Once all of the residues are simplified we obtain the expression for the trace heat kernel's leading term as given in the proposition. ***Qed***

s_m	Residue
0	$\zeta_{L_2}(0))$
1/2	$\frac{3}{8\sqrt{\pi}\sqrt{t}}$
1	$\frac{1}{16t\log 2}$
$1 \pm \frac{2\pi i m}{\log 4}$	$\frac{1}{16t\log 2}\frac{6\zeta_R(2+\frac{4\pi i m}{\log(4)})\Gamma(1+\frac{2\pi i m}{\log(4)})}{t^{\frac{2\pi i m}{\log(4)}}\pi^{2+\frac{4\pi i m}{\log(4)}}}$
$\frac{1}{2} + \frac{2i\pi}{\log 4}$	0 for $m \neq 0$

Table 6.5: Residues of the integrand of the inverse Mellin transform for given poles of the spectral zeta function for Laakso spaces with a fixed $j = 2$

The power of 1 of t in the denominator of the leading term in the proposition implies that the spectral dimension d_s for L_2 is 2. Knowing that the Hausdorff dimension $d_h = 2$ from Table 6.1, we conclude that the walk dimension $d_w = 2$ since $d_s = 2d_h/d_w$. Notice the poles and dimensions of this fractal were explicitly calculated. But Corollary 6.5.4 and Proposition 6.5.2 yield the same result once $r = \lim_{n\to\infty} d_n^{1/n} = \lim_{n\to\infty}(2^n)^{1/n} = 2$ is known.

6.5.2 Laakso Space with $j = \{2, 3, 2, 3...\}$

Proposition 6.5.6. For the Laakso space with $j_{2k} = 3$ and $j_{2k-1} = 2$ where $k \geq 1$, the trace of the heat kernel is

$$\begin{aligned} Z_L(t) \sim & \zeta_L(0) + \\ & \frac{1}{24t^{\frac{1}{2}+\frac{\log(2)}{\log(6)}}\log(6)}\left(\frac{\Gamma\left(\frac{1}{2}+\frac{\log(2)}{\log(6)}\right)\zeta_R\left(1+\frac{2\log(2)}{\log(6)}\right)}{\pi^{1+\frac{2\log(2)}{\log(6)}}} + \right. \\ & \sum_{m=1}^{\infty} 2Re\left(\frac{\Gamma\left(\frac{1}{2}+\frac{\log(2)}{\log(6)}+\frac{2\pi im}{\log(6)}\right)\zeta_R\left(1+\frac{2\log(2)}{\log(6)}+\frac{4\pi im}{\log(6)}\right)}{\pi^{1+\frac{2\log(2)}{\log(6)}+\frac{4\pi im}{\log(6)}}t^{-\frac{2\pi im}{\log(6)}}}\right) \\ & \left.\left(\frac{2^{2+\frac{4\log(2)}{\log(6)}+\frac{8\pi im}{\log(6)}}+10\cdot 2^{1+\frac{2\log(2)}{\log(6)}+\frac{4\pi im}{\log(6)}}+12}{2^{1+\frac{2\log(2)}{\log(6)}+\frac{4\pi im}{\log(6)}}}\right)\right). \end{aligned} \tag{6.5.12}$$

Proof. In this case $r = \lim_{n\to\infty} d_n^{1/n} = \lim_{n\to\infty}(2^{n/2}3^{n/2})^{1/n} = \sqrt{6}$. This locates the poles with largest real part at $s_m = \frac{1}{2} + \frac{\log(2)}{\log 6} + \frac{2\pi im}{\log 6}$.

The next step is to obtain and simplify the spectral zeta function associated with the trace of heat kernel given in (6.5.2). Since j_i alternates between 2 and 3, the following values can be directly substituted in, for any k we have:

$$d_1 = 2 \quad d_2 = 6 \quad d_{2k-2} = 6^{k-1} \quad d_{2k-1} = 2\times 6^{k-1} \quad d_{2k} = 6^k$$

In preparation for substituting these values into (6.5.2) the sum is split into two sums, one over even n and the other over odd

$$\begin{aligned} & \zeta_L(s) = \\ & \sum_{n=2}^{\infty}\frac{2^{n-1}(d_{n-1}-1)+2^{n-2+2s}(d_{n-1}-1)+2^{n+2s}-2^n+2^{n-1}d_{n-1}(j_n-2)}{d_n^{2s}} \\ & = \frac{2(d_1-1)+2^{2s}(d_1-1)+2^{2+2s}-2^2+2d_1}{d_2^{2s}} \\ & \quad + \sum_{k=2}^{\infty}\left(\frac{2^{2k-2}(d_{2k-2}-1)+2^{2k-3+2s}(d_{2k-2}-1)+2^{2k-1+2s}-2^{2k-1}}{d_{2k-1}^{2s}}\right. \\ & \quad \left. + \frac{2^{2k}(d_2k-1)+2^{2k-2+2s}(d_{2k-1}-1)+2^{2k+2s}-2^{2k}+2^{2k-1}(d_{n-1})}{d_{2k}^{2s}}\right). \end{aligned} \tag{6.5.13}$$

Substituting the known values of d_{2k}, d_{2k+1}, j_{2k}, and j_{2k+1} we obtain

$$\begin{aligned} \zeta_L(s) = \frac{\zeta_R(2s)}{\pi^{2s}}\left[\left(\frac{2^{2s}+4}{12}+\frac{s^{2s-1}+1}{2^{2s}}\right)\frac{24}{6^{2s}-24}+\right. \\ \left.\left(3\cdot 2^{2s}-6+\frac{6\cdot 2^{2s}-12}{2^{2s}}\right)\frac{1}{6^{2s}-4}\right]. \end{aligned} \tag{6.5.14}$$

To apply the inverse Mellin transform as was done in (6.4.5) to obtain an expression for $Z_L(t)$. Then $Z_L(t)$ can be calculated using the sum of the residues of $\zeta_L(s)\Gamma(s)t^{-s}$ using the poles obtained in (6.5.7) as well as $s = 1/2$ (obtained from the Riemann zeta function, $\zeta_R(2s)$ and $s = 0$ (from $\Gamma(s)$). Table 6.6 lists the residues for those poles.

s_m	Residue
0	$\zeta_L(0)$
$\frac{1}{2}$	$\frac{2}{3\sqrt{\pi t}}$
$s_m = \frac{1}{2} + \frac{\log(2)}{\log 6} + \frac{2\pi i m}{\log(6)}$	$\frac{\Gamma(s_m)\zeta_R(2s_m)}{t^{s_m}\pi^{2s_m}} \frac{2^{-2s_m}}{24\log(6)} \left(2^{4s_m} + 10 \cdot 2^{2s_m} + 12\right)$
$s_k = \frac{\log(2)}{\log(6)} + \frac{2\pi i m}{\log(6)}$	$\frac{\Gamma(s_k)\zeta_R(2s_k)}{t^{s_k}\pi^{2s_k}} \frac{3}{8\log(6)} \frac{4^{2s_k}-4}{4^{s_k}}$

Table 6.6: Residues of the integrand of the inverse Mellin transform for given poles of the spectral zeta function for the {2,3,2,3...} Laakso spaces

The sum of the residues in Table 6.6 expresses the trace of the heat kernel with the leading terms as shown in the statement of the proposition. Note that the general terms in $Z_L(t)$ are shown in the proposition to indicate the behavior of the trace of the heat kernel in more detail. ***Qed***

Corollary 6.5.7. The exponent of t, $\frac{\log(2\sqrt{6})}{\log 6}$, in the leading term as t goes towards zero implies that the spectral dimension of this Laakso space is $d_s = \log 24/\log 6$. The Hausdorff dimension for this fractal is given in Table 6.1 as $d_h = \log 24/\log 6$.

Again, the same results are obtained by simply applying Corollary 6.5.4 and Proposition 6.5.2.

Bibliography

[1] M. Abramowitz and I. Stegun, "Handbook of Mathematical Functions: with Formulas, Graphs, and Mathematical Tables," Dover Publications, 1965

[2] E. Akkermans, A. Comtet, J. Desbois, G. Montambaux, and C. Texier, *Spectral Determinant on Quantum Graphs*, Annals of Physics, **284** (2000) 10–51.

[3] A. Allan, M. Barany, and R. S. Strichartz, Spectral operators on the Sierpinski gasket I, *Complex Variables and Elliptic Equations* **54** 521-543 (2009).

[4] D. Applebaum. "Lévy Processes and Stochastic Calculus," Cambridge University Press, Cambridge. 2005.

[5] G. Arfken and H. Weber, *Mathematical Methods for Physicists*, Elsevier Academic Press, 2005

[6] N. Bajorin, T. Chen, A. Dagan, C. Emmons, M. Hussein, M. Khalil, P. Mody, B. Steinhurst, A. Teplyaev, *Vibration Modes of 3n-gaskets and other fractals* J. Phys. A: Math Theor. **41** (2008) 015101 (21pp).

[7] N. Bajorin, T. Chen, A. Dagan, C. Emmons, M. Hussein, M. Khalil, P. Mody, B. Steinhurst, A. Teplyaev, *Vibration Spectra of Finitely Ramified, Symmetric Fractals.* Fractals **16**:3 (2008) 243-258.

[8] M.T. Barlow, *Which values of the volume growth and escape time exponent are possible for a graph?* Rev. Mat. Iberoamericana, **20** (2004), 1-31.

[9] M.T. Barlow and R.F. Bass, *The construction of Brownian motion on the Sierpinski carpet*, Ann. de l'Institut H. Poincar, **25** (1989), 225-257.

[10] M.T. Barlow and R.F. Bass, *Brownian motion and harmonic analysis on Sierpinski carpets*, Canadian J. Math, **54** (1999), 673-744.

[11] M. T. Barlow, R. F. Bass, T. Kumagai, A. Teplyaev. *Uniqueness of Brownian Motion on Sierpinski Carpets.* **arXiv:0812.1802v1** (to appear in Journal of the European Mathematical Society)

[12] M. Barlow and S. Evans. Markov processes on vermiculated spaces. *Random walks and geometry*, (ed. V. Kaimanovich), de Gruyter, Berlin, 2004.

[13] M.T. Barlow and E.A. Perkins, *Brownian motion on the Sierpinski gasket*, Probab. Th. Rel. Fields, **79** (1988) 543-623.

[14] L. Barthold, R. Grigorchuk, *Spectra of non-commutative dynamical systems and graphs related to fractal groups*, C. R. Acad. Sci. Paris Sér. I Math. **331**:6 (2000) 429–434

[15] L. Bartholdi, R. Grigorchuk, V. Nekrashevych, *From fractal groups to fractal sets.* Fractals in Graz 2001, p. 25–118, Trends Math., Birkhuser, Basel, (2003).

[16] M. Begue, L. DeValve, D. Miller, B. Steinhurst, *Heat Kernel Asymptotics On General Laakso Spaces* **arXiv:0912.2176**.

[17] J.-P. Bode and A. M. Hinz, *Results and open problems on the Tower of Hanoi*, Congr. Numer. **139** (1999), 113-122.

[18] Stefan Boettcher and Bruno Gonçalves, *Anomalous Diffusion on the Hanoi Networks*, **arXiv:0802.2757v2**.

[19] S. Boettcher, B. Gonçalves and H. Guclu, *Hierarchical Regular Small-World Networks*, J. Phys. A **41** (2008), no. 25, 252001, 7 pp.

[20] E. Bondarenko and V. Nekrashevych, *Post-critically finite self-similar groups*, Algebra Discrete Math. **2** (2003), no. 4, 21–32.

[21] N. Bourbaki, Trans: S. Berberian, "Integration," Springer-verlag, New York, 2004.

[22] J. Cheeger, *Differentiability of Lipschitz functions on metric measure spaces*, Geom. and Funct. Anal., **9** (1999), 413-640.

[23] R. Grigorchuk, *On Burnside's problem on periodic groups (Russian)*, Funktsional. Anal. i Prilozhen. **14** (1980), no. 1, 53–54.

[24] R. Grigorchuk and Z. Šuník, *Asymptotic aspects of Schreier graphs and Hanoi Towers groups*, C. R. Math. Acad. Sci. Paris **342** (2006), no. 8, 545-550.

[25] R. Grigorchuk and Z. Šuník, *Schreier spectrum of the Hanoi Towers group on three pegs*, *Analysis on graphs and its applications*, 183–198, Proc. Sympos. Pure Math, vol. 77, Amer. Math. Soc., Providence, RI, 2008.

[26] S. Evans and R. Sowers. *Pinching and twisting Markov processes.* The Annals of Probability, Vol. **31**, No. 1. (Jan., 2003), 486-527.

[27] K. Falconer, "The Geometry of Fractal Sets," Cambridge University Press, 1985.

[28] K. Falconer, "Fractal Geometry: Mathematical Foundations and Applications." John Wiley & Sons Ltd., Chichester (1990).

[29] D. Ford and B. Steinhurst, *Vibration Spectra of the m-Tree Fractal*, To appear in Fractals (2010).

[30] B. Franchi, Piotr Hajłasz, P. Koskela, *Definitions of Sobolev Classes on Metric Spaces*, Annales de l'insitut Fourier, **49** (1999) 1903-1924.

[31] M. Fukushima, Y. Oshima and M. Takeda, "Dirichlet Forms and Symmetric Markov Processes," deGruyter Studies in Mathematics: 19. 1995.

[32] M. Fukushima, T. Shima, *On a Spectral Analysis for the Sierpinski Gasket*, Potential Analysis **1** (1992), 1-35.

[33] P. Hajłasz, *Sobolev Spaces on an Arbitrary Metric Space*, Potential Analysis, **5** (1996), 403-415.

[34] P. Hajłasz, *Sobolev spaces on metric-measure spaces*, Contemp. Math., **338** (2003) 173-218.

[35] J. Heinonen, "Lectures on Analysis on Metric Spaces," Springer-verlag, New York, 2001.

[36] J. Heinonen, *Nonsmooth Calculus*, Bulletin of the AMS, **44** (2007), 163-232.

[37] J. Hocking and G. Young, "Topology," Dover Publications, Mineola NY, 1988.

[38] K. Igudesman, *Lacunary Self-similar Fractal Sets and Intersection of Cantor Sets,* Lobachevskii Journal of Mathematics **12** pp 41-50 (2003).

[39] N. Kajino, *Spectral asymptotics for Laplacians on self-similar sets*, J. of Func. Anal. **258** (2010), 1310-1360.

[40] J. Kigami, *Harmonic calculus on p.c.f. self-similar sets*, Trans. Amer. Math. Soc., **335** (1993), 721-755.

[41] J. Kigami. *Harmonic Calculus on Limits of Networks and its Applications to Dendrites*, J. Func Anal. **128** (1995), 48-86.

[42] J. Kigami, *Hausdorff dimensions of self-similar sets and shortest path metrics*, J. Math. Soc. Japan **47** (1995), no. 3, 381–404.

[43] Jun Kigami, "Analysis on Fractals," Cambridge Tracts in Mathematics, vol. 143. Cambridge University Press, Cambridge, 2001.

[44] J.Kigami, *Harmonic analysis for resistance forms,* J. Funct. Anal. **204**, (2003), 399–444.

[45] J. Kigami, *Measurable Riemannian geometry on the Sierpinski gasket: the Kusuoka measure and the Gaussian heat kernel estimate*, Math. Ann., **340** (2008), 781-804.

[46] J. Kigami, M. Lapidus, *Weyl's Problem for the Spectral Distribution of Laplacians on P.C.F. Self-similar Fractals* Comm. Math. Phys, **158** (1993), no. 1, 93-125.

[47] P. Koskela, K. Rajala, and N. Shanmugalingam. *Lipschitz continuity of Cheeger-harmonic functions in metric measure space.* J. Funct. Anal. **202** (2003), 147-173.

[48] P. Koskela, N. Shanmugalingam, and J. Tyson. Dirichlet forms, *Poincaré inequalities, and the Sobolev spaces of Korevaar-Schoen.* Potential Analysis **21** (2004), no 3, 241-262.

[49] P. Kuchment, *Quantum graphs I. Some basic structures.* Waves in random media, **14** (2004), S107–S128.

[50] P. Kuchment, *Quantum graphs II. Some spectral properties of quantum and combinatorial graphs.* J. Phys. A. **38** (2005), 4887–4900.

[51] S. Kusuoka, *Dirichlet forms on fractals and products of random matrices*, Publ. RIMS Kyoto Univ., **25** (1989), 659-680.

[52] T.J. Laakso, *Ahlfors $Q-$regular spaces with arbitrary $Q > 1$ admitting weak Poincaré inequality*, Geom. and Funct. Anal., **10** (2000), 111-123.

[53] M. Lapidus and M. van Frankenhuysen, "Fractal Geometry and Number Theory: Complex Dimensions of Fractal Strings and Zeros of Zeta Functions," Birckhäuser, Boston, 2000

[54] M. Lapidus, J.W. Neuberger, R.J. Renka, *Snowflake harmonics and computer graphics: numerical computation of spectra on fractal drums*, Internat. J. Bifur. Chaos Appl. Sci. Engrg., **6** (1996), 1185-1210.

[55] M. Lapidus and M. Pang, *Eigenfunctions of the Koch Snowflate Drum*, Comm. in Math. Phys., **172** (1995), 359-376.

[56] P. Lax, "Functional Analysis," Wiley Interscience, New York, 2002.

[57] R. Lehoucq, D. Sorensen, and C. Yang, "ARPACK Users' Guide: Solution of Large-Scale Eigenvalue Problems with Implicitly Restarted Arnoldi Methods," SIAM Publications, Philadelphia, 1998.

[58] T. Lindstrøm, *Brownian Motion on Nested Fractals*, Memoirs Amer. Math. Soc., **420** (1990).

[59] S. Makisumi, G. Stadnyk, B. Steinhurst, *Modified Hanoi Towers Groups and Limit Spaces* **arXiv:0909:3520** (submitted)

[60] P. A. P. Moran, *Additive functions of intervals and Hausdorff measure*, Proc. Cambridge Philos. Soc. **42** (1946), 15–23.

[61] V. Nerashevych, "Self-similar groups," Mathematical Surveys and Monographs vol. 117. Amer. Math. Soc., Providence, RI, 2005.

[62] V. Nekrashevych and A. Teplyaev, *Groups and analysis on fractals*, *Analysis on graphs and its applications*, 143–180, Proc. Sympos. Pure Math., vol. 77, Amer. Math. Soc., Providence, RI, 2008.

[63] M. Newman and D. Watts, *Renormalization group analysis of the small-world network model*, Physics Letters A **263** (1999), 341-346.

[64] L.C.G. Rogers and D. Williams. "Diffusions, Markov Processes and Martingales: Vol. 1 Foundations," Cambridge Mathematical Library, Cambridge. 2000.

[65] S. Roman, "Advanced Linear Algebra." Springer Science+Business Media, LLC., New York (2008).

[66] K. Romeo and B. Steinhurst, *Spectrum of a Laplacian on Laakso Spaces,* Complex Analysis and Elliptic Equations, **54**:6, pp. 623-636, 2009.

[67] W. Rudin, "Functional Analysis," McGraw-Hill Book Company, New York, 1973.

[68] S. Semmes, *Finding curves on general spaces through quantitative topology with application for Sobolev and Poincaré inequalities*, Selecta Math. (N.S.), **2** (1996), 155-295.

[69] N. Shanmugalingam, *Newtonian spaces: an extension of Sobolev spaces to metric measure spaces*, Rev. Mat. Iberoamericana, **16** (2000), 243–279.

[70] T. Shima, *On Eigenvalue Problems For Laplacians on PCF Self-similar Sets,* Japan Journal of Industrial and Applied Mathematics, **13** (1996), 1-23.

[71] B. Steinhurst, *Dirichlet Forms on Laakso and Barlow-Evans Fractals of Arbitrary Dimension.* **arXiv:0811.1378v2** (2008)

[72] B. Steinhurst, *Uniqueness of Brownian Motion on Laakso Spaces*, in preparation.

[73] B. Steinhurst and A. Teplyaev, *Spectral Analysis and Dirichlet Forms on Barlow-Evans Fractals,* in preparation.

[74] R. Strichartz, *Differential Equations on Fractals: A Tutorial.* Princeton University Press, Princeton (2006).

[75] A. Teplyaev, *Harmonic coordinates on fractals with finitely ramified cell structure*, Canad. J. Math., **60** (2008), 457-480.

[76] D. J. Watts and S. H. Strogatz, *Collective dynamics of 'small-world' networks*, Nature **393** (1998), 440–442.

[77] D. Zhou, *Criteria for Spectral Gaps of Laplacians on Fractals*, J. Fourier Anal. and Appl., **16** (2010), 76-96.

[78] D. Zhou, *Spectral Analysis of Laplacians on the Vicsek Set* Pacific J. Math. **241** (2009) 369-398.